GEOPHYSICAL ELECTROMAGNETICS AT VERY-HIGH AND ULTRA-HIGH FREQUENCIES

by

© ELIZABETH BARANYI

A Thesis submitted to the Faculty of Graduate studies and Research in Partial Fulfillment of the Requirements for the Degree of Master of Science in Applied Geophysics.

Department of Mining and Metallurgical Engineering

McGill University

Montreal, CANADA

GEOPHYSICAL ELECTROMAGNETICS AT VERY HIGH AND ULTRA-HIGH FREQUENCIES

by

ELIZABETH BARANYI

To my Father

ABSTRACT

This thesis concerns the geophysical theory of electromagnetic fields and waves, mainly for the near field induction problem, for very-high and ultra-high frequencies. The major contribution of this research is to allow for geophysical models of a half-space in which the basic electromagnetic parameters are complex-valued and frequency-dependent. With less emphasis, other dependencies (i.e. temperature, porosity, salinity, water content and grain size) are also discussed. In spite of the lack of a theoretical basis in solid-state physics, the Cole-Cole model of complex conductivity, permittivity and permeability has been employed because of their relatively simple mathematical formulation while closely corresponding to the Kirkwood-Fuoss physical permittivity model. This geophysical electromagnetic theory is described, in parallel, in both the time and frequency domains in order to describe the domain-equivalence of the complex-valued frequency-dependent models.

Olhoeft (1975) recognized the need for describing permafrozen materials with complex-valued permittivities which contribute to an additional conductivity-like loss at frequencies beyond few Hertz. Spectra of Olhoeft's observations on permittivity and conductivity of real materials have been inverted in this work to allow for frequency dependent

complex-valued electrical parameters. The results support the formulated theory. Furthermore, the resulting parameters have been used to calculate the geophysical electric and magnetic fields caused by theoretically simple transmitting dipole antennas.

This thesis offers a substantial review of the contemporary models of geophysical electromagnetic parameters which allow for the better understanding of high frequency electromagnetic effects which can now be usefully observed with modern geophysical prospecting survey instruments.

RESUME

Cette recherche présente la théorie géophysique des champs et ondes électromagnétiques du problème d'induction au champ proche, aux très hautes et ultra hautes fréquences. La contribution majeur de cette recherche est qu'elle permet des modèles géophysiques du demi-espace, dans lequel les parametres géophysiques de base sont complexes et sont fonctions de la fréquence. D'autres dépendances (ex: température, porosité, salinité, contenance d'eau et taille des graines) sont aussi brèvement citées. Malgré le manque d'explication théorique en état solide, les modèles Cole-Cole de conductivité, permittivité et perméabilité ont été choisis, à cause de leurs

formes mathématiques simples tout en ayant une proche correspondance avec le model Kirkwood-Fuoss de permittivité. La description de la théorie d'électromagnétisme en géophysique est élaborée en parallèle, dans le domaine de fréquence, et le domaine de temps, pour en déduire la nature complexe des parameters.

Olhoeft (1975) souligne la nécessité de decrire les matières pergélisoles au-dessus de quelques Hertz, par une permittivité complexe. Cette dernière participant à une perte additionnelle d'ordre conductive. Dans cette oeuvre, des spectres de résistivité et permittivité observés appartenant a de matières réelles, ont été inversés en permettant des parametres électriques complexes, et fonction de la fréquence. Les résultats obtenus soutiennent la théorie formulée. Ces même parametres ont été par la suite utilisés pour en deduire les champs électriques et magnétiques causés par deux configurations d'antenne dipolaire théoriquement simple.

Cette thèse offre une revue substantielle des modèles contemporains de parametres électromagnétiques géophysiques, ce qui nous espèrons, permettra une meilleure compréhension des effets électromagnétiques de hautes fréquences, observés par les instruments modernes de prospection géophysique.

Nous espèrons que la lecture de cette thèse offrira une référence convainquante et substantielle pour d'éventuelles recherches futurs.

TABLE OF CONTENTS

ACKNOWLEDGEMENT

The author wishes to express her sincere appreciation to Professor O.G. JENSEN for his encouragement and assistance.

Continuing support of this research which was provided by the EMR Research agreements number 138/4/81, 90/4/82 and 54/04/83 as awarded to Professor O. G. JENSEN is greatfully acknowledged.

LIST OF FIGURES

LIST OF TABLES

LIST OF APPENDICES

CHAPTER I

GENERAL INTRODUCTION

1.1 INTRODUCTION

The purpose of this thesis is to assemble a useful description of the electrical and magnetic properties of real geological materials, which is appropriate for the wide range of frequencies now employed in geophysical measurements, and which allows for the variety of source-receiver configurations of electrical, magnetic and electromagnetic instruments in common use. We shall limit our attention to homogeneous and isotropic geological materials which can, however, exhibit strong frequency dependencies in their electromagnetic physical properties. The description must be consistant with Maxwell's electromagnetic theory and known natural laws. We shall find it convenient to use the Cole-Cole (1941) dispersion formulae , in describing the complex frequency dependence of the dielectric permittivity, the electrical conductivity (or resistivity), and the magnetic permeability of naturally occuring materials. We shall compare these theoretical models to examples derived from the existing empirical data which now spans frequencies from essentially DC (Van Voorhis et al. 1973, Carmichael 1982) to ultra-high frequency band (Hoekstra & Delaney 1974, Poley et al. 1978, Coon et al. 1981 etc...).

In addition we shall obtain appropriate theoretical formulations for the description of geophysical measurements in relation to the geological electrical and magnetic parameters.

1.2 NATURAL ROCKS

Natural rocks are heterogeneous materials, which show considerable complexity with respect to their electrical and magnetic properties. In general, a rock is a multicrystalline matrix, comprising a large density of surface contacts between different materials, elements and solutions. The evolving theories of solid state physics can essentially describe the electrical and magnetic phenomena which arise on the microscopic surfaces and within microscopic volumes of rocks. The macroscopic properties of a composite material, containing phases with very different physical properties, depend not only on the volume fractions of the constituents, but are extremely sensitive to the geometry and topology of the boundary surfaces between the phases. Nevertheless rocks typically show some **"mean"** macroscopic behavior. Geophysically our interest is with the macroscopic measures and therefore, for convenience, in the development of this work we shall describe the electrical and magnetic behavior of an equivalent homogeneous medium, which is conductive permittive and permeable.

The magnetic permeability of general rock types does not differ much from that of free space, except for the common naturally occuring "magnetic" materials. At zero frequency, and under low inducing fields, the magnetization is essentially directly proportional to the magnitude of the inducing field. That is, we may employ a real valued constant of proportionality, the magnetic susceptibility, to describe the field-magnetization relationship. At low frequencies the magnetization of most materials closely follows the alternating field (that is, remains in phase with the alternating field) but as frequency increases the field oscillations become too rapid for the molecular and grain boundary adjustments to be maintained in equilibrium with the applied field so that the magnetization becomes phase-delayed in reference to this field. At even higher frequencies (typically beyond 10 KHz, except in the narrow-bands of nuclear and electronic resonances) the induced magnetization of macroscopic volumes of real materials essentially vanishes (Landau and Lifshitz, 1960). Since we are here dealing mainly with very high frequency electromagnetic (VHF-EM) fields, the magnetic effects are generally insignificant, and we shall reasonably assume rock permeabilities equivalent to the permeability of free space μ_o.

A similar situation holds for the dielectric polarization of rocks, although the analogous phenomena typically arise at much higher frequencies (Debye, 1929). At low frequencies, the dielectric polarization easily follows an alternating

inducing electric field. The electrical susceptibility, which is the constant of proportionality relating the electric polarization to the inducing field, is essentially real valued and therefore no power loss occurs. At extremely high frequencies, in the microwave and infrared band, the field alternates so quickly that electrical polarization cannot become established and only a small residual level of polarization remains. This results in most materials showing a minimum in dielectric permittivity at sufficiently high frequencies. This residual permittivity will approach that of free space for non-polar molecules, while for substances like water, alcohol and barium titanite, which are molecules possessing a natural permanent electric dipole moment due to the asymmetry of their electrical charge distribution, the residual permittivity will exceed that of free space.

Conductivity of physical materials can show a relatively complex frequency dependence. As well, the range of real conductivities of common materials is extremely wide: from the order of 10^{-15} S/m for quartz and mica to the order of 10^{9} S/m for silver, gold and copper. At extremely low temperatures, some metals and alloys posses a practically infinite superconductivity (e.g. lead below 7.2°K). In such metals the current continues to flow without measurable dissipation even after the electric field has been removed.

Often, the conductive properties of rock masses dominate all other effects at frequencies in the submicrowave range.

However, in the infrared to X-ray frequency range, conductivity can show a considerable complexity of frequency dependence. Our interest in these frequency-dependent electrical and magnetic material properties will not concern the various strongly resonant phenomena such as nuclear magnetic resonances.

1.3 OUTLINE

In chapter II, we define the essential electromagnetic fields and in restricting their description impose linearity, isotropy and homogeneity conditions on the geophysical media. Constitutive equations and Ohm's law are then stated both in the time and frequency domains. We shall require realizability (i.e. we require that the phenomena be causal and stable), a condition which leads to Hilbert transform restrictions. Maxwell's equations and charge continuity equation follow, from which we deduce the wave equation for the E- and H-field and derive the general equation of the propagation constant and wave impedance for far fields. Also, propagation depth and apparent resistivity as functions of frequency and average material properties are obtained. For near field, we shall consider potential functions described in terms of Hertz vector from which, by appropriate differentiation, the E- and H-field, and consequently all other electromagnetic fields, can be described.

In Chapter III, common dielectric phenomena and dielectric hysterisis are described followed by Debye's "Polar Molecules" description in introduction to the Cole-Cole model which has been adopted as the basic dielectric dispersion model in this research. After the description of each dielectric model in the frequency domain, its time domain equivalent is obtained via Fourier transformation. The Cole-Davidson dielectric dispersion model is compared to the Cole-Cole model; the Maxwell-Wagner effect is discused.

The final section of Chapter III deals with conductivity, its temperature dependence and time and frequency domain relationships. The Cole-Cole resistivity model which is now commonly used in geophysical analysis of high-frequency resistivity and induced polarization data is described; the Cole-Davidson resistivity model which describes the membrane polarization effect is also discussed.

Chapter IV describes the general equations of apparent dielectric permittivity and resistivity and from these equations deduces the several limiting cases which are commonly used in geophysical theory. Example inversions of actual resistivity data are attempted to obtain estimates of the essential Cole-Cole parameters of the geophysical media. The general equation of the "formation factor", taking into account complex resistivity and permittivity properties, is then obtained and subsequently reduced to the equation commonly employed in geophysical electromagnetic theory. The effect of

porosity, water content and salinity are discussed and examples and references are given. Finally, practical measurements are compared to the elaborated theory.

Chapter V essentially deals with alternating current sounding for simple configurations of antennas. The objective is to study the variation of the electric and magnetic fields with depth, height and particularly frequency. First the E- and H-field equations are developed for vertical and horizontal dipoles, in terms of the Hertz vector, then profiles for different varying parameters are calculated, considering Cole-Cole parameters.

Chapter VI comprises the conclusion and further suggestions for study.

CHAPTER II

THE GENERALIZED MATERIAL PROPERTIES RELATING THE VECTOR FIELD QUANTITIES OF ELECTRICITY AND MAGNETISM.

2.1.1 VECTOR FIELD QUANTITIES

The essential vector measures which represent an electrical and magnetic field, are $\vec{D}$, the electric displacement (C/m^2), $\vec{E}$, the electric field (V/m), $\vec{J}$, the electric current density (Amp/m^2), which are primarely of electric nature, and $\vec{H}$, the magnetic field (Amp/m) and $\vec{B}$, the magnetic induction (Teslas) which are of magnetic nature. These vector quantities are interrelated by Maxwell's equations, the equation of charge continuity, the constitutive relationships, and Ohm's law.

In free space, the constitutive relationships and Ohm's law describe linear functional dependencies between the $\vec{D}$ & $\vec{E}$, $\vec{B}$ & $\vec{H}$, $\vec{J}$ & $\vec{E}$ vector fields pairs respectively.

$D=\epsilon_o E$ $\quad \epsilon_o=8.854*10^{-12}$ Farads/m 2-1-1

$B=\mu_o H$ $\quad \mu_o=4\pi*10^{-7}$ Henry/m 2-1-2

$J=\sigma_o E$ $\quad \sigma_o=0.0$ S/m for free space 2-1-3

In real materials, the generalization of these relationships can give rise to a need for much more complex mathematical formalisms. In any real material, we may

establish these relationships using the general functional forms:

$$D=f(\mathcal{E},E)\,, \qquad 2\text{-}1\text{-}4$$

$$B=f(\mathcal{M},H)\,, \qquad 2\text{-}1\text{-}5$$

$$J=f(\mathcal{Z},E)\,. \qquad 2\text{-}1\text{-}6$$

Where the $\mathcal{E}$, $\mathcal{M}$ and $\mathcal{Z}$ represent a location dependent complex series of tensor coefficients which may be involved in a nonlinear way with the vectors.

2.1.2 LINEARITY AND ISOTROPY

For real materials, in the presence of sufficiently small E- and H-fields these relationships can normally be assumed to be locally represented by linear, homogeneous functions,

$$D=\mathcal{E}.E\,, \qquad 2\text{-}1\text{-}7$$

$$B=\mathcal{M}.H \qquad 2\text{-}1\text{-}8$$

and

$$J=\mathcal{Z}.E \qquad 2\text{-}1\text{-}9$$

where $\mathcal{E}$, $\mathcal{M}$ and $\mathcal{Z}$ can be either scalar or second-rank tensor quantities describing the essential material properties.

In an anisotropic (but linearly homogeneous) medium, each component of the resulting field depends upon all components of

the applied field and the material constants (i.e. the ϵ, γ, σ) must have a general tensor form. Then, the individual components of the vector quantities can be related by the tensor equations:

$$D_i = \epsilon_{ij} E_j, \qquad 2\text{-}1\text{-}10$$

$$B_i = \gamma_{ij} H_j \qquad 2\text{-}1\text{-}11$$

and

$$J_i = \sigma_{ij} E_j. \qquad 2\text{-}1\text{-}12$$

where, now, each material constant is described by a second rank tensor. For example

$$\Sigma = \begin{pmatrix} \sigma_{11} & \sigma_{12} & \sigma_{13} \\ \sigma_{21} & \sigma_{22} & \sigma_{23} \\ \sigma_{31} & \sigma_{32} & \sigma_{33} \end{pmatrix} = \sigma_{ij} \qquad 2\text{-}1\text{-}13$$

where

i,j=1,2,3 represent three orthogonal spatial coordinates.

Similarly

$$E = \epsilon_{ij}$$

and

$$\mathcal{M} = \gamma_{ij}$$

Equation 2-1-13 shows that 9 coefficients are required to define the property of conductivity at any point. Commonly, however, $\sigma_{ij} = \sigma_{ji}$, and this symmetric conductivity tensor contains only 6 independent elements. It is further possible to adjust the coordinates in such manner that $\sigma_{ik}=0$ if $i \neq k$ so that

$$\sigma_{ij} = \begin{pmatrix} \sigma_{11} & 0 & 0 \\ 0 & \sigma_{22} & 0 \\ 0 & 0 & \sigma_{33} \end{pmatrix} \qquad 2\text{-}1\text{-}14$$

reduces to a diagonal tensor. If any two elements of this tensor are equal, the medium is uniaxially anisotropic. For isotropic media all three coefficients are equal and the tensor relationships reduce to scalar ones (i.e. a zero rank tensor). Then, Ohm's law reduces to its common form,

$$J = \sigma . E \qquad 2\text{-}1\text{-}15a$$

and the constitutive equations simplify:

$$D = \epsilon . E, \qquad 2\text{-}1\text{-}16a$$

$$B = \mu . H. \qquad 2\text{-}1\text{-}17a$$

These scalar constants are

ϵ , the dielectric permittivity measured in $F.m^{-1}$,

μ , the magnetic permeability measured in $H.m^{-1}$ and

σ , the electric conductivity measured in $S.m^{-1}$.

These much simplified relationships hold at any point within linear and isotropic materials; they also hold everywhere within materials which are homogeneous.

2.1.3 HARMONIC COMPONENTS OF THE VECTOR FIELDS.

Commonly in the development of the physical theory of electromagnetism, we implicitly consider harmonic components of the field quantities. The constitutive equations and Ohm's law

can be more explicitly written in the following form:

$$\vec{D}(\omega) = \epsilon(\omega).\vec{E}(\omega)\,, \qquad 2\text{-}1\text{-}18$$

$$\vec{B}(\omega) = \mu(\omega).\vec{H}(\omega) \qquad 2\text{-}1\text{-}19$$

and

$$\vec{J}(\omega) = \sigma(\omega).\vec{E}(\omega)\,. \qquad 2\text{-}1\text{-}20$$

These equations are analogous to the input-output relations describing linear systems in which the material property (i.e. the $\epsilon(\omega)$, $\mu(\omega)$ and $\sigma(\omega)$) corresponds to the system transfer function, and the vector field quantities correspond to the input-output pairs (Fuller and Ward, 1970). Equivalently then, in the **"time domain"** of the real world of measurements, these relationships are represented by the convolutional forms:

$$\vec{d}(t) = e(t) * \vec{e}(t)\,, \qquad 2\text{-}1\text{-}21$$

$$\vec{b}(t) = m(t) * \vec{h}(t) \qquad 2\text{-}1\text{-}22$$

and

$$\vec{j}(t) = A(t) * \vec{e}(t)\,. \qquad 2\text{-}1\text{-}23$$

Here the symbolic notation * represents the general superpositon integral; for example:

$$\vec{j}(t) = \int_{-\infty}^{\infty} A(\tau).e(t-\tau)\ d\tau \qquad 2\text{-}1\text{-}24a$$

or equivalently

$$\vec{j}(t) = \int_{-\infty}^{\infty} A(t-\tau).e(\tau)\ d\tau\,. \qquad 2\text{-}1\text{-}24b$$

[Note: Unless otherwise indicated, throughout this thesis, upper-case Latin and Greek symbols apply to the frequency domain and their lower-case equivalents to the time domain. However, in order to minimize the confusion of the reader who has typically learned his electromagnetic formalism in the frequency domain, we shall maintain the symbols σ, ρ, ϵ and φ to describe the frequency-domain material properties and use s, r, e and m for their time-domain equivalents.]

Only in the particular case where the material property is independent of the frequency is its Fourier transform of the time function a scaled Dirac function, and consequently in this case the time-domain convolution can be replaced by the simple multiplication by the scaled conductivity permittivity or permeability. This simple case is not of basic interest in the subsequent development of this thesis.

In the real world, measurements are made in time domain, but mathematical manipulation in this domain is often cumbersome, especially when dealing with inversion and interpretation of geophysical data. Frequency domain mathematical manipulations are usually much easier, even though the material properties must be then represented by complex-valued functions of frequency. Throughout this thesis, we will be concerned with the parallel formulation of the required electromagnetic equations in both the frequency and time domains.

The Fourier transform relates the frequency and time

representations of the electrical or magnetic vector field quantities or material properties as follows:

$$\vec{X}(\omega) = \frac{1}{2\pi}\int_{-\infty}^{\infty} \vec{x}(t) \cdot e^{-i\omega t}\, dt \qquad 2\text{-}1\text{-}25$$

and

$$\vec{x}(t) = \int_{-\infty}^{\infty} \vec{X}(\omega) \cdot e^{+i\omega t}\, d\omega \qquad 2\text{-}1\text{-}26$$

where $\vec{x}(t)$ and $\vec{X}(\omega)$ represent any of these quantities in each of the two domains. For example;

1- If the time domain E-field is a scaled impulse function

$$E(t=\emptyset) = E_o\, \delta(t) \qquad 2\text{-}1\text{-}27a$$

then the frequency domain E-field will be frequency independent and

$$E(\omega) = E_o \ . \qquad 2\text{-}1\text{-}27b$$

2- If

$$E(t) = E_o \cdot e^{i\omega_o t} \qquad 2\text{-}1\text{-}28a$$

where ω_o is the angular frequency of a continuous wave oscillation, then

$$\vec{E}(\omega) = E_o \cdot 2\pi\delta\,(\omega - \omega_o) \ . \qquad 2\text{-}1\text{-}28b$$

Generally in the following development of this thesis, we shall omit the factor $e^{i\omega_o t}$ when describing harmonic electromagnetic waves and fields in the time domain. Equivalently, we shall often omit the factor $\delta(t)$ when describing essentially temporally impulsive fields in the Fourier frequency domain.

2.1.4 REALIZABILITY, REALITY AND THE HILBERT TRANSFORM

The functional representation of the properties of real materials must be **"realizable"**. That is the quantities $e(t)$, $m(t)$ and $\mathcal{A}(t)$ must be both causal and stable, for if they were acausal they would violate what appears to be nature's most basic law that a response must follow the excitation and if they were unstable, they would violate the law of energy conservation. Furthermore, in 2-1-21 both e(t) and d(t) must be real-valued (Fuller and Ward, 1970); this requires that $e(t)$ be real-valued. Mathematically, we can establish the causality and reality conditions by requiring that:

$$e(t),\ m(t),\ \mathcal{A}(t) = \begin{cases} 0 \text{ for } t<0 \\ \text{real for } t>0 \end{cases} \qquad 2\text{-}1\text{-}29$$

and we can establish the stability condition by requiring that

$$\int_0^\infty e^2(t)\,dt < \infty \qquad 2\text{-}1\text{-}30$$

which implies that

$$\int_0^\infty |e(t)|\ dt < \infty \qquad 2\text{-}1\text{-}31$$

which guarantees that the Fourier transform of $e(t)$ is everywhere finite.

The Fourier transform pair representing the dielectric permittivity property must have the form:

$$\epsilon(\omega) = \frac{1}{2\pi}\int_0^\infty e(t)\ e^{-i\omega t}\ dt \qquad 2\text{-}1\text{-}32$$

$$e(t) = \int \epsilon(\omega)\ e^{+i\omega t}\ d\omega\ . \qquad 2\text{-}1\text{-}33$$

Since the time domain material functions are properly causal and real valued, the corresponding frequency domain functions $\epsilon(\omega)$, $\mu(\omega)$ and $\sigma(\omega)$ must be complex-valued. The complex nature of these material functions allows that the related vector field quantities need not be exactly in phase with each other. The reality of the time-domain function implies further conditions: the real part of $\epsilon(\omega)$ (also $\mu(\omega)$ and $\sigma(\omega)$) must be an even function of frequency while the imaginary part must be an odd function of frequency. Furthermore, for a system to be physically realizable implies a well-known relationship between the real and imaginary parts of its frequency domain functional representation which is described by the **"Hilbert Transform"**.

Given

$$R(i\omega) = P(\omega) + iQ(\omega) = A(\omega)\ e^{\,i\phi(\omega)} \qquad 2\text{-}1\text{-}34$$

the Fourier transform of a causal temporal function r(t), $P(\omega)$ and $Q(\omega)$ must be Hilbert transform pairs. That is

$$P(\omega) = \frac{1}{2\pi}\int_{-\infty}^{\infty} Q(u)/(\omega - u)\ du \qquad 2\text{-}1\text{-}35$$

$$Q(\omega) = \int_{-\infty}^{\infty} P(u)/(\omega - u)\ du. \qquad 2\text{-}1\text{-}36$$

Furthermore if

$$R(\omega) = A(\omega).e^{i\,\phi\ (\omega)} \qquad 2\text{-}1\text{-}37$$

obeys the stronger condition of minimum phase (Ulrych & Lasserre, 1966), then the real and imaginary principal components of the logarithm of $R(\omega)$ are also Hilbert transform pairs. That is

$$\ln A(\omega) = \frac{1}{2\pi} \int_{-\infty}^{\infty} \phi(u)/(\omega-u)\, du \qquad 2\text{-}1\text{-}38$$

$$\phi(\omega) = \int_{-\infty}^{\infty} \ln A(\omega)/(\omega-u)\, du \qquad 2\text{-}1\text{-}39$$

It appears to be a natural law that simple passive systems are **"minimum phase"**. This property is manifest in the time domain response of a system as its ability to pass energy from input to output as rapidly as possible given that it modifies signal frequency composition.

2.2.1 SOME ELEMENTARY ELECTROMAGNETIC THEORY.

Maxwell's field equations, shown here in time domain, are as follows:

Ampere's law $$\nabla \times \vec{h}(t) = \vec{j}(t) + \frac{\partial}{\partial t}\vec{d}(t), \qquad 2\text{-}2\text{-}1$$

Faraday's law $$\nabla \times \vec{e}(t) = -\frac{\partial}{\partial t}\vec{b}(t), \qquad 2\text{-}2\text{-}2$$

Coulomb's law $$\nabla \cdot \vec{d}(t) = \rho(t) \qquad 2\text{-}2\text{-}3a$$

and

$$\nabla \cdot \vec{b}(t) = \emptyset. \qquad 2\text{-}2\text{-}4$$

In a homogeneous isotropic medium equation 2-2-3a reduces to

obeys the stronger condition of minimum phase (Ulrych & Lasserre, 1966), then the real and imaginary principal components of the logarithm of $R(\omega)$ are also Hilbert transform pairs. That is

$$\ln A(\omega) = \frac{1}{2\pi} \int_{-\infty}^{\infty} \phi(u)/(\omega-u)\, du \qquad 2\text{-}1\text{-}38$$

$$\phi(\omega) = \int_{-\infty}^{\infty} \ln A(\omega)/(\omega-u)\, du \qquad 2\text{-}1\text{-}39$$

It appears to be a natural law that simple passive systems are **"minimum phase"**. This property is manifest in the time domain response of a system as its ability to pass energy from input to output as rapidly as possible given that it modifies signal frequency composition.

2.2.1 SOME ELEMENTARY ELECTROMAGNETIC THEORY.

Maxwell's field equations, shown here in time domain, are as follows:

Ampere's law $$\nabla \times \vec{h}(t) = \vec{j}(t) + \frac{\partial}{\partial t}\vec{d}(t), \qquad 2\text{-}2\text{-}1$$

Faraday's law $$\nabla \times \vec{e}(t) = -\frac{\partial}{\partial t}\vec{b}(t), \qquad 2\text{-}2\text{-}2$$

Coulomb's law $$\nabla \cdot \vec{d}(t) = \rho(t) \qquad 2\text{-}2\text{-}3a$$

and

$$\nabla \cdot \vec{b}(t) = \emptyset. \qquad 2\text{-}2\text{-}4$$

In a homogeneous isotropic medium equation 2-2-3a reduces to

$$\nabla \cdot \vec{d}(t) = \emptyset \ . \qquad 2\text{-}2\text{-}3b$$

In equation 2-2-1, noting the analogy between the current density $\vec{j}$ and and the field quantity $\frac{\partial \vec{d}}{\partial t}$, this latter term is called the displacement current density. Depending on whether $\frac{\partial \vec{d}}{\partial t}$ or $\vec{j}$ dominates, the material will be essentially either a dielectric or a conductor.

The charge continuity equation

$$\nabla \cdot \vec{j}(t) + \frac{\partial \rho(t)}{\partial t} = \emptyset \qquad 2\text{-}2\text{-}5a$$

completes Maxwell's four equations in generally describing electricity and magnetism. In any region of non-vanishing conductivity, the charge density will reach its equilibrium very quickly, so that there will usually be no accumulation of charge during the flow of current and

$$\nabla \cdot \vec{j}(t) = \emptyset \ . \qquad 2\text{-}2\text{-}5b$$

Maxwell's equations show that electromagnetic fields should be capable of propagation through space as waves.

Fourier transformation of equations 2-2-1 and 2-2-2 obtains

$$\nabla \times \vec{H}(\omega) = \vec{J}(\omega) + i\omega\vec{D}(\omega) \qquad 2\text{-}2\text{-}6$$

and

$$\nabla \times \vec{E}(\omega) = -i\omega\vec{B}(\omega) \ . \qquad 2\text{-}2\text{-}7$$

Often, in geophysical electrimagnetic theory, the term $\omega\vec{D}(\omega)$ in equation 2-2-6 is neglected for low frequencies; however, as we increase frequency we may reach a condition where $\omega\vec{D}(\omega)$

we increase frequency we may reach a condition where $\omega\vec{D}(\omega)$ becomes comparable in magnitude with $\vec{J}(\omega)$.

Introducing the equivalent Fourier transformations of the constitutive equations and Ohm's law into equations 2-2-6 and 2-2-7 we obtain:

$$\nabla x\vec{H}(\omega) = (\sigma(\omega)+i\omega\epsilon(\omega)) \vec{E}(\omega) \qquad 2\text{-}2\text{-}8$$

and

$$\nabla x\vec{E}(\omega) = -i \mu(\omega) \vec{H}(\omega) . \qquad 2\text{-}2\text{-}9$$

These two equations can be reformed as wave equations in $\vec{E}(\omega)$ and $\vec{H}(\omega)$.

2.2.2 THE ELECTROMAGNETIC WAVE EQUATION

In a general linear homogeneous isotropic material characterized by complex valued frequency-dependent parameters σ, ϵ, and μ we can derive the relationships governing the propagation of electromagnetic fields. Replacing 2-2-9 in 2-2-8 and using the identity

$$\nabla x\nabla x\vec{A} = \nabla(\nabla .\vec{A}) - \nabla \vec{A} \qquad 2\text{-}2\text{-}1\emptyset$$

we find that

$$\nabla^2\vec{E}(\omega) = i\omega \mu(\omega) [\sigma(\omega)+i\omega\epsilon(\omega)] \vec{E}(\omega) , \qquad 2\text{-}2\text{-}11$$

and equivalently we obtain a complimentary equation in $\vec{H}(\omega)$

$$\nabla^2\vec{H}(\omega) = i\omega \mu(\omega) [\sigma(\omega)+i\omega \epsilon(\omega)]\vec{H}(\omega) . \qquad 2\text{-}2\text{-}12$$

If we further recognize that

$$k^2 = -i\omega\mu\ (\ \sigma + i\omega\epsilon\ ) \qquad 2\text{-}2\text{-}13$$

is the squared wavenumber for waves propagating within the material, we can rewrite equations 2-2-12 & 2-2-13 as follows:

$$\nabla_r^2 E(\omega) + k^2\ E(\omega) = \emptyset \qquad 2\text{-}2\text{-}14a$$

and

$$\nabla_r^2 H(\omega) + k^2\ H(\omega) = \emptyset\ . \qquad 2\text{-}2\text{-}14b$$

where r is the position vector, measured from any arbitrarily chosen origin for a coordinate system. Equations 2-2-14a and 2-2-14b describe waves propagating through an absorbing medium. The general solution of the wave equation for $\vec{E}$ in Cartesian coordinates, restricting our immediate interest to plane waves:

$$E(\omega,r) = E_o\ e^{i(\pm k.r \pm \omega t)} \qquad 2\text{-}2\text{-}15$$

where E_o is independent of frequency and position and using Cartesian coordinates,

$$k.r = ux+vy+wz$$

so that the propagation vector,

$$k = \sqrt{u^2+v^2+w^2}$$

and

$$r = \sqrt{x^2+y^2+z^2}.$$

2.2.3 THE PROPAGATION CONSTANT AND LOSS TANGENT

Equation 2-2-13 shows that the magnitude of the propagation constant must be generally complex-valued

$$k = \alpha - i\beta \quad . \qquad 2\text{-}2\text{-}16$$

Rearranging equation 2-2-13

$$k^2 = -i\omega\mu_e(\sigma_e + i\omega\epsilon_e)$$

where now μ_e, σ_e and ϵ_e are real values, then (compare Crossley (1982)):

$$\alpha = \left(\frac{\omega\mu\sigma_e}{2}\right)^{1/2} \left[(1+\nu^2)^{1/2} + \nu \right]^{1/2} \qquad 2\text{-}2\text{-}17$$

and

$$\beta = \left(\frac{\omega\mu\sigma_e}{2}\right)^{1/2} \left[(1+\nu^2)^{1/2} - \nu \right]^{1/2} \qquad 2\text{-}2\text{-}18$$

where

$$\nu = \omega\epsilon_e/\sigma_e \qquad 2\text{-}2\text{-}19$$

The ratio of imaginary to real components of k^2

$$\tan\delta = \nu = \omega\epsilon_e/\sigma_e \qquad 2\text{-}2\text{-}20$$

is called the loss tangent. Below the critical frequency where $\tan\delta = 1$, the propagation vector depends more upon effective material conductivity than its dielectric conductivity. Above this frequency, the effect of material permittivity dominates. Typically at frequencies for which $\tan\delta << 1$, we may neglect

the presence of a material dielectric permittivity while for frequencies for which $\tan\delta >> 1$, the permittivity dominates the conductivity. This critical frequency is of the order of 10^4 Hz for quartz and gneiss and 10^5 Hz for granite and gabbros.

2.2.4 WAVE IMPEDANCE

A particular situation arises when we have a homogeneous half space and a harmonic current flows along the x-axis. Thus the E-field components vanish along the y-axis and z-axis and,

$$E_x = Ae^{-ikz+i\omega t} = A\, e^{-\beta z}\, e^{+i(\omega t - \alpha z)} \qquad 2\text{-}2\text{-}20$$

where the $e^{-\beta z}$ term represents a damping term and $e^{i\alpha z}$ is the phasor. Here E_x is time varying and generates a time variant orthogonal magnetic field in the y direction.

$$H_y = k/\omega\mu\ A\ e^{-ikz+i\omega t} \qquad 2\text{-}2\text{-}21$$

The surface wave impedance of the homegeneous ground, defined as the ratio E_x/H_y and denoted by Z has SI-dimensions of ohms.

$$Z = H_y/E_x = k/\omega\mu = \left(\frac{\sigma + i\omega\epsilon}{i\omega\mu}\right)^{1/2} \qquad 2\text{-}2\text{-}22$$

In free space where $\sigma = 0$ $\mu = \mu_o$ and $\epsilon = \epsilon_o$, the wave impedance is simply real-valued;

$$Z = \sqrt{\epsilon_o/\mu_o} = 120\pi \quad \text{ohms.}$$

2.2.5 DEPTH OF PENETRATION OF VHF EM-WAVES

In the conventional solution for the skin depth of electromagnetic fields, which is generally valid at low frequencies, the depth of penetration is obtained as:

$$\delta = \left(\frac{2}{\sigma\mu\omega}\right)^{1/2} \qquad 2\text{-}2\text{-}23$$

Using this equation at very high frequencies predicts very small values of δ in the frequency range of our interest. The electromagnetic theory however does not justify this simple form for higher frequencies. Starting with the general equation for the propagation constant;

$$k = \left[\omega^2\mu\epsilon_e - i\omega\mu\sigma_e\right]^{1/2} \quad , \qquad 2\text{-}2\text{-}24$$

the depth of penetration (i.e. that depth at which the amplitude of the field component has decayed to 1/e of its original value) becomes

$$\delta = \left[\left(\frac{2\epsilon_e}{\sigma_e^2\mu}\right)\left[\left(1+\left(\frac{\sigma_e}{\omega\epsilon_e}\right)^2\right)^{-1/2}+1\right]\right]^{1/2} \qquad 2\text{-}2\text{-}25$$

and, since σ_e & ϵ_e are functions of the frequency, the penetration depth is not simply dependent on either parameter.

In soft rocks such as limestone and dolomite, a pulse radar has detected lithological contrasts at a depth beyond 12 m. This is not yet the upper limit of these systems: Moffat & Puskar (1976) estimated a penetration in these rocks of around 16m.(50 ft.). For hard rocks, considering the

differences in their electrical properties, it is estimated that the depth of penetration should be greater than that of soft rocks by at least a factor of 4. Reflections from voids have been detectable at 16.4 m. in the frequency range of 10 to 160 MHz. Coon et al. (1981) estimated the depth of penetration of 20-500 MHz to 33 m(100 ft) through coal seams. In addition, the EM energy polarized normal to the bedding planes is less attenuated than energy polarized parallel to the bedding planes. Lafleche (1984) has obtained penetrations beyond 50 m. at 445 Mhz in the Big Nickel Mine, Sudbury, Ontario.

2.2.6 APPARENT RESISTIVITY

From equation 2-2-22 we obtain the absolute ratio

$$\left|\frac{E_x}{H_y}\right|^2 = \frac{\omega\mu}{\sigma_e}\left[1+\nu^2\right]^{-1/2} \qquad 2\text{-}2\text{-}26$$

At low frequencies, is neglected and if we write

$$\rho_{app} = \frac{1}{\sigma_e}$$

we obtain

$$\rho_{app} = \frac{1}{\omega\mu}\left|\frac{E_x}{H_y}\right|^2 \qquad 2\text{-}2\text{-}27$$

However if the medium is dielectric or if we increase the frequency, ν can not be neglected and

$$\rho_{app} = \frac{1}{\omega\mu}\left|\frac{E_x}{H_y}\right|^2\left[1-\left(\frac{\epsilon_e}{\mu}\right)^2\left|\frac{E_x}{H_y}\right|^4\right]^{-1/2} \qquad 2\text{-}2\text{-}29$$

where now the equation also depends upon the dielectric property of the medium. The apparent resistivity values will be larger than those estimated under the low frequency assumption.

2.2.7 POTENTIAL FUNCTIONS AND THE HERTZ VECTOR

Often in solving problems in electromagnetics, potential functions are introduced (Sommerfeld 1949, Patra and Mallick 1980). The fields are then derived by differentiation of these potential functions. Since $\vec{B}$ is necessarily solenoidal, it can be expressed in terms of another vector $\vec{A}$ so that

$$\vec{B} = \nabla \times \vec{A} \qquad 2\text{-}2\text{-}30$$

and

$$\nabla \times (\vec{E} + i\omega\vec{A}) = 0; \qquad 2\text{-}2\text{-}31$$

therefore $(\vec{E} + i\omega\vec{A})$ is irrotational, and consequently

$$\vec{E} + i\omega\vec{A} = -\nabla\vec{\Phi} \qquad 2\text{-}2\text{-}32$$

where Φ is a scalar function.

The functions $\vec{A}$ & Φ are known as the vector & scalar potentials. Introducing the Lorentz restriction,

$$\nabla \cdot \vec{A} + i\omega^2\mu\epsilon\Phi + \mu\sigma\Phi = 0 \quad ,$$

both functions must obey wave equations, similar to those of the E- & H-fields as above.

Hertz has shown that electromagnetic fields can be expressed in terms of a single vector function $\vec{\Pi}$. If we set:

$$\vec{A} = \mu\omega(\nabla + i\omega\epsilon)\vec{\Pi} \qquad 2\text{-}2\text{-}33$$

this equation satisfies Lorentz' restriction so that

$$\vec{\Phi} = -\nabla\cdot\vec{\Pi}. \qquad 2\text{-}2\text{-}34$$

Substituting 2-2-33 & 2-2-34 into 2-2-32 we find

$$\vec{E} = \nabla\times\nabla\times\vec{\Pi} \qquad 2\text{-}2\text{-}35$$

or

$$\vec{E} = \nabla(\nabla\cdot\vec{\Pi}) + k^2\vec{\Pi} \qquad 2\text{-}2\text{-}36$$

and similarly

$$\vec{H} = -\frac{k^2}{i\omega\mu}\ \nabla\times\vec{\Pi} \qquad 2\text{-}2\text{-}37$$

Equation 2-2-35 & 2-2-37 are the general equations of electric and magnetic fields in terms of the Hertz vector. Hence, once $\vec{\Pi}$ is known, the resulting fields can be derived directly. Sommerfeld (1949) has treated this subject in detail.

In electrodynamics the Hertz vector potential $\vec{\Pi}$ replaces the scalar potential of electrostatics. The $\vec{E}$ and $\vec{H}$ fields, and the related $\vec{B}$ and $\vec{D}$, as well as J fields can be all expressed in terms of $\vec{\Pi}$. This Hertz vector potential can be shown to obey the wave equation itself,

$$(\nabla^2 + k^2)\vec{\Pi}(\omega) = 0 \qquad 2\text{-}2\text{-}38$$

and its Fourier transform is:

$$\vec{\pi}(t) = \int_{-\infty}^{\infty} \vec{J}(\omega)\, e^{i\omega t}\, d\omega \,. \qquad 2\text{-}2\text{-}39$$

CHAPTER III

ELECTRICAL AND MAGNETIC PROPERTIES OF ROCKS

3.1.1 DIELECTRIC PHENOMENA

Dielectric materials are good insulators; they are composed of molecules with bound charges, which when placed in an electric field E, become di-polarized in the direction of the applied external field. This resulting polarization accounts for their refractive indices being different from those of free space. At sufficiently low field, the polarization is linear in the applied field as follows:

$$\vec{P} = \propto \vec{E} \qquad 3\text{-}1\text{-}1$$

where

$$\propto = \epsilon_o \chi_e \qquad 3\text{-}1\text{-}2$$

$\propto$ = polarizability ($F.m^{-1}$)

ϵ_o = dielectric permittivity of free space ($F.m^{-1}$)

χ_e = dielectric susceptibility (dimensionless)

A measure called electric displacement, $\vec{D}$, is due to both the polarization of the bound charges, $\vec{P}$, and to the applied external field, $\vec{E}$.

$$\vec{D} = \epsilon_o \vec{E} + \vec{P} \qquad 3\text{-}1\text{-}3$$

or

$$\vec{D} = \epsilon \vec{E} \qquad 3\text{-}1\text{-}4$$

where

$$\epsilon = \epsilon_o(1+\chi_e) . \qquad 3\text{-}1\text{-}5$$

ϵ is the factor of proportionality between the external electric field $\vec{E}$ and the resulting electric displacement $\vec{D}$ in a dielectric, and is known as the dielectric permittivity.

In the simplest case, ϵ is considered to be a scalar constant, independent of all other physical parameters and coordinates. For free space (and approximately for air):

$$\chi_e = \emptyset ,$$

$$\epsilon = \epsilon_o$$

and

$$\vec{D} = \epsilon_o \vec{E} . \qquad 3\text{-}1\text{-}6$$

For real materials, the dielectric permittivity is often much more complex and in general ϵ is a complex tensor, function of frequency (ω), temperature (T) and location (r). It is also known to be pressure, porosity, salinity and grain size dependent. For the moment, we will consider ϵ as being a complex frequency dependent scalar quantity describing the dielectric condition of a homogeneous medium thus:

$$\epsilon = \epsilon^*(\omega) \qquad 3\text{-}1\text{-}7$$

where

$$\epsilon^* = \epsilon' - i\epsilon'' \qquad 3\text{-}1\text{-}8$$

The choice of sign is arbitrary; here, the sign is chosen so that $\epsilon'' > 0$. The negative sign indicates that the phase of the imaginary component lags that of the real component. The complex nature of ϵ^* requires that within the material, under the application of an external alternating field, there is energy dissipation. Table 1 (from Poley et al., 1978) shows some measures of complex ϵ^* .

In most dielectric materials the displacement of charges is proportional to the applied electric field E. However in some materials like Rochelle Salt [orthorombic hemihedral-holoaxial crystalline structure, chemical composition; $(K,NH_4)NaC_4H_4O_6 \cdot 4H_2)$] the dielectric displacement is not uniquely determined by the applied field, but also depends on its previous value. This phenomena is known as the "dielectric hysteresis".

3.1.2 DIELECTRIC HYSTERESIS

In the hysteresis phenomena, the displacement traces out a hysteresis loop quite similar to the magnetic hysteresis loop. By analogy to ferromagnetism is this effect is called "ferroelectricity". The hysteresis implies that the substance has a spontaneous polarization,(i.e. a polarization which persists when the applied field is removed). The susceptibility in such materials depends on the present applied field and

Table 1. (After Poley et al., 1978). Real and imaginary permittivity versus frequency.

f (Mc/s)		ϵ'	ϵ''	δ (cm)
10	measured	28	380	36
100		18	36	14.7
200		16	16	13.2
500		14	5.6	13.1
800	extrapol.	13.2	3.2	13.7
1000		13	2.6	14.4
3000		11	0.65	16.0

Penetration depth for salt-water-saturated sandstone.
(Porosity 15%, salinity 15% by weight)

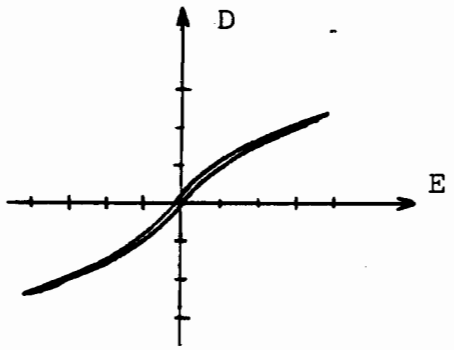

At 10°C.

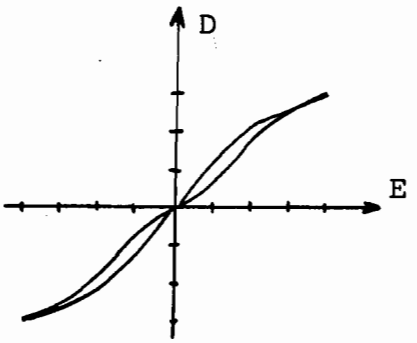

At 0°C.

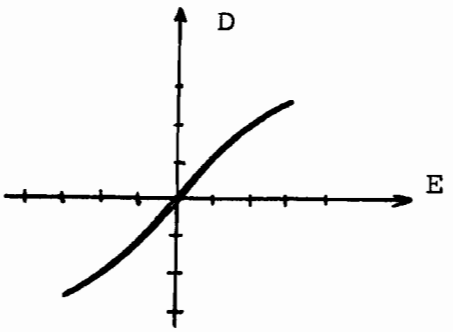

At -20°C.

Figure 1. (Reproduced from Megaw, 1957)
D-E Hysterisis loops at various temperatures, for Kh_2PO_4.

the history of previously applied fields.

Ferroelectricity is typically sensitive to temperature. In the case of Rochelle Salt, increasing temperature above $0^{o}C$ causes the hysteresis loop to decrease slightly in height, while the width undergoes a more important decrease. At around $24^{o}C$ both sides of the loop merge into one line and the salt's spontaneous polarization disappears. The temperature at which this occurs is the ferroelectric Curie point of the substance. On the other hand, by decreasing the temperature below $0^{o}C$, at some lower temperature, near $-20^{o}C$, the spontaneous polarization disappears again (see figure 1).

Other materials which show the property of dielectric hysteresis are: Potasium Hydrogen Phosphate KH_2PO_4, Barium Titanite $BaTiO_3$ and Cadmium Niobate $Cd_2Nb_2O_7$. This strongly non-linear dielectric hysteresis effect will not be considered further. I will, rather, restrict my attention to the much more common condition of linearity.

3.1.3 TEMPERATURE VARIATION

Increasing the temperature increases thermal agitation which in turn usually decreases the degree of polarization of a molecule, and hence, produces a decrease in the electric susceptibility. Later it will become clear that the parameters describing the permittivity are themselves temperature dependent. We will, at present, assume the material temperature to be a constant (see Figure 2).

3.1.4 POLAR MOLECULES

The "Polar Molecules" model was described by Debye (1929). Although now of little practical use, it was the first step in the development toward the definitive model which has been adopted in this research. The development of the Debye dispersion equation for polar molecules can be found in the literature (Debye, 1929 and Bottcher, 1952). It determines the following complex pemittivity:

$$\overset{*}{\epsilon}(\omega) - \epsilon_\infty = (\epsilon_o - \epsilon_\infty) / (1 + i\omega\tau) \qquad 3\text{-}1\text{-}9$$

where

ω = angular frequency

τ = intrinsic relaxation time which for a material of spherical polar molecules is:

$$\tau = 8\pi\eta\alpha^3/2kT \qquad 3\text{-}1\text{-}10$$

η = viscosity,

α = average radius of the molecule,

ϵ_∞ = real asymptotic value of permittivity at very high frequencies

$$\epsilon_\infty = \lim_{\omega \to \infty} \epsilon'$$

ϵ_o = real permittivity at zero frequency

$$\epsilon_o = \lim_{\omega \to o} \epsilon'$$

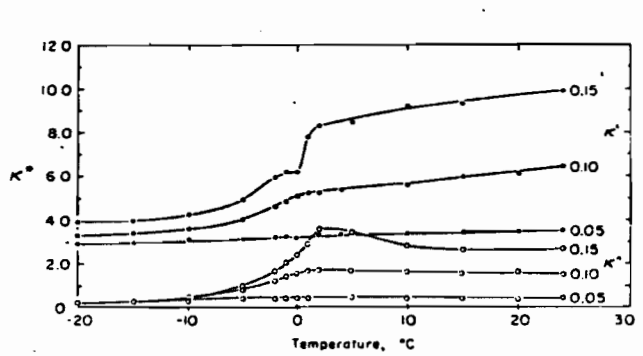

Fig. *a*.

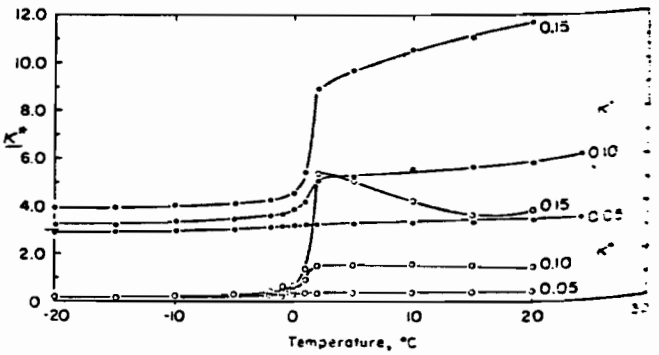

Fig. *b*.

The complex dielectric constant at 10×10^9 Hz as a function of temperature at three water contents (g H_2O/g soil) for (*a*) Goodrich clay and (*b*) Fairbanks silt.

Figure 2. (From Hoekstra and Delaney, 1974)

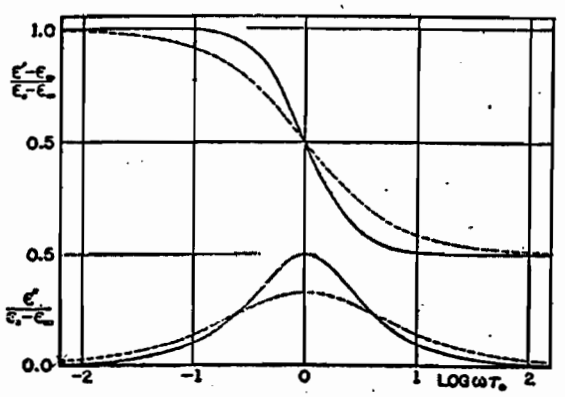

Real and imaginary parts of the dielectric constant plotted against frequency. The solid curves are for the Debye Eqs. (2), the dashed curves indicate the type of behavior frequently found experimentally.

Figure 3. (From Cole and Cole, 1941)

so that $\epsilon_o > \epsilon_\infty$.

Within the two real limits of permittivity ϵ_o and ϵ_∞, there is a range of dispersion which is characterized by an out-of-phase component of permittivity. In this transition region of dispersion, since this permittivity component is in phase with any possible real conductivity component, it is often called the absorption conductivity. This dispersion imposes a decrease on the real component of permittivity from ϵ_o to ϵ_∞.

It is worth noting the model symmetry of permittivity function of log-frequency about about $\log \omega\tau = 0$. Actually measured components also possess such symmetry. Separating the real and imaginary components in equation 3-1-9, the real component becomes:

$$\epsilon' - \epsilon_\infty = (\epsilon_o - \epsilon_\infty) / [1 + (\omega\tau)^2] \qquad 3\text{-}1\text{-}11$$

and the imaginary component,

$$\epsilon'' = (\epsilon_o - \epsilon_\infty)\, \omega\tau / [1 + (\omega\tau)^2] \,. \qquad 3\text{-}1\text{-}12$$

The phase angle of the complex-valued permittivity is:

$$\delta = \tan^{-1} \frac{\epsilon''}{\epsilon'} = \tan^{-1} \left[\frac{(\epsilon_o - \epsilon_\infty)}{(\epsilon_o \epsilon_\infty)^{1/2}} \frac{\omega\tau_x}{(1 + (\omega\tau_x)^2)} \right] \qquad 3\text{-}1\text{-}13$$

where

$$\tau_x = \left(\frac{\epsilon_\infty}{\epsilon_o}\right)^{1/2} \tau$$

Maximum loss occurs at frequency at $\omega = \frac{1}{\tau}$ where the dielectric components are

$$\epsilon' = \frac{\epsilon_0 + \epsilon_\infty}{2} \qquad 3\text{-}1\text{-}14$$

$$\epsilon'' = \frac{\epsilon_0 - \epsilon_\infty}{2} \; . \qquad 3\text{-}1\text{-}15$$

The most rapid variation of the absorption and dispersion curves occurs in the two decades of $\omega\tau$ centered about $\log \omega\tau = 0$. This range is called the dispersion range (see Figure 3).

The relaxation time τ requires further consideration. Rewriting equation 3-1-10,

$$\tau = 8\pi\eta\alpha^3/2kT \qquad 3\text{-}1\text{-}10$$

Here, η is the viscosity; one therefore should expect the range dispersion to occur at lower frequencies for more viscous liquids. These dependencies have been found in many cases (i.e. glycerine, glycols) which are extremely viscous at low temperatures. Experimentally η shows an exponential dependence of the form of $e^{B/kT}$ on temperature, thus the relaxation time τ will increase even faster with decreasing temperature since it is proportional to

$$\tau \propto e^{B/kT}/kT \; .$$

The molecular explanation of the temperature dependence is that the relative influence of the molecular interaction energy decreases with respect to that of the thermal energy when the temperature increases. The relaxation time is also proportional to the volume of the molecules, so that for larger molecules the dispersion occurs at lower frequencies. In addi-

tion to τ, ϵ_o also decreases with temperature; also, ϵ_∞ is to a minor extent, temperature dependent.

Changing the temperature displaces the profiles of the ϵ' and ϵ'' curves but their general form is preserved on the frequency axis.

In equation 3-1-1Ø, the molecules are considered to be spherical while, more generally, Cole and Cole (1941) suggest that they are ellipsoidal. Thus, instead of a single relaxation time, three must be considered, one for each of the axial ratios of the ellipsoid. Consequently the term

$$\frac{1}{1+i\omega\tau}$$

should be replaced by

$$\sum_{k=1}^{3} \frac{c_k}{1+i\omega\tau_k} \qquad 3\text{-}1\text{-}16$$

3.1.5 FOURIER TRANSFORMATION OF THE DEBYE DISPERSION MODEL

The Fourier transform of the permittivity function of frequency described by Debye's dispersion model is

$$e(t) = \int_{-\infty}^{\infty} \left[\epsilon_\infty + \frac{\epsilon_o - \epsilon_\infty}{1+i\omega\tau} \right] e^{\,i\omega t} \, d\omega \,. \qquad 3\text{-}1\text{-}17$$

The first term on the right side of this equation is a constant and its Fourier transform is a scaled Dirac delta function. Thus;

$$e(t) = \epsilon\,\delta(t) + \frac{\epsilon_o - \epsilon_\infty}{\tau}\int_{-\infty}^{\infty} \frac{1 - ix}{1+x^2}\, e^{ixt/\tau}\, dx \qquad 3\text{-}1\text{-}18$$

where $x = \omega\tau$.

The imaginary part in this integral is odd with respect to x and its integral reduces to zero. The real part is even and

$$e(t) = \epsilon_\infty \delta(t) + \frac{\epsilon_o - \epsilon_\infty}{\tau}\int_{0}^{\infty} \frac{\cos xt/\tau + x \sin xt/\tau}{1+x^2}\, dx \qquad 3\text{-}1\text{-}19$$

Integrating equation 3-1-19 obtains

$$e(t) = \epsilon_\infty \delta(t) + \frac{\epsilon_o - \epsilon_\infty}{\tau}\, e^{-t/\tau} \qquad t>=\emptyset \qquad 3\text{-}1\text{-}20a$$

Thus, the time-domain measure of the permittivity is entirely real as required and is simply an exponentially decreasing function of time. For negative times, causality requires that

$$e(t) = \emptyset \qquad t<\emptyset \qquad 3\text{-}1\text{-}20b$$

In addition $\int_{0}^{\infty} |e(t)|\, dt = \epsilon_o$ must be finite for stability.

We shall now verify the physical realizability of the Debye models; the real and imaginary components of ( ) must be Hilbert transform pairs:

$$\epsilon'(\omega) - \epsilon_\infty = \frac{1}{2\pi}\int_{0}^{\infty} \frac{\epsilon''(\nu)\nu}{\nu^2 - \omega^2}\, d\nu \qquad 3\text{-}1\text{-}21$$

and

$$\epsilon''(\omega) = \int_{0}^{\infty} \frac{[\epsilon'(\nu) - \epsilon_\infty]}{\nu^2 - \omega^2}\, \omega\, d\nu$$

This is easily verified, for equation 3-1-21

$$\epsilon'(\omega) - \epsilon_\infty = \frac{\epsilon_o - \epsilon_\infty}{2\pi}\int_{0}^{\infty} \frac{\nu'^2 d\nu}{[\nu'^4 + (1+\omega^2\tau^2)\nu'^2 + \omega^2\tau^2]}$$

where $\nu' = \nu\tau$.

This integral in this equation can be found in standard tables (Abramowitz and Stegun, 1968):

$$\int_0^\infty \frac{\nu'^2 d\nu}{(\nu'^4 + (1+\omega^2\tau^2)\nu'^2 + \omega^2\tau^2} = \frac{2\pi}{1+\omega^2\tau^2}$$

and thus,

$$\epsilon'(\omega) - \epsilon_\infty = \frac{\epsilon_o - \epsilon_\infty}{1+\omega^2\tau^2}$$

3.1.6 RELAXATION AND RESONANCE

Electrical responses can be classified as a "resonance phenomenon" or "relaxation phenomenon" according to whether or not the time domain response function oscillates or smoothly decays toward some assymptotic value. In the range of frequencies of our interest, the Debye model responses are purely relaxational. However all real materials appear to show resonances at sufficiently high frequencies. In condensed matter the lowest resonant frequencies are in the infrared range (10^{13} Hz.), where lattice and molecular vibrations start to take place. For water, relaxation occurs roughly between 3 and 300 GHz and the atomic rotational and vibrational polarization is between 1 and 100 THz.

3.1.7 DISTRIBUTION OF RELAXATION TIMES

Equation 3-1-9 describes Debye's dielectric dispersion model in polar molecules. This equation, in a very few cases, appears to describe real dielectricity. Most dielectric materials deviate from Debye's model although they show similar general behavior and symmetry. Usually their dispersion profile is flatter and extends over a much wider range of frequencies, while the absorption curve is broader and with a smaller maximum value.

The reason for this deviation is that the Debye model is too simple and considers only a single relaxation time. That is, all molecules in the substance are assumed to be spherical and identical. In real materials, the local conditions on each molecule are, however, strongly variable: the magnitude of the interaction forces, directing forces, thermal influences all change from place to place and time to time and consequently every dipole possesses a particular relaxation time. Hence, instead of a single relaxation time, we must describea distribution of relaxation times centered about some most probable value. The term

$$\frac{1}{1+i\omega\tau}$$

in Debye's simple model must be replaced by

$$\int_0^\infty \frac{G(\tau)d\tau}{1+i\omega\tau} \qquad 3\text{-}1\text{-}22$$

where G( ) is a normalized distribution function; that is,

$$\int_0^\infty G(\tau)\,d\tau = 1. \qquad 3\text{-}1\text{-}23$$

This extended dispersion model is described by the form

$$\epsilon^*(\omega) = \epsilon_\infty + (\epsilon_o - \epsilon_\infty)\int_0^\infty \frac{G(\tau)\,d\tau}{1+i\omega\tau} \qquad 3\text{-}1\text{-}24$$

with the real component

$$\epsilon'(\omega) = (\epsilon_o - \epsilon_\infty)\int_0^\infty \frac{G(\tau)\;d\tau}{1+(\omega\tau)^2} + \epsilon_\infty$$

and imaginary component

$$\epsilon''(\omega) = (\epsilon_o - \epsilon_\infty)\int_0^\infty \frac{G(\tau)\,\omega\tau\,d\tau}{1+(\omega\tau)^2}$$

The theory of distributed relaxation times was first described by von Schweidler (1913), but he did not obtain an equation for $G(\tau)$. If we consider that an infinite number of causes disturb the original relaxation time τ_o, it would be a good assumption to consider a Gaussian probability distribution form for $G(\tau)$.

$$G(\tau)\,d\tau = \frac{b}{\sqrt{\pi}}\, e^{-b^2y^2}\, dy \qquad 3\text{-}1\text{-}25$$

where $y = \ln \tau/\tau_o$

Here b determines the width of the distribution and τ_o is the most probable value for the relaxation time.

Kirkwood and Fuoss (1941) suggested another distribution function for $G(\tau)$:

$$G(\tau) = \tfrac{1}{2}(\cosh y + 1)^{-1} \qquad 3\text{-}1\text{-}26$$

which closely fits the experimental obtained dispersion curves for many real materials. ϵ'' should then be represented as

$$\epsilon''(\omega) = \epsilon''_m \operatorname{sech}\left[\beta \ln \omega\tau_0\right] \qquad 3\text{-}1\text{-}27$$

where β is a free parameter for selection:

$\beta=1$ results a system with a single relaxation time while $\beta=0$ represents infinitely wide distribution of relaxation times. Another empirical formula for dielectric dispersion was suggested by Cole and Cole (1941):

$$\epsilon^*(\omega) - \epsilon_\infty = (\epsilon_0 - \epsilon_\infty)/\left[1 + (i\omega\tau)^{1-\alpha}\right] . \qquad 3\text{-}1\text{-}28$$

This function is also symmetrical about $\ln \omega\tau = 1$ (This property will be discussed in more detail later). An interesting property of the Cole-Cole model is that it satisfies many experimental results and is in good agreement with the Kirkwood and Fuoss (1941) dispersion if the relation between parameters

$$\beta = \frac{\alpha\sqrt{2}}{2\cos\alpha\pi/2} \qquad 3\text{-}1\text{-}29$$

It has the major advantage of being a much simpler representation and free of integrals. Its disadvantage is that no physical theory has been suggested which determines the parameter β .

Qualitatively, in concentrated solutions, we would expect a broadening of the distribution and lowering of ϵ''_m, because coupling of any sort between the molecules would superimpose

another set of relaxation times on those characteristic of individual molecules. In the case of a very wide distribution of relaxation, times (mica, ceramic, glasses), however, the Cole-Cole equation (3-1-28) becomes rather innacurate and the Kirkwood-Fuoss relationship should be used instead.

3.1.8 COLE-COLE DISPERSION MODEL

The Cole and Cole (1941) dispersion equation 3-1-28

$$\epsilon^{*}(\omega)-\epsilon_{\infty} = (\epsilon_{o}-\epsilon_{\infty}) / [1+(i\omega\tau)^{1-\alpha}] \qquad 3\text{-}1\text{-}28$$

is commonly preferred in the current geophysical literature in describing dielectrics and especially conductivity properties by analogy (Pelton et al., 1978). Here,

τ = the most probable relaxation time.

α = the distribution parameter which is a measure of distribution of the relaxation times.

Necessarily, $0 < \alpha < 1$.:

$\alpha = 0$ reduces equation 3-1-28 to the Debye equation with a single relaxation time while the limit $\alpha = 1$ is physically non-realizable because it imposes $\epsilon'' = 0$. Approaching the $\alpha = 1$. limit produces very wide dispersions nearly independent of frequency (with a time domain response, proportional to the logarithm of time).

As their basis for description of their dielectric dispersion model, Cole and Cole chose to use the Argand diagram in complex plane, in which the imaginary component is plotted versus the real component. Each point characterizes a single frequency; the locus of points describes basic properties of the empirical model. The Argand locus for Debye's model is represented by a semicircle with its center on the real axis at the point $\frac{\epsilon_o+\epsilon_\infty}{2}$ (see Fig. 4). This locus of points can be represented by the following vectorial sum:

$$\vec{u}+\vec{v} = \epsilon_o-\epsilon_\infty \qquad 3\text{-}1\text{-}29$$

which is the equation of a circle with

$$\vec{u} = \epsilon^*-\epsilon_\infty, \qquad \vec{v} = i\omega\tau(\epsilon^*-\epsilon_\infty) \qquad 3\text{-}1\text{-}30$$

Measurments made for real materials do not fit the Debye semicircle. Rather they form a locus of points in a circular arc (particularly at lower temperatures) having its center below the real axis. From Figure 5, we can see that the angle $(1-\alpha)\pi/2$ is independent of the frequency. It follows then that

$$\vec{u}+\vec{v} = \vec{u}\left[1+f(\omega)\, e^{-i(1-\alpha)\pi/2}\right] = \epsilon_o-\epsilon_\infty \qquad 3\text{-}1\text{-}31$$

where $f(\omega)$ is a real undetermined function of frequency and other parameters. Substituting from 3-1-30

$$\epsilon^*-\epsilon_\infty = (\epsilon_o-\epsilon_\infty)/\left[1+f(\omega)\, e^{-i(1-\alpha)\pi/2}\right] \qquad 3\text{-}1\text{-}32$$

since

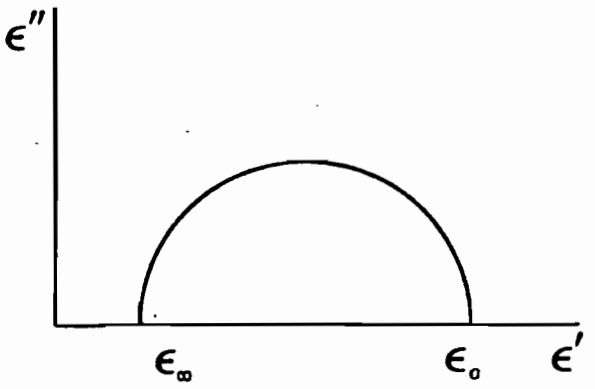

Figure 4. (From Alvarez, 1973). Argand diagram of the Debye model.

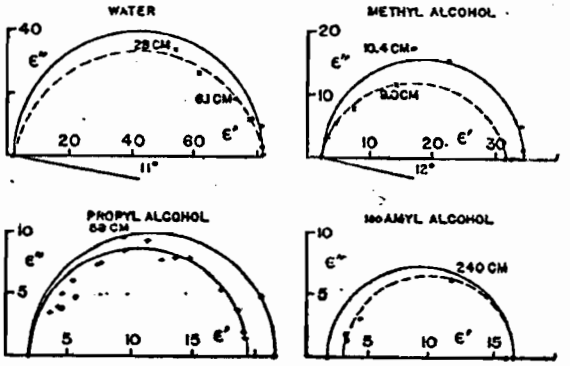

Complex dielectric constants of water and alcohols.

Figure 5. (From Cole and Cole, 1941). Argand diagram of the Cole-Cole model for four substances.

$$e^{i(1-\alpha)\pi/2} = i^{(1-\alpha)},$$

$$\epsilon^*(\omega) - \epsilon_\infty = (\epsilon_o - \epsilon_\infty) / [1 + f(\omega) i^{(1-\alpha)}].$$

Also, since the complex form of ϵ^* is a result of considering an applied field of the form

$$E = E_o e^{i\omega t}$$

in which i and ω show identical exponential dependence, the dependence of f (ω) on frequency can be considered to have the form $\omega^{1-\alpha}$. This follows from the fact that any theory in which ω appears as a result of linear operations on the complex exponential will lead to the same dependence on the unit imaginary i, as on ω.

$$\epsilon^*(\omega) - \epsilon_\infty = (\epsilon_o - \epsilon_\infty) / [1 + (i\omega T)^{1-\alpha}]. \qquad 3\text{-}1\text{-}28$$

The real and imaginary components of 3-1-28 are respectively:

$$\epsilon'(\omega) - \epsilon_\infty = (\epsilon_o - \epsilon_\infty)[1 + (\omega T)^{1-\alpha} \sin \alpha\pi/2]/A \qquad 3\text{-}1\text{-}33$$

$$\epsilon''(\omega) = (\epsilon_o - \epsilon_\infty)(\omega T)^{1-\alpha} \cos \alpha\pi/2 / A \qquad 3\text{-}1\text{-}34$$

where

$$A = 1 + 2(\omega T)^{1-\alpha} \sin \alpha\pi/2 + (\omega T)^{2(1-\alpha)}$$

Without any loss of generality we can require in the following conditions

$$\epsilon'(\omega<0) = \epsilon'(\omega>0) \qquad 3\text{-}1\text{-}36$$

and

$$\epsilon''(\omega<0) = -\epsilon''(\omega>0)$$

so that the causality restriction (equation 2-1-26) will be respected. The maximum dispersion occurs at $\omega_m = 1/\tau$ where

$$\epsilon''_m = \frac{1}{2}(\epsilon_o - \epsilon_\infty) \tan\left[(1-\alpha)\pi/4\right]. \qquad 3\text{-}1\text{-}37$$

The condition of the Hilbert transformation, requires that ϵ' or ϵ'' are uniquely determined by the knowledge of the other component. This has been verified by Kramers (Cole and Cole, 1941):

$$\epsilon'(\omega) - \epsilon_\infty = \frac{1}{2\pi}\int_o^\infty \frac{\epsilon''(\nu)\,\nu\,d\nu}{\nu^2 - \omega^2}$$

and

$$\epsilon''(\omega) = \int_o^\infty \frac{[\epsilon'(\nu) - \epsilon_\infty]\,\omega\,d\nu}{\nu^2 - \omega^2} \qquad 3\text{-}1\text{-}38$$

Because of technical difficulties in obtaining measurements for real materials, ϵ' and ϵ'' are only determined near the low or high frequency limits. However, since ϵ' and ϵ'' are uniquely determined by the knowledge of the other, it is possible to interpolate the known data to form an arc locus and determine the parameters of an equivalent homogeneous dielectric model.

TABLE 2

SUBSTANCE	DIELECTRIC CONSTANT ϵ_o
Quartz	4.5 - 4.7
Calcite	7 - 8
Gas	1
Oil	2.2
Water	8Ø
Shale	13 - 15

3.1.9 TRANSIENT COLE-COLE PERMITTIVITY MODEL

The Fourier transform of the Cole-Cole equation is

$$e(t) = \epsilon_\infty \delta(t) + (\epsilon_o - \epsilon_\infty) \mathcal{F}\left[1 + (1 + (i\omega\tau)^{1-\alpha}\right] \qquad 3\text{-}1\text{-}39$$

The term $\frac{1}{1+(i\omega\tau)^{1-\alpha}}$ will have a Fourier transform which will show much slower than exponential decay of the Debye equation where α. was equal to zero. To derive the time domain response of this term following Jain (1981), let us for convenience temporarily absorb into :

$$H(\omega) = \frac{1}{1+(i\omega\tau)^{1-\alpha}} \qquad 3\text{-}1\text{-}40$$

We know that $H(\omega)$ is the Fourier transform of the impulse response h(t). If we rearrange 3-1-40

$$H(\omega) + (i\omega)^{1-\alpha} H(\omega) = 1. \qquad 3\text{-}1\text{-}41$$

If $\alpha = 0$ the time domain Fourier transform of the above would be

$$h(t) + \frac{\partial}{\partial t} h(t) = \delta(t) \qquad 3\text{-}1\text{-}42$$

and obviously likewise Debye's equation, the response would be

$$h(t) = e^{-t/\tau}. \qquad 3\text{-}1\text{-}43$$

If we denote the fractional derivative by $\frac{\partial^{1-\alpha}}{\partial t^{1-\alpha}}$ for $\alpha > 0$ we would have

$$h(t) + \frac{\partial^{1-\alpha}}{\partial t^{1-\alpha}} h(t) = \delta(t) \qquad 3\text{-}1\text{-}44$$

Using the property that

$$\frac{\partial^c}{\partial t^c}\ \frac{t^k}{\Gamma(1+k)} = \frac{t^{k-c}}{\Gamma(1+k-c)} \qquad 3\text{-}1\text{-}45$$

where Γ is the gamma-function, we would obtain the form for h(t) as

$$h(t) = \sum_{n=1}^{\infty} (-1)^{n+1}\ \frac{t^{n(1-\alpha)-1}}{\Gamma(n-n\alpha)} \qquad 3\text{-}1\text{-}46$$

Then the equivalent unit step function response would be

$$U(t) = \sum_{n=1}^{\infty} (-1)^{n+1}\ \frac{t^{n(1-\alpha)}}{\Gamma(n-n\alpha+1)} \qquad 3\text{-}1\text{-}47$$

Returning to equation 3-1-39, the Fourier transform of the Cole-Cole model will then obtain

$$e(t) = \epsilon_\infty \delta(t) + (\epsilon_o - \epsilon_\infty) \sum_{n=1}^{\infty} \frac{(-1)^{n+1}\ t/\tau^{n(1-\alpha)}}{\Gamma(n-n\alpha+1)} \quad . \qquad 3\text{-}1\text{-}48$$

We require that e(t) be finite when $t \rightarrow \infty$. For t/τ <=1, the above equation is finite, but for t/τ >1, in order to keep the transient e(t) finite we must replace

$$e(t) = (\epsilon_o - \epsilon_\infty) \sum_{n=1}^{\infty} \frac{(-1)^n\ (t/\tau)^{-n(1-\alpha)}}{\Gamma(1-n+n\alpha)} \qquad t > \tau \qquad 3\text{-}1\text{-}49$$

so that the series will converge. The above discussion holds for reversible absorption but does not take into account the effect of irreversible Joule conductivity (Jain, 1981).

From Figure 6 it is apparent that for t>=τ the transient permittivity decreases to less than half its initial value.

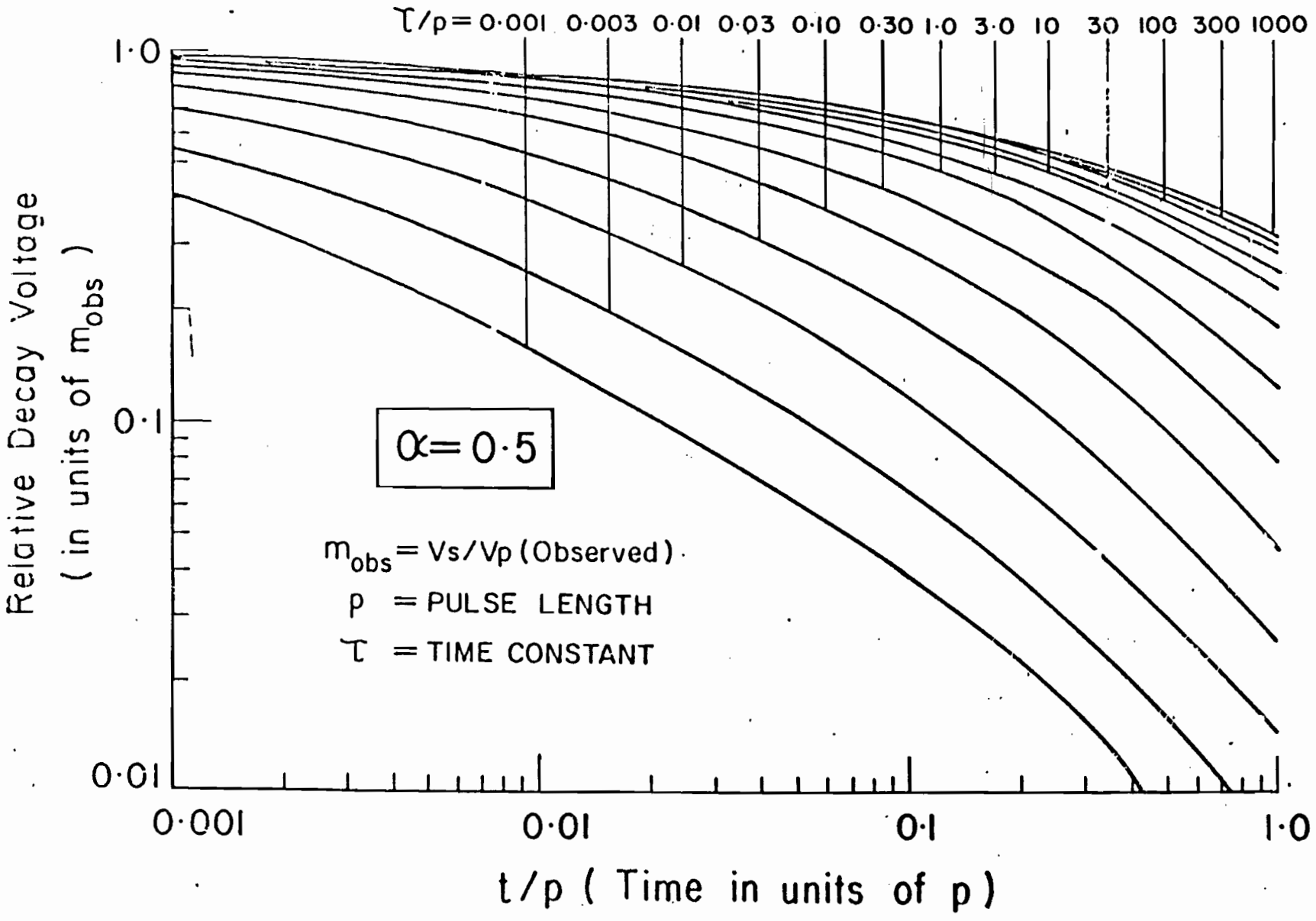

Figure 6. (From Jain, 1981). Decay voltage versus t/p for various τ/p.

3.1.1Ø COLE-DAVIDSON DISPERSION MODEL

R. Cole and Davidson (1951), observed a non-symmetric behavior in some substances like glycerol, propylene glycol and few others. They developed the following empirical formula to fit their dispersion curves

$$\epsilon^* - \epsilon_\infty = (\epsilon_o - \epsilon_\infty)/(1 + i\omega\tau)^\beta \qquad 3\text{-}1\text{-}5Ø$$

$$0 \leq \beta \leq 1$$

where now β is a measure of skewness

The real and imaginary components of the complex permittivity ϵ^* are then

$$\epsilon' - \epsilon_\infty = (\epsilon_o - \epsilon_\infty)(\cos\phi)^\beta \cos\beta\phi \qquad 3\text{-}1\text{-}51$$

$$\epsilon'' = (\epsilon_o - \epsilon_\infty)(\cos\phi)^\beta \sin\beta\phi \qquad 3\text{-}1\text{-}52$$

where $\tan\varphi = \omega\tau$

This model is not symmetric about $\ln\omega\tau = Ø$ but consists of contributions that diminish in importance as the frequency increases, producing smaller values of ϵ'' toward higher frequencies in comparision with Debye's model.

3.1.11 MAXWELL-WAGNER EFFECT

In addition to the polarization in dielectrics as discussed previously, there is another polarizaton rising in a heterogeneous material from the accumulaton of charges due to differences in mobility between anions and cations in adjacent zones. At the interfaces, a membrane polarization arises. Physical descriptions of polarization usually omit this phenomenon since it is of little fundamental interest. However in geophysical measurements in geological conditions, it is of considerable practical interest.

Maxwell-Wagner (Alvarez, 1973) described the charge built up at the microscopic interface of two media differing in conductivity and/or dielectric permittivity. This Maxwell-Wagner polarization is then due to concentration gradients that develop at zone boundaries in response to current flow. Their theory considers spherical particles with constant parameters ϵ_2 and σ_2 uniformly distributed in a medium with constant parameters ϵ_1 and σ_1 to arrive at a relaxation spectrum with a single relaxation time. In the frequency domain:

$$\nabla . D = \nabla(\epsilon E) = \nabla(\epsilon . E) + \epsilon . \nabla E = \rho \qquad 3\text{-}1\text{-}53$$

and

$$\nabla . J = \nabla(\sigma J) = \nabla(\sigma . J) + \sigma . \nabla J = -i\omega\rho \qquad 3\text{-}1\text{-}54$$

so that

$$i\omega\rho = \sigma/\epsilon \left[-(i\omega\rho) + \sigma\left[\nabla(\epsilon/\sigma) . E(\omega)\right]\right] \qquad 3\text{-}1\text{-}55$$

and for $\omega = \emptyset$

$$\rho(o) = \sigma(o)\left[\nabla[\epsilon(o)/\sigma(o)] \cdot \vec{E}(o)\right] . \qquad 3\text{-}1\text{-}56$$

Consequenly if ϵ and σ vary as a function of position, $\nabla(\epsilon/\sigma)$ will be non-zero and as a result there can be a concentration of charges at the microscopic interface. The term $\nabla(\epsilon/\sigma)$ gives then rise to the Maxwell-Wagner effect which produces an additonal dispersion of the system.

3.2.1 CONDUCTIVITY

Conductive materials are characterized by the abundance of contained free charges. Under the application of any external electric field E, the free charges will flow along the field lines producing a current density J, which is a function of the applied field:

$$\vec{J} = f(\sigma, \vec{E}) \qquad 3\text{-}2\text{-}1$$

Recalling the discussion of linearity at low field levels, isotropy and homogeneity, we expect a linear relationship between the current density $\vec{J}$ and the field strength $\vec{E}$, scaled by a complex conductivity σ^*.

$$\vec{J} = \sigma^* \cdot \vec{E} \qquad 3\text{-}2\text{-}2$$

$\vec{J}$ = current density (Amp/m^2)

σ^* = conductivity in S/m

$\vec{\sigma}^* = \vec{\sigma}(\omega, T)$

$\sigma^* = \sigma' + i\sigma''$

In the simplest situation the conductivity is a constant scalar and, in particular, for a material like air where the conductivity is approximately zero,

$$J_{air} = \emptyset \ . \qquad 3\text{-}2\text{-}4$$

However in general like permittivity, conductivity is also a complex tensor, dependent on frequency, temperature, location and pressure.

3.2.2 THERMAL DEPENDENCE OF CONDUCTIVITY

To deal with the temperature dependence, let us rather consider the inverse of conductivity, the resistivity.

$$\rho^* = \frac{1}{\sigma^*} \qquad 3\text{-}2\text{-}5$$

$$\rho^* = \rho' - j\rho'' \qquad 3\text{-}2\text{-}6$$

$$\rho' = \frac{\sigma'}{|\sigma^*|^2} \ , \qquad \rho'' = \frac{\sigma''}{|\sigma^*|^2} \qquad 3\text{-}2\text{-}7$$

The electrical resistivity of conductors is dominated at room temperature by the collision of conduction electrons with lattice phonons and at very low temperatures by collision with impurity atoms and mechanical imperfections in the lattice. The net resistivity is given by Mathieson's rule (Kittel, 1958).

$$\rho = \rho_l + \rho_i \qquad 3\text{-}2\text{-}8$$

where ρ_l is the thermal resistivity, and ρ_i is independent of temperature and due to the atomic structure of the matter. The electrical conductivity is not a simple matter to deal with

because of its complex dependence on many parameters. However, Kittel shows that ρ_1 can be represented by the empirical function

$$\rho_1 \propto (T/M\theta_R^2) f(T/\theta_R)$$

where f approaches unity at high temperatures and is proportional to $(T/\theta_R)^4$ at very low temperatures.

Above,

M is the atomic mass,

θ_R the Debye temperature and

T, the absolute temperature.

The proportionality of ρ_1 with $T/M\theta_R^2$ at high temperature follows because the electron-phonon scattering is proportional to the mean square thermal strain. Additional discussion of the dependence of resistivity on temperature is beyond the scope of this thesis, but has been discussed by Kittel (1958). Very generally, we expect resistivity to be approximately linear in temperature, in the range of temperatures of our interest, so that

$$\rho = \rho_i + T/M\theta_R^2 \qquad 3\text{-}2\text{-}9$$

Some curves of thermal conductivity as function of absolute temperature, are shown below (Fig. 7). The behavior of these particular elements with respect to temperature is closely related to their atomic crystalline structure but this is not the interest of this work. Henceforth, we will constrain the temperature to a constant.

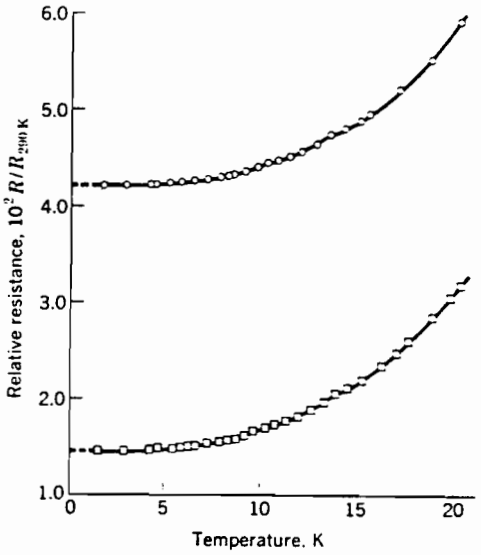

Resistance of potassium below 20 K, as measured on two specimens by D. K. C. MacDonald and K. Mendelssohn, Proc. Roy. Soc. (London) **A202**, 103 (1950). The different intercepts at 0 K are attributed to different concentrations of impurities and static imperfections in the two specimens. For measurements below 4.2 K, see D. Gugan, Proc. Roy. Soc. (London) **A325**, 223 (1971).

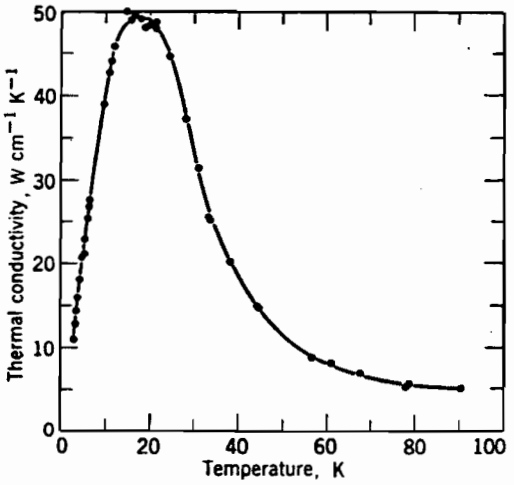

The thermal conductivity of copper, after Berman and MacDonald.

Figure 7. (From Kittel, 1958). Resistance and thermal conductivity curves versus temperature.

3.2.3 TIME DOMAIN CONDUCTIVITY AND RESISTIVITY

In good conductors the property practically measured is their resistivity, while in poor conductors conductivity is practically measured. The logical foundation of linear response theory is the principle of superposition, which is expressed by the following expression in which conductivity relates an imposed electric field to the resulting current density within the medium:

$$\vec{j}(t) = \int_0^\infty s(t)\, e\,(t-\tau)\, d\tau. \qquad 3\text{-}2\text{-}10$$

In a parallel description material resistivity relates an electric field due to current-density generation:

$$\vec{e}(t) = \int_0^\infty r(t)\, j(t-\tau)\, d\tau. \qquad 3\text{-}2\text{-}11$$

Above, s(t) and r(t) are the real conductivity and resistivity impulse response functions. According to the causality restriction we require

$$s(t) = r(t) = 0 \qquad \text{for } t<0 \qquad 3\text{-}2\text{-}12$$

Note then that

$$s(t) \neq r(t)^{-1} \qquad \text{for } t<0.$$

These respective functions describe the response $\vec{j}(t)$ and $\vec{e}(t)$ due to a short impulse in $\vec{e}(t)$ and $\vec{j}(t)$. For their equivalent step responses, we would obtain

$$R(t) = \int_0^t r(\tau)\, d\tau \qquad 3\text{-}2\text{-}13$$

$$c(t) = \int_0^t s(\tau)\, d\tau$$

where R(t) and C(t) are the output waveforms of $\vec{e}(t)$ and $\vec{j}(t)$ due to an input unit step $\vec{j}(t)$ and $\vec{e}(t)$. We define the Fourier transforms of s(t) and r(t) by:

$$\sigma^*(\omega) = \int_0^\infty s(t)\, e^{-i\omega t}\, dt$$
$$\rho^*(\omega) = \int_0^\infty r(t)\, e^{-i\omega t}\, dt \qquad 3\text{-}2\text{-}14$$

and equivalently

$$s(t) = \int_{-\infty}^{\infty} \sigma^*(\omega)\, e^{i\omega t}\, d\omega$$
$$r(t) = \int_{-\infty}^{\infty} \rho^*(\omega)\, e^{i\omega t}\, d\omega \qquad 3\text{-}2\text{-}15$$

In the latter pair, the path of integration is along the real w-axis. If σ^* and ρ^* have singularities for any real w, the path of integration is properly displaced infinitesimally in the positive imaginary direction.

The two components of $\rho^*(\omega)$ contributing to the line integral are those associated with the semicircle path at infinity and the path enclosing th negative imaginary axis . The second contribution depends only upon the difference between the values taken by the integrand on the two sides of the real w-axis. The decay spectrum are defined by the difference (Shuey and Johnson, 1973):

$$A_r(\omega) = \frac{\rho(-i\omega+\alpha) - \rho(-i\omega-\alpha)}{2i\pi} \qquad 3\text{-}2\text{-}16$$

and equivalently for $\sigma(\omega)$

$$A_c(\omega) = -\frac{\sigma(-i\omega+\alpha) - \sigma(-i\omega-\alpha)}{2i\pi} \qquad 3\text{-}2\text{-}17$$

In addition, if we consider that both $\rho(\omega)$ and $\sigma(\omega)$ are finite at $w \longrightarrow \infty$ which is a realizability requirement, the decomposed impulse responses become

$$r(t) = \rho_\infty \delta(t) + \int_0^\infty A_r(k)\, e^{kt}\, dk$$
$$s(t) = \sigma_\infty \delta(t) - \int_0^\infty A_c(k)\, e^{-kt}\, dk \qquad 3\text{-}2\text{-}18$$

where A_r and A_c are real resistivity and conductivity decay spectra. The resistivity and conductivity responses in terms of A_r and A_c are obtained by the use of the Cauchy integral theorem:

$$\rho(\omega) = \rho_\infty + i\int_0^\infty \frac{A_r(k)\, dk}{\omega + ik}, \qquad 3\text{-}2\text{-}19$$

$$\sigma(\omega) = \sigma_\infty - i\int_0^\infty \frac{A_c(k)\, dk}{\omega + ik}. \qquad 3\text{-}2\text{-}20$$

The step response in terms of the decay spectra are also obtained by integration of 3-2-18:

$$R(t) = \rho_\infty + \int_{-\infty}^{\infty} (1 - e^{-kt})\, A_r\, dk/k$$
$$C(t) = \sigma_\infty - \int_{-\infty}^{\infty} (1 - e^{-kt})\, A_c\, dk/k \qquad 3\text{-}2\text{-}21$$

or in terms of ρ_0 and σ_0

$$R(t) = \rho_0 - \int_{-\infty}^{\infty} e^{-kt}\, A_r\, dk/k$$
$$C(t) = \sigma_0 + \int_{-\infty}^{\infty} e^{-kt}\, A_c\, dk/k \qquad 3\text{-}2\text{-}22$$

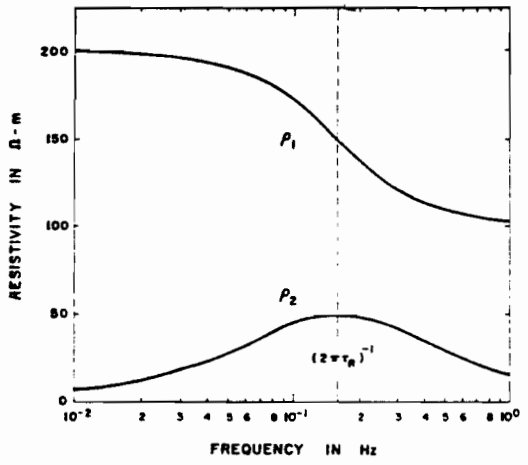

Figure 8. (After Shuey and Johnson, 1973). Complex resistivity for the Debye model with $\rho(\infty) = 100$ Ωm, $\rho(0) = 200$ Ωm, $\tau_f = 1$sec.

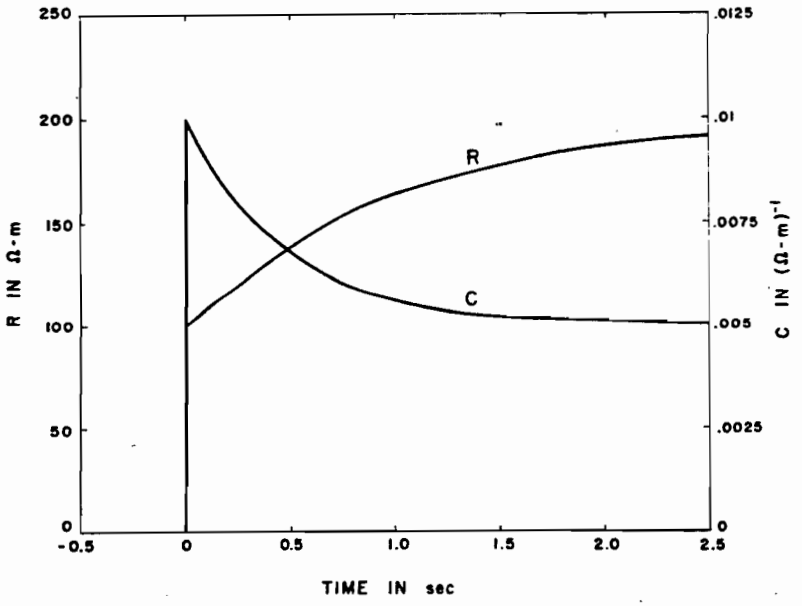

Figure 9. (After Shuey and Johnson, 1973). Step responses for the Debye model with $\tau_R = 1$ sec, $\tau_c = 0.5$ sec.

3.2.4 THE DEBYE MODEL

For a single decay time, the Debye model is described in frequency domain by the form

$$\rho(\omega) = \rho_\infty + \frac{\rho_0 - \rho_\infty}{1 + i\omega\tau} \qquad 3\text{-}2\text{-}23$$

which has one pole at $\omega = -\frac{1}{\tau}$. The resistivity decay spectrum becomes

$$A_\gamma = \frac{\rho_0 - \rho_\infty}{\tau} \quad \delta(\omega - 1/\tau)$$

and the voltage response to a unit current step (see figure 9),

$$R(t) = \rho_0 - (\rho_0 - \rho_\infty) \exp(-t/\tau).$$

3.2.5 COLE-COLE RESISTIVITY MODEL

Until now, permittivity and resistivity (or conductivity) have been discussed in parallel formalism and have been shown to posses similar behavior. Thus, it should be useful to consider a Cole-Cole resistivity model of dispersion. This model was introduced into the geophysical literature by Pelton et al. (1978). The reason they have suggested this model is that it comprises two additional parameters which may well provide a means for recognition of the mineralization by use of high-frequency resistivity (or induced polarization) geophysical surveys. In addition, this simple model has been found to

fit a large variety of laboratory complex measurements of resistivity (Madden and Cantwell, 1967 and Pelton et al., 1978).

A mineralized rock sample having both blocked and unblocked pore passages (Fig. 10) can be simulated by the circuit of Figure 11. The complex frequency dependent impedance of this circuit is

$$Z(\omega) = R_o\left[1 - m\left(1 - \frac{1}{1+(i\omega\tau)^c}\right)\right] \qquad 3\text{-}2\text{-}29$$

where m is the chargeability:

$$m = \frac{1}{\frac{R_1}{R_o}+1} \qquad 3\text{-}2\text{-}30$$

R_o is the unblocked pore path resistance,

R_1 is the resistance of the solution in blocked passages,

c is the degree of frequency dependence of the impedance

$$0 <= c <= 1$$

τ is the relaxation time.

With some manipulation we can rewrite equation 3-2-29:

$$Z(\omega) - Z_\infty = \frac{R_o - Z_\infty}{1+(i\omega\tau)^c} \qquad 3\text{-}2\text{-}31$$

where

$$Z_\infty = \left(\frac{1}{R_o} + \frac{1}{R_1}\right)^{-1}$$

Equation 3-2-31 is the Cole-Cole dispersion equation as commonly presented in the geophysical literature. At very low frequencies the current flows through unblocked pore passages, and the assymptotic value of the impedance will be R_o. At very high frequencies the flow is through both blocked and unblocked passages in parallel and the impedance assymptote becomes Z_∞.

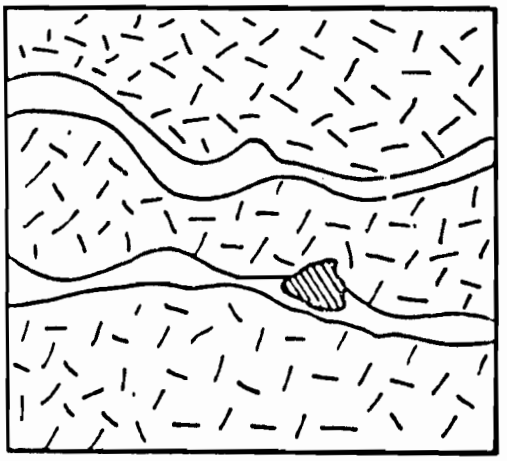

Mineralised Rock

Figure 10. (From Pelton et al., 1976). Small section of mineralized rock with both blocked and unblocked pore passages.

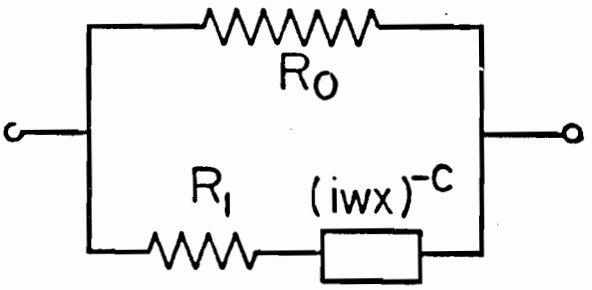

$$Z(w) = Ro\left[1 - m\left(1 - \frac{1}{1+(iwc)^c}\right)\right]$$

Equivalant Circuit

Figure 11. (From Pelton et al., 1976). The equivalent circuit of the above.

Among the mineralizations to which the Cole-Cole resistivity model has been fitted is the Lornex Porphyry Copper deposit in Highland Valley British Colombia (Fig. 12) for which the following parameters have been determined in interpretation of broad-band, high-frequency induced polarization survey data

$$R_o = 126.0 \pm 0.9 \ \Omega m$$
$$Z = 68.0 \pm 1.2 \ \Omega m$$
$$\tau = (1.0 \pm 0.6) \times 10^{-4}$$
$$c = 0.16 \pm 0.006$$

In another case of dry porphyry from Copper Cities deposits, Arizona, in addition to the normal dispersion, a second dispersion appears at higher frequencies, which is possibly due to membrane polarization. The dispersion curve has been fitted by 2 Cole-Cole terms. In addition to the above, there is a high frequencies inductive coupling due to the common dipole-dipole configuration used in the Induced polarization survey method. Millett (1967) gives complete tables for this inductive electromagnetic coupling and thus it can be reduced from the raw dispersion.

Obviously, the cole-cole model is simple. The dominant mechanism controlling the current passage through blocked passages is diffusion. In natural rocks, many different pore passages blocked by different minerals having different grain sizes occur. The result of this is a broad dispersion with a slight frequency dependence. Despite weaknesses, the model

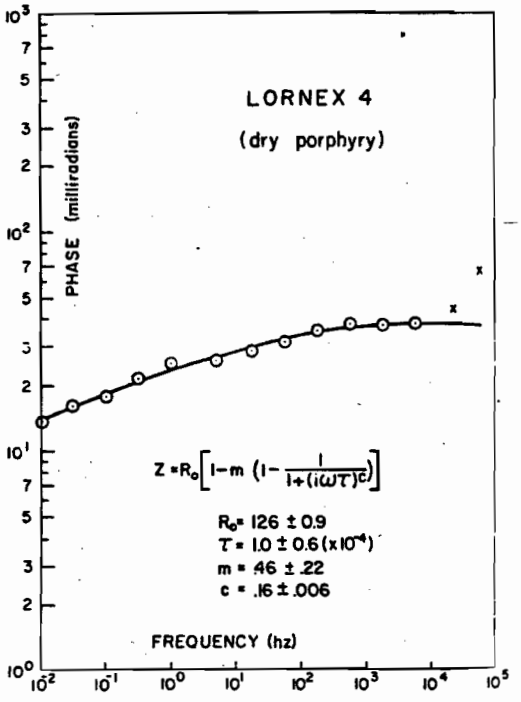

Phase angle spectra from the Lornex porphyry copper deposit in Highland Valley region of British Columbia. Dipole-dipole array: $n = 1$, $x = 1$ m. The circles represent the observed data, the solid line represents the best-fitting theoretical curve, and the crosses represent possibly noisy data which were not used in the inversion.

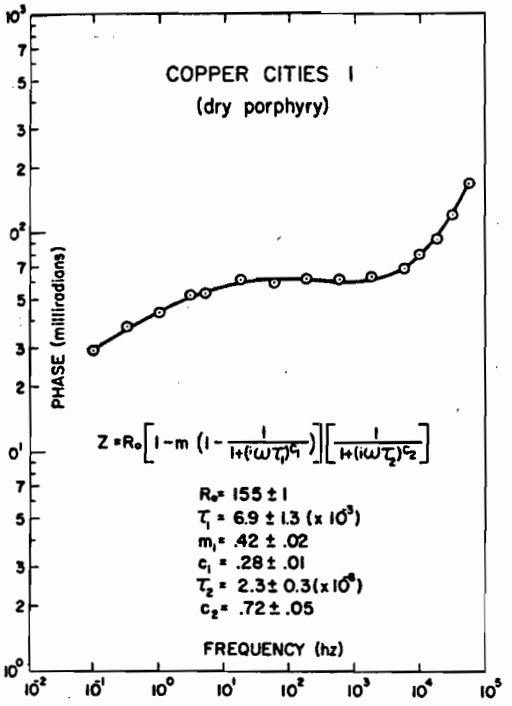

Phase angle spectra from the Copper Cities porphyry copper deposit in the Globe-Miami district of Arizona. Dipole-dipole array, $n = 1$, $x = 1$ m.

Figure 12. (After Pelton et al., 1976). Two phase angle spectra and their equivalent Cole-Cole equations.

slight frequency dependence. Despite weaknesses, the model fits a large variety of laboratory samples and in-situ measurements.

3.2.6 TIME DOMAIN EQUIVALENT RESPONSE OF COLE-COLE RESISTIVITY MODEL

If the frequency dependent exponent c = 1, the time domain decay has the familiar negative exponential form,

$$V(t) = m \frac{R_o}{I} e^{-t/\tau} \qquad 3\text{-}2\text{-}31$$

where, now, I is the chargeability current.

But, if c < 1, the decay will be slower than exponential. Proceeding in the same way as for dielectric permittivity, we can determine the step decay for resistivity to have the form:

$$V(t) = m \frac{R_o}{I} \sum_{n=0}^{\infty} \frac{(-1)^n (t/\tau)^{nc}}{\Gamma(1+nc)} \qquad t/\tau <= 2\pi$$

$$V(t) = m \frac{R_o}{I} \sum_{n=1}^{\infty} \frac{(-1)^{n+1} (t/\tau)^{-nc}}{\Gamma(1-nc)} \qquad t/\tau > 2\pi \qquad 3\text{-}2\text{-}32$$

See Figure 13.

3.2.7 COLE-DAVIDSON RESISTIVITY MODEL

Madden and Marshall (1959) developed a theoretical model for membrane polarization. Their model describes clay-bearing sandstone and comprises of a series combination of zones. Zone

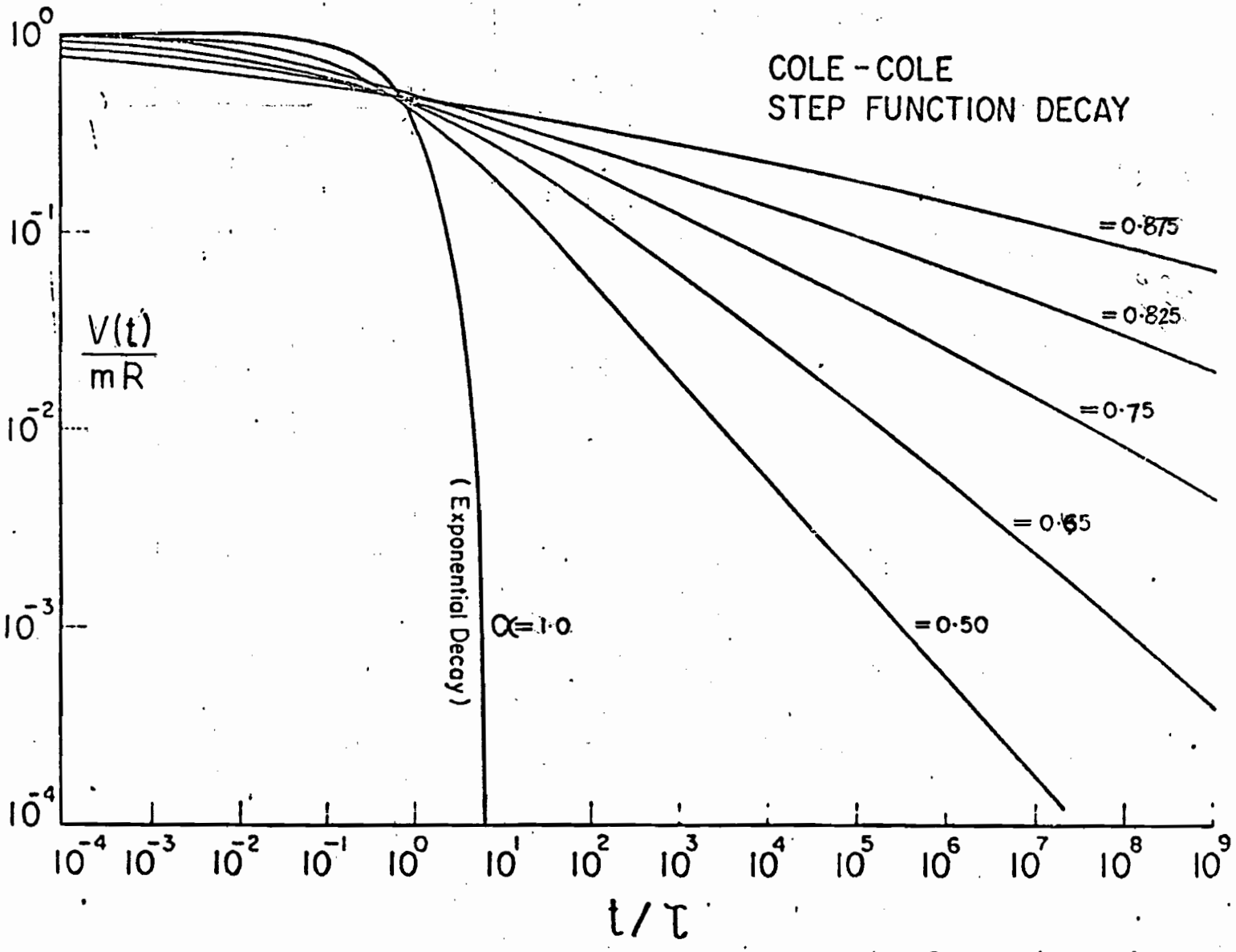

Figure 13. (From Jain, 1981). Step decay verus t/τ, for various α's.

1 contains pore fluid uninfluenced by clay while the pore fluid in zone 2 is in near proximity to clay particles so that when current is passed through zone 2 it is predominantly carried by transport of cations rather than anions. Upon linearizing the appropriate equations of motion and matching boundary conditions between zones, Madden and Marshall derive a rather complicated expression for the impedance combinations of zones,

$$Z(\omega) = \frac{L_1}{\mu_1 P_0 F}\left[\frac{1}{\sigma_1\theta_1} + \frac{B}{A\sigma_2\theta_2} + \frac{(\sigma_2-\sigma_1)^2}{\sigma_1^2\sigma_2^2\theta_1\theta_2}\left[\frac{x_1\theta_2}{\tan x_1} + \frac{x_2\theta_1 A}{B\tan x_2}\right]^{-1}\right]$$

Klein and Sill (1982) have shown that the Cole-Davidson distribution provides a close fit to the Madden-Marshall model while reducing number of parameters required so that it offers a more practical tool for characterizing clay's EM response. They have fitted the Cole-Davidson parameters by inversion, for an artificially produced sample of clay-glass bead mixtures of varying size and pore solution conductivity. they descibe

$$Z(\omega) = R_0\left[1-m\left(1-\frac{1}{(1+(i\omega\tau)^c)^\alpha}\right)\right] \qquad 3\text{-}2\text{-}33$$

where

R_0 = background resistivity, $\frac{1}{\frac{R_1}{R_0}+1}$,

m = $1-R_\infty/R_0$ chargeability,

τ = time constant,

and

R_1 = high frequency asymptote.

Madden and Marshall's description suggests that τ would provide information of the clay occurence and texture while the chargeability m should depend upon the amount of clay present in

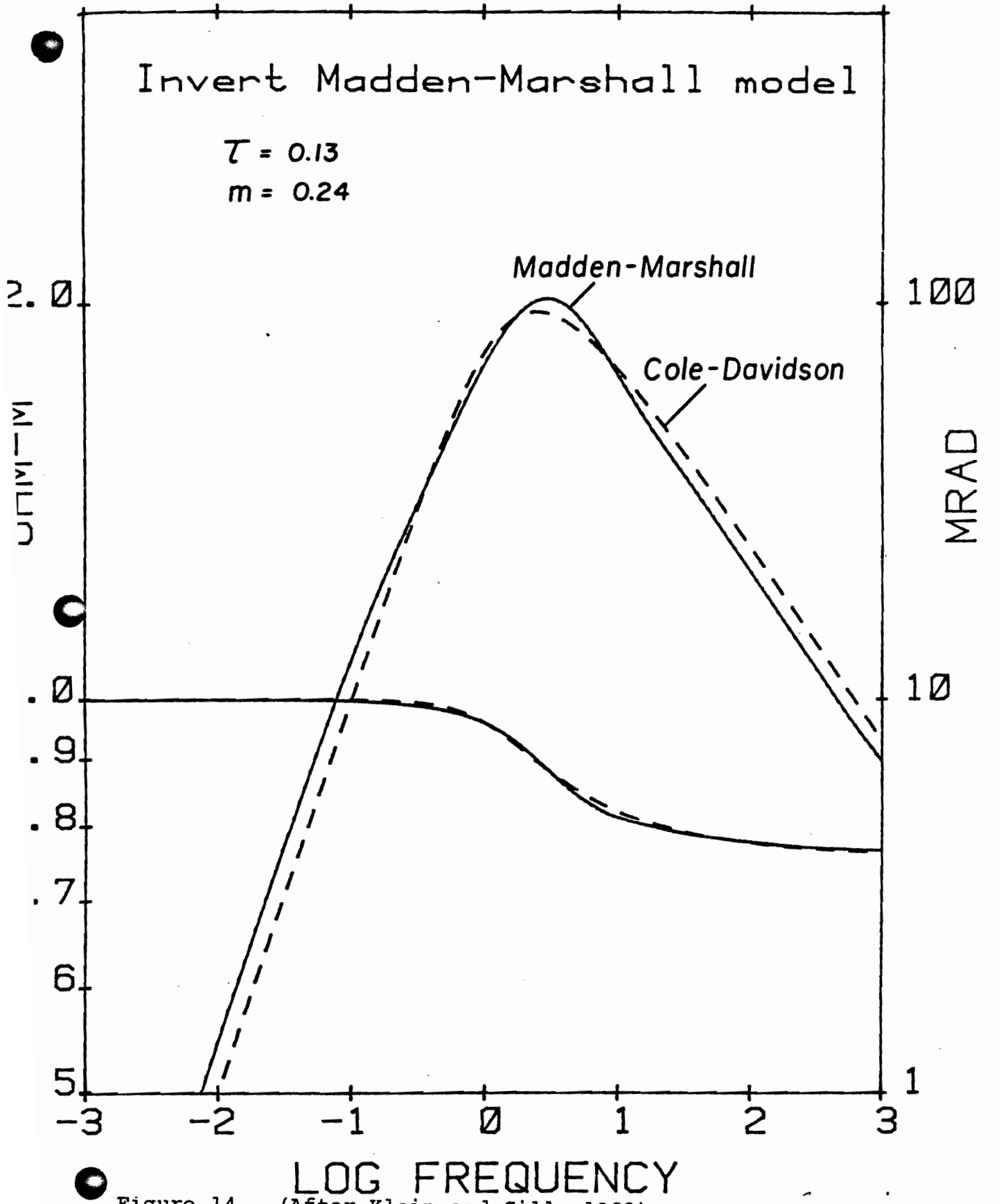

Figure 14. (After Klein and Sill, 1982). Amplitude and phase angle spectra versus frequency.

isolated zones. Clay particles providing a continuous path for surface conduction would be expected to decrease R_o, but have no effect on m (see Figure 14).

If membrane polarizaton could be completely characterized by a diffusion-like process, we would expect more symmetrical phase peaks with the parameter c close to 1, but for the artificial samples :

$$.5<c<1.$$

also most values of α were less than Ø.5. These results suggest that essential membrane polarization effects can be empirically described by the generalized Cole-Davidson model.

Klein and Sill (1982) show that increasing grain size shifts the relaxation toward lower frequencies (Fig. 15).

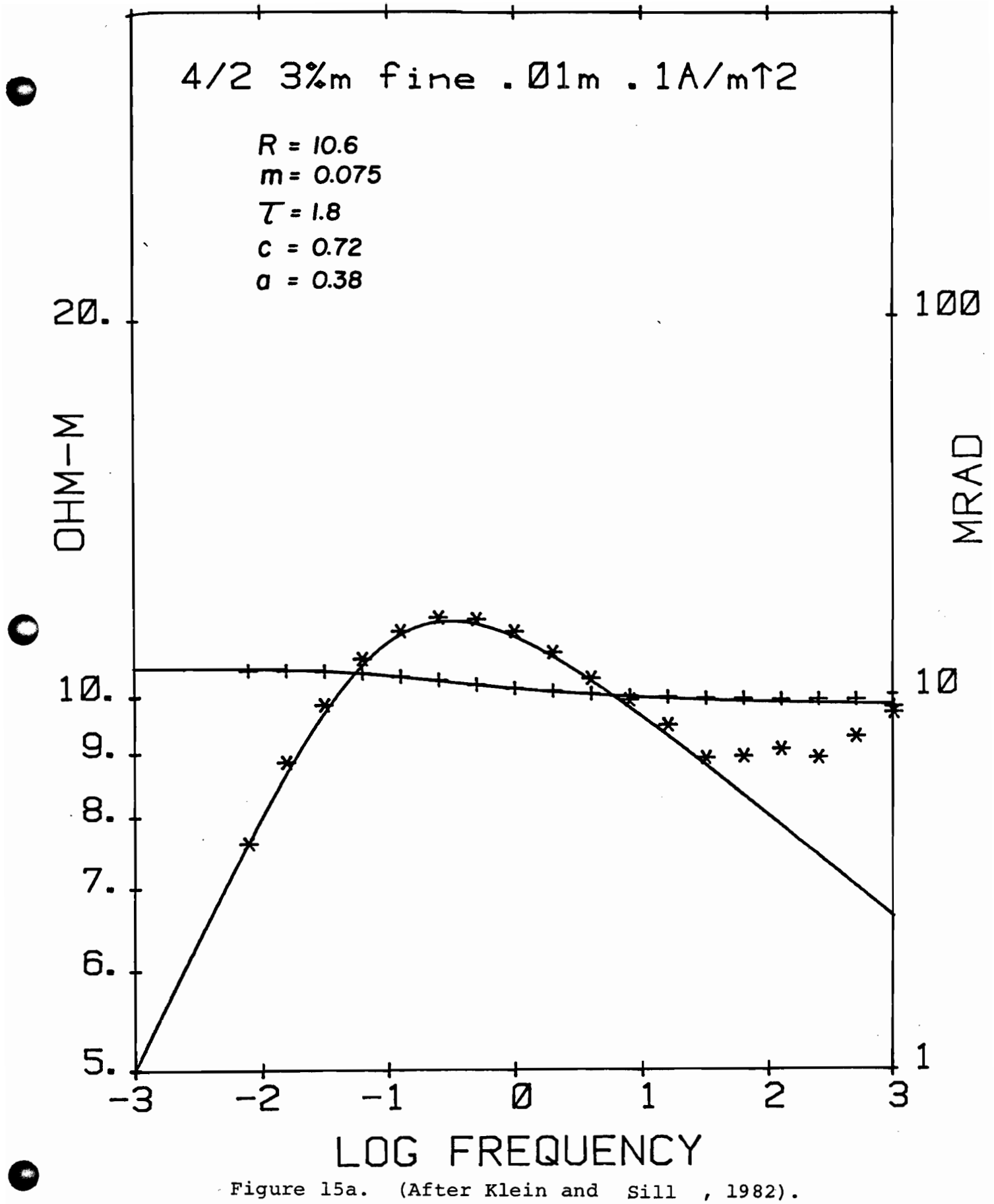

Figure 15a. (After Klein and Sill , 1982).

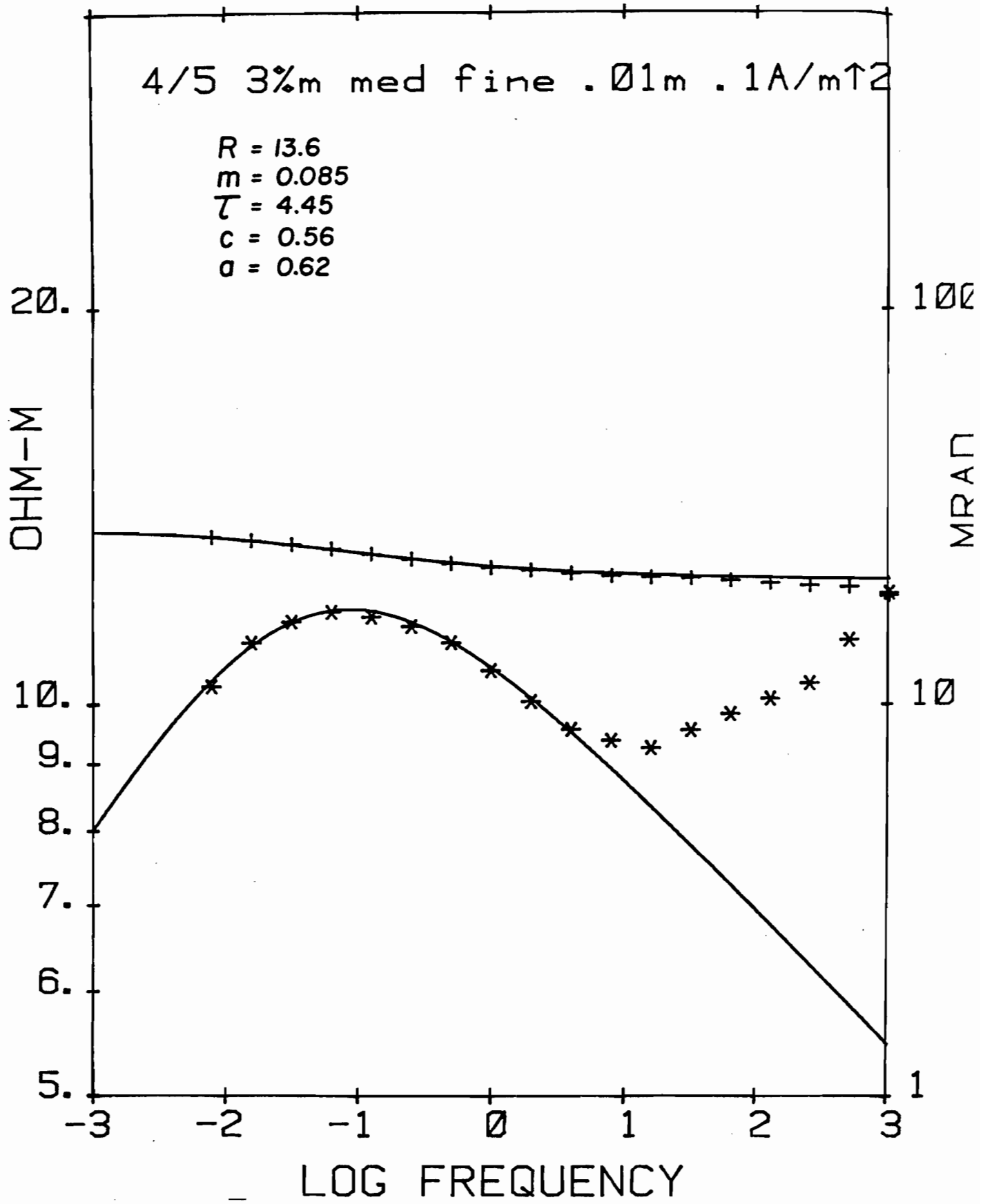

Figure 15b. (After Klein and Sill, 1982).

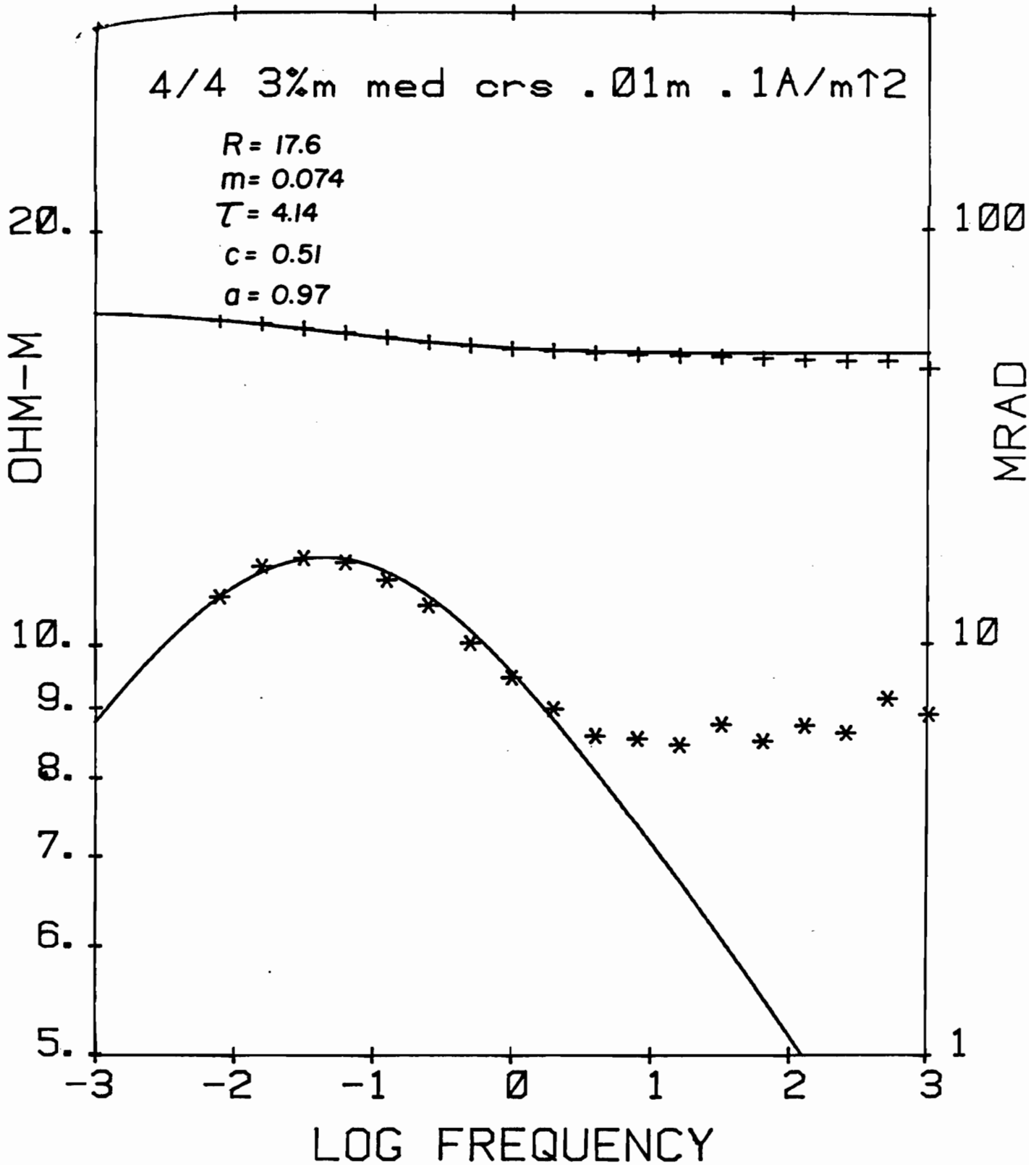

Figure 15c. (After Klein and Sill , 1982).

3.3.1 MAGNETIC INDUCTION

An external magnetic field H_{ext}, applied to a medium will align the internal magnetic poles of the body and thus produce a secondary polarization field M. This quantity is commonly known as the magnetization and increases the total field within most materials. The sum of the external field and magnetization scaled by the free space permeability determines the magnetic induction B,

$$B = \mu_o (H_{ext} + M) \qquad 3\text{-}3\text{-}1$$

where $\mu_o = 4\pi \times 10^{-7}$ H/m is the magnetic permeability of free space especially, in free space, M=Ø and 3-3-1 reduces to

$$B = \mu_o H_{ext} \qquad 3\text{-}3\text{-}2$$

Equation 3-3-1 can be rewritten,

$$B = \mu_o H_{ext} (1 + \chi_m) \qquad 3\text{-}3\text{-}3$$

where now, χ_m is the magnetic susceptibility, a dimensionless quantity. By definition, the ratio of the magnetic induction to the applied field is called the magnetic permeability,

$$\mu = \mu_o (1 + \chi_m) \qquad 3\text{-}3\text{-}4$$

All known materials exhibit a non-zero magnetic susceptibility. For most (paramagnetic) materials the magnitude of

susceptibility is small and of positive sign, for some (diamagnetic) materials, it is small and of negative sign. The most common materials which are colloquially regarded as the "magnetic" ones are properly ferromagnetic and may show relative large values of positive susceptibility. The most common of the ferromagnetic minerals are the oxides fo iron (certain ones), nickel and titanium. Further explanation of the common magnetic conditions follows:

Diamagnetism: Diamagnetic materials contain no permanent magnetic dipoles, but dipoles can be induces by an external field. The field of the dipoles opposes the external field and is negative,

$$\chi_m < 0 \qquad 3\text{-}3\text{-}5$$

Paramagnetism: Paramagnetism occurs in substances which contain permanent magnetic dipoles. Paramagnetism occurs when an external magnetic field lines up the permanent dipoles in oppositionto their thermal agitation. For thes group of materials,

$$\chi_p > 0 \qquad 3\text{-}3\text{-}6$$

Ferromagnetism: In ferromagnetics materials, quantum mechanical effects cause the magnetic moments of many electrons to align with each other even in the absence of an external field. Typically,

$$\chi_F > \chi_p \qquad 3\text{-}3\text{-}7$$

also is a function of the external field and past history of magnetization.

Antiferromagnetism: Some substances which contain magnetic ions are not substantially magnetized since every oriented spin couples with an antiparallel spin in a nearby atom so that the net result is zero. Hematite is an example of such a material.

3.3.2 MAGNETIC HYSTERESIS EFFECT

Let us allow that the magnetization, M, is a general polynimial function of the applied field. A Maclaurin's series expansion of M, in the applied field obtains

$$M = A_1 H + A_2 H^2 + A_3 H^3 + \ldots\ldots \qquad 3\text{-}3\text{-}8$$

where A_i are coefficients.

Since we are dealing with low fields in geophysics, the third and higher order terms are often negligible, and thus:

$$M \cong A_1 H + A_2 H^2 \qquad 3\text{-}3\text{-}9$$

This is known as Lord Rayleigh's relationship.

Magnetic materialx may be classed as follows:

A - Soft magnetic materials which show linear effects with the applied field for which A_2 is negligible.

B - Hard magnetic materials that are non-linear with the applied field $A_2 \neq \emptyset$ and possessing a memory of its past magnetization.

To describe the intrinsic magnetic hardness of a ferromagnetic material, it is sufficient to introduce the coercive force H_c and the remanent coercive force M_r. Figure 16 shows the classical hysteresis loop in which $\mu(H)$ is the tangent to the curve at each particular point, and depends upon the applied field. The degree of hysteresis is determined by the area enclosed by the loop. For soft magnetic materials, the hysteresis loop encloses essentially no area. The form of the hysterisis loop is dependent upon mineral grain-size, composition and shape.

For both hard and soft magnetic materials the magnetization tends to a saturation asymptote at very high fields. Saturation requires all dipoles to be magnetized in the direction of the external field so that further magnetization is not possible.

In general equation 3-3-10 can be written in the form,

$$\vec{B} = \mu^*(\omega, H) \cdot \vec{H} \ , \qquad 3\text{-}3\text{-}11$$

but fo the soft magnetic materials which are the basic interest, here, equation 3-3-11 simplifies and

$$\vec{B} = \mu^*(\omega) \cdot \vec{H} \ . \qquad 3\text{-}3\text{-}12$$

Fourier transformation of this obtains the time domain equivalent form:

$$\vec{b}(t) = m^*(t) \cdot \vec{h}(t, r) \ . \qquad 3\text{-}3\text{-}13$$

3.3.3 TEMPERATURE DEPENDENCE OF MAGNETIZATION

All materials are to some extent magnetic in presence of an external field, but ferromagnetic materials can become permanently magnetized through acquiring an ordering energy. Thermal vibrations tend to disorder this magnetization. As long as the ordering energy is larger than the thermal vibration energy the materials maintains ferromagnetic characterisics but when the thermal energy dominates, the material loses its magnetic properties. The limiting temperature for permanent magnetization is the Curie temperature,

$$T_c = \mu_o M/k \ , \qquad 3\text{-}3\text{-}14$$

where k is Boltzmann's Constant 1.38×10^{-6} erg/^oK.

A characteristic curve of ferromagnetic temperature dependence is shown in Figure 17.

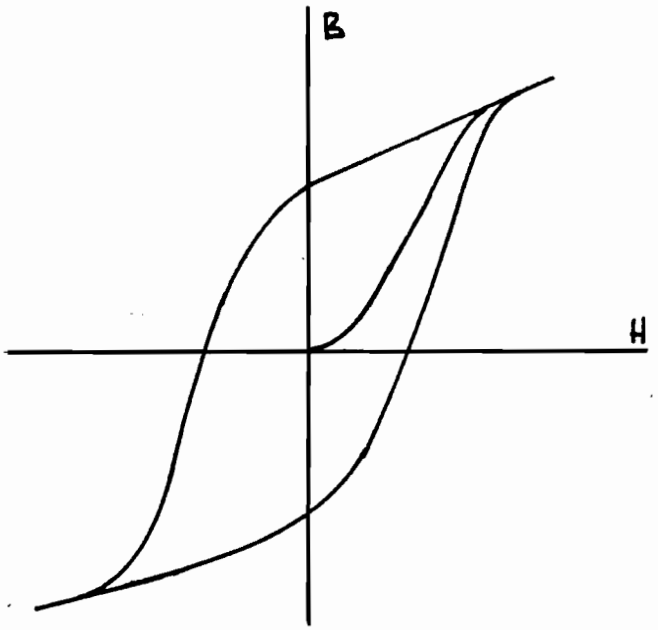

Figure 16. Classical magnetic hysteresis loop.

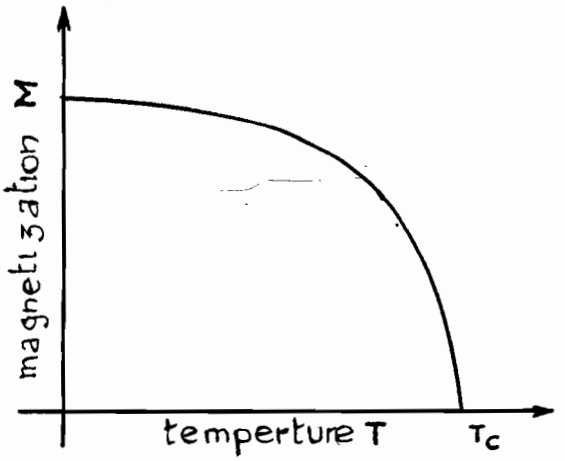

Figure 17. (After Strangway, 1967). Curve of magnetization versus temperature.

3.3.4 MAGNETIC LOSSES

Neel's (1955) model of non-interacting single-domain particles has been used in the description of the magnetization of lunar paricles. The magnetic behavior of lunar samples is dominated by metallic iron grains, a large fraction of which are smaller than 300 Å in diameter and essentially of single-domain. In addition, the low iron content (0.01% to 0.5% by weight) isolates the particles. Consider a sample of N_t non-interacting single-domain iron particles of volume v, suspended in a material of magnetic permeability of μ_o. When a field is applied, thermal interaction will cause N particles to reorient themselves so that there is a net magnetization m parallel to the direction of the applied field. The rate of change of the net magnetization of the N particles is:

$$\frac{dm}{dt} = \alpha\frac{h}{\tau} - \frac{m}{\tau} \qquad 3\text{-}3\text{-}15$$

where

$$\alpha = J_s \, {}^{v}/_{kT}$$

J_s is the saturation magnetization,
h is the applied magnetic field,
T is the absolute temperature,
k is Boltzmann's constant and
τ is the time constant of the system of N particles.

For an applied sinusoidally-varying magnetic field

$$h(t) = h_o \; e^{i\omega t} \qquad 3\text{-}3\text{-}16$$

resulting in magnetization

$$m(t) = m_o \; e^{i\omega t} \qquad 3\text{-}3\text{-}17$$

the total magnetization as a function of the applied field in frequency domain is

$$m_o = \frac{\omega\alpha}{3}\left(\frac{1}{1+i\omega\tau}\right) \quad h_o \qquad 3\text{-}3\text{-}18$$

The ratio m_o/h_o is complex magnetic susceptibility

$$\chi_m = \frac{\omega\alpha}{3}\left(\frac{1}{1+i\omega\tau}\right); \qquad 3\text{-}3\text{-}19$$

the time constant τ is determined by the shape and size of the magnetic grains. In real materials, particles possess different shapes and sizes which produce a distribution of relaxation time constants.

Recalling the similarity between the Kirkwood-Fuoss distribution of relaxation times in dielectrics and the Cole-Cole model, we can recognize its analogy to the following magnetic relaxation model suggested by Olhoeft and Strangway (1974), which also possesses the Cole-Cole behavior.

3.3.5 COLE-COLE MAGNETIC RELAXATION

Magnetic minerals show a measurable magnetic lossiness through various mechanisms. This effect has been measured by Olhoeft and Strangway (1974) in the range of 125 to 4000 Hz.

Magnetic losses can cause distinct but small changes in the electromagnetic response of a medium. The effect can be detected provided the peak magnetic loss is of lower frequency than the electric and dielectric losses.

Olhoeft and Strangway (1974) suggested that a Cole-Cole dispersion with a broad distribution magnetic relaxation times well fitted their data. The complex magnetic permeability can be described

$$\mu^* = \mu' - i\mu'' \qquad 3\text{-}3\text{-}21$$

where

$$\mu' = (1+\chi')\mu_0$$

and

$$\mu'' = \mu_0\chi''$$

so that

$$\mu^* - \mu_\infty = \frac{\mu_s - \mu_\infty}{[1+(i\omega\tau)^\alpha]}$$

where:

$$\mu_\infty = \lim_{\omega\to\infty} \mu' \qquad 3\text{-}3\text{-}22$$

$$\mu_s = \lim_{\omega\to 0} \mu'$$

Since magnetic relaxation is a low frequency effect, the approximation

$$k^2 \simeq -i\sigma\mu^*\omega$$

holds and the propagation constant has the form

$$k = \sqrt{\frac{\omega}{2}}\left[((\kappa^2+\beta^2)^{1/2}+\alpha)^{1/2} - i((\alpha^2+\beta^2)^{1/2}-\alpha)^{1/2}\right],$$

where

$$\alpha = (\mu'\sigma'' - \sigma'\mu''),$$

$$\beta = (\mu'\sigma' + \mu''\sigma'').$$

In the case of negligible conductivity losses

$$k = \sqrt{\frac{\omega\sigma'\mu''}{2}} \left[((1+\delta^2)^{1/2}+1)^{1/2} - i\,((1+\delta^2)^{1/2}-1)^{1/2} \right] \qquad 3\text{-}3\text{-}23$$

where

$$\delta = \mu'/\mu''$$

Figure 18 compares Galt's (1952) data for single crystal magnetics with relaxation curves with = 0.67, allowing a relatively broad distribution of relaxation times. In fact, the distribution is typically broader for magmetic relaxation than for electrical and dielectric relaxation. Figure 19 shows the variation of the loss tangent with changing quantities of magnetite in artificial samples. Experimentally, the magnetic loss peaks for magnetite in the audio-frequency range neat 350-1000 Hz independent of geometry. The effect of magnetic dispersion and absorption, is small in comparision to the equivalent eletrical effects and is usually insignificant in most geophysical materials. Only in highly resistive rocks for which the electrical losses in the audio-frequency range are small does the magnetic loss become an important background effect.

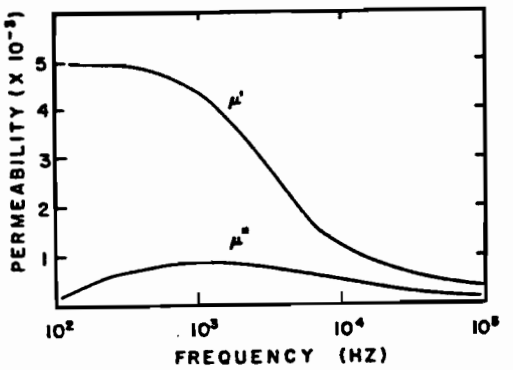

Galt (1952) single crystal magnetite permeability spectrum.

Figure 18. (After Olhoeft and Strangway, 1974)

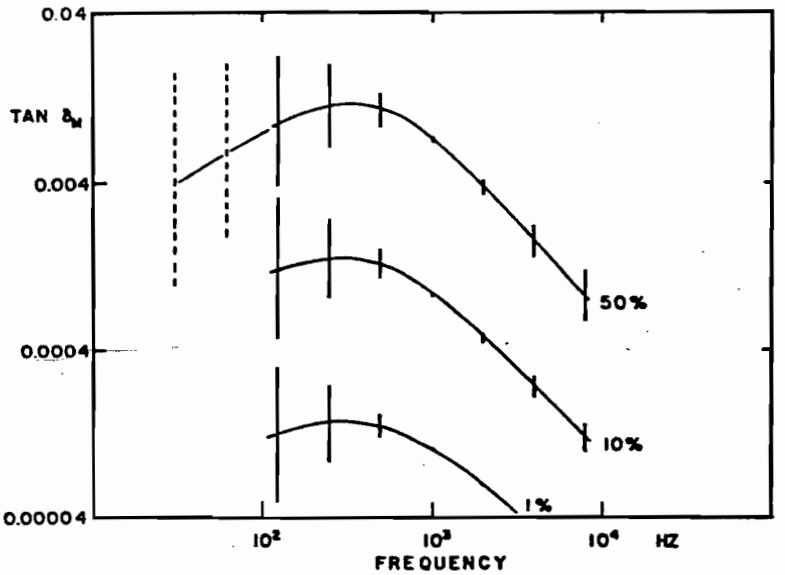

Several loss tangent spectra for artificial samples with varying magnetite content; the weight percentages of magnetite are indicated.

Figure 19. (After Olhoeft and Strangway, 1974).

CHAPTER IV

4.1 APPARENT DIELECTRIC PERMITTIVITY AND CONDUCTIVITY

Recall equation 2-2-13 which determines the propagation constant, k,

$$k^2 = \omega^2 \mu^* \epsilon^* - i\sigma^* \mu^* \omega \qquad 4\text{-}1\text{-}1$$

Ferromagnetic materials exepted, in general, the magnetic polarization of most materials is so weak that μ^* can be replaced by μ_o, the permeability of free space, for all practical purposes. If we now substitude for the real and imaginary components of permittivity and conductivity, we find,

$$k^2 = \omega^2 \mu (\epsilon' + \sigma''/\omega) - i\mu\omega (\sigma' + \omega\epsilon''). \qquad 4\text{-}1\text{-}2$$

and rewriting this equation, we form

$$k^2 = \omega^2 \mu \epsilon_e - i\mu\omega\sigma_e \qquad 4\text{-}1\text{-}3$$

where the subscript e stands for "effective" and defines the total in-phase and total quadrature components see Figure 2Ø).

$$\epsilon_e(\omega) = \epsilon'(\omega) + \sigma''(\omega)/\omega \qquad 4\text{-}1\text{-}4$$

$$\sigma_e(\omega) = \sigma'(\omega) + \omega\epsilon''(\omega) \qquad 4\text{-}1\text{-}5$$

The parameters which are actually, or perhaps more properly

apparently, measured are $\sigma_e(\omega)$ and $\epsilon_e(\omega)$, (Fuller and Ward, 1970). Thus the measured conductivity and permittivity are a combination of the true parameters. In fact, most substances, substances in addition to their dielectric properties, have free moving charges. Upon the application of an electric field the mechanism of absorption due to the charge transport toward the electrodes contributes to the dielectric losses. Inspection of equations 4-1-4 and 4-1-5 leads us to expect large $\epsilon_e(\omega)$'s at low frequencies if $\sigma''(\omega) \neq 0$ and large $\sigma_e(\omega)$ at high frequencies if $\epsilon''(\omega) \neq 0$.

Observations show that in moist rocks, conductivity increases with frequency, but levels off around a "critical" frequency (Fuller and Ward, 1970). Permittivity, however, decreases continually with increasing frequency. This is in agreement with the above equations. At very low frequencies, some rocks show an abnormally high permittivity (e.g. $\epsilon_e = 10^4 \epsilon_o$ for shale with 3.8% pore electrolite by volume, (figure 20). These high values are simply due to the ω^{-1} factor in equation 4-1-4, and are not in any way the characteristic of the medium. Some approximations are possible in the following cases:

For "wet" rocks, we can reasonably expect free charge conduction to be the dominant mechanism. By letting:

$$\sigma'(\omega) \gg \omega\epsilon''(\omega) \quad \text{and} \quad \sigma''(\omega) \gg \omega\epsilon'(\omega)$$

the following approximation will hold:

$$\sigma_e(\omega) \cong \sigma'(\omega) \qquad 4\text{-}1\text{-}6$$

$$\epsilon_e(\omega) \approx \sigma''(\omega)/\omega \qquad 4\text{-}1\text{-}7$$

Fuller and Ward's observations for wet rocks show that the conductivity is a slowly varying function of ω. In 6 orders of frequency the conductivity seldom exceeds one order of magnitude ($\sigma \approx 10^{-1}$ and 10^{-5} S/m). The dielectric permittivity is typically inversely proportional to the frequency and can reach values beyond 10^7 below 1Hz (see Figure 21). At high frequencies, though, the dielectric constant assymptotes to $80\epsilon_0$ which is the dielectric constant of water.

For "dry" rocks, the opposite approximation holds:

$$\epsilon'(\omega) >> \sigma''(\omega)/\omega \quad \text{and} \quad \epsilon''(\omega) >> \sigma'(\omega)/\omega$$

Thus

$$\sigma_e(\omega) \cong \omega \epsilon''(\omega) \qquad 4\text{-}1\text{-}8$$

and

$$\epsilon_e(\omega) \cong \epsilon'(\omega) \qquad 4\text{-}1\text{-}9$$

The observed data shows a conductivity approximately proportional to the frequency ($\sigma \cong 10^{-6}$ to 10^{-12} S/m) and a dielectric permittivity decreasing slowly with frequency such that for 6 orders of frequency it varies about one order of magnitude (Figure 22).

Complex dielectric permittivity values have been measured above 20MHz by Poley et al. Their measurements for sandstones with 15% porosity showed that for dry samples ϵ' showed small decrease with frequency while an air-humid sample has an increasing ϵ' toward lower frequencies. Salt water saturated samples also showed an increasing contribution of ϵ' with

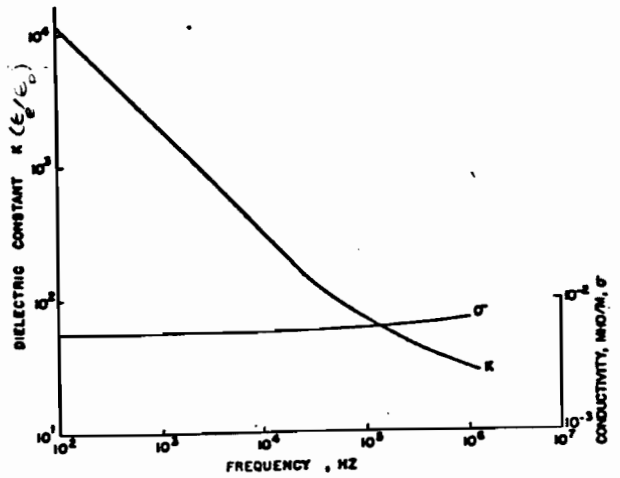

Dielectric constant and electrical conductivity spectra of a shale with 3.8 percent pore electrolyte by volume [27] measured by two-electrode cell.

Figure 20. (After Fuller and Ward, 1970).

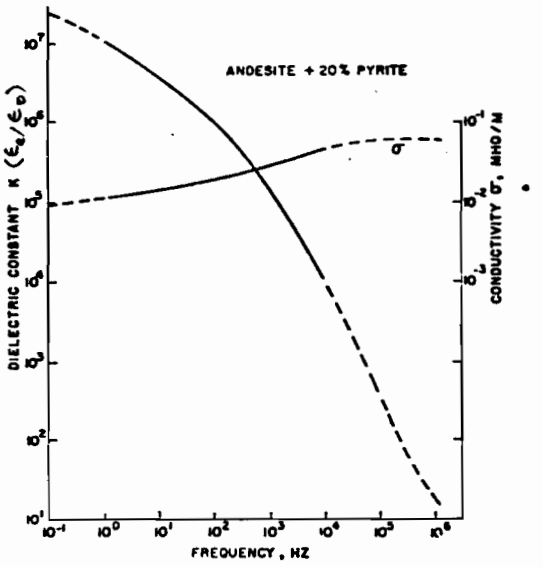

Dielectric constant and electrical conductivity spectra for a synthetic *mineralized rock* made of a mixture of 20 percent pyrite (FeS^2) grains in andesite grains with NaCl as the electrolyte. A four-electrode cell was used.

Figure 21. (After Fuller and Ward, 1970).

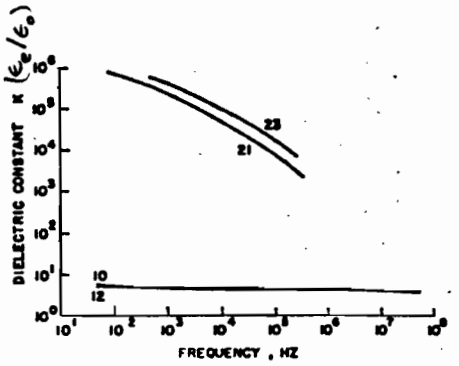

Dielectric constant spectra of four specimens of sandstone from the Morrison formation in the Colorado Plateau. Specimens 10 and 12 were "dry" while specimens 21 and 23 were "wet" [16].

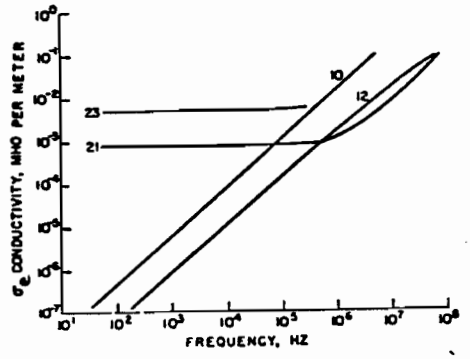

Conductivity spectra of four specimens of sandstone from the Morrison formation in the Colorado Plateau. Specimens 10 and 12 were "dry" while specimens 21 and 23 were "wet" [16].

Figure 22. (After Fuller and Ward, 1970). Dielectric constant and electrical conductivity of four specimens of sandstone from the Morrison formation in the Colorado Plateau. Specimens 10 and 12 were dry, while specimens 21 and 23 were wet.

frequency up to a critical frequency where the curve levels off. Very high values of ϵ' were found at lower frequencies. All these measurements are in agreement with the above approximations but we must not forget that these are approximations and so must be used carefully. Often, these approximations have been considered to hold in general, but we shall avoid this assumption here.

The above discussion applies properly to homogeneous media. Fuller and Ward's measurements on rock salt has shown dispersion to be practically absent, and with very low quadrature components which means that it allows an appreciable depth of field penetration.

4.1.1 INVERSION OF RESISTIVITY

Fitting of real resistivity data with the effective resistivity equations 4-1-4, 4-1-5 and the Cole-Cole conductivity and resistivity has been attempted in demonstration of the need for more complex electromagnetic models. The resistivity data used here were obtained by Olhoeft (1975), for clay permafrost at $-27^{o}C$, for which there is a notable decrease of apparent effective resistivity with frequency in the range of 10^{3}Hz to 10^{7}Hz. The inversion method used in the following analysis is the "singular value decomposition" approach.

First, equation 4-1-5 was modelled with constant

permittivity and conductivity with frequency (see table 3). The inversion resulted in the following parameters:

$$\sigma' = 0.1772E\text{-}5 \text{ S/m},$$

$$\epsilon'' = 40.35 \quad \epsilon_o \text{ F/m}$$

and

$$\Delta = 0.158.$$

The ϵ'' value is not realistic and the relative error measure for the inversion is very large. Next, a Cole-Cole dielectric permittivity and a constant conductivity model was considered. The fit was less reliable than that of the first case above, the reason being that the data describe effective resistivity values and so we cannot expect these data to well determine the dielectric constant. Next, the same equation was modelled with a Cole-Cole resistivity and imaginary permittivity; the results obtained were:

$$\epsilon'' = 43.1 \quad \epsilon_0 \text{ F/m},$$

$$\rho_o = 47.36E+4 \quad \Omega m,$$

$$\rho_\infty = 5.687 \quad \Omega m,$$

$$f_c = 2.14E+4 \text{ Hz},$$

$$\alpha = 0.958$$

and

$$\Delta = 0.299E\text{-}1. \qquad 4\text{-}1\text{-}11$$

The error, clearly, has been decreased by almost one order of magnitude, (see table 3), consequently we have adopted this latter model instead of the first. We can further improve the model by considering both Cole-Cole resistivity and permittivity models. The results are as follows:

ρ_o = Ø.4364E+6 Ωm ϵ_o = 4Ø.35 $\epsilon_Ø$F/m

ρ_∞ = 5.68 Ωm ϵ_∞ = 2.67 $\epsilon_Ø$ F/m 4-1-12

f_r = 135.5 Hz f_c = 849.7 Hz

α_r = Ø.92 α_c = Ø.122

with a relative error,

Δ = Ø.21E-2,

one order of magnitude smaller than for the previous case. See Figure 23.

A similar fitting for the same clay permafrost at -1Ø°C has also been accomplished using a combined resistivity-permittivity Cole-Cole dispersion models:

ρ_o = Ø.2819E+6 Ωm ϵ_o = 4Ø.35 $\epsilon_Ø$ F/m

ρ_∞ = 7.Ø6 Ωm ϵ_∞ = 2.98 $\epsilon_Ø$ F/m 4-1-13

f_r = 61.62 Hz f_c = 838.4 Hz

α_r = Ø.87 α_c =Ø.122

Δ = Ø.17E-2.

See Figure 24.

Above, we discovered that the Cole-Cole parameters and especially the relaxation time are frequency dependent and shift toward lower values with increasing temperature which accords with these results. Olhoeft's (1975) resistivity data for ice at -27°C has been fitted with two Cole-Cole dispersion functions to obtain:

ρ_o = Ø.6912E+6 Ωm ϵ_o = 7Ø.32 $\epsilon_Ø$ F/m

ρ_∞ = 2.52 Ω m

ϵ_∞ = 24.70 ϵ_0 F/m

4-1-20

f_r = 2.07 Hz

f_c = 4645. Hz

α_r = 0.92

α_c = 0.122

Δ = 0.105E-1.

See Figure 25.

A joint inversion has been performed on two sets of data after Carmichael (1982), belonging to the effective resistivity and permittivity of serpentinite at 200°C, (see Figure 26). The listing of the program is provided in appendix B. The relative error in the data is higher by one order of magnitude than the previous fit, that results from using a joint inversion. The fitted parameters of the combined resistivity/permittivity Cole-Cole models are as follows:

ρ_o = 0.4827E+5

ϵ_o = 40.56

ρ_∞ = 0.7590E+3

ϵ_∞ = 2.0

f_r = 0.2070E+4

f_c = 0.200E+3

α_r = 0.55

α_c = 0.95

Δ = 0.121

Toble 3. Observed and fitted resistivity values for various models

FREQUENCY (HZ)	OBSERVED RESISTIVITY ϱM	FITTED WITH TWO COLE-COLE PARAMETERS ϱM	FITTED WITH COLE-COLE RESISTIVITY ϱM	FITTED WITH CONSTANT AND ϱM
0.2153E+2	0.4642E+6	0.4266E+6	0.4622E+6	0.5494E+6
0.4645E+2	0.4500E+6	0.4168E+6	0.4498E+6	0.5330E+6
0.1000E+3	0.4472E+6	0.3957E+6	0.4252E+6	0.5010E+6
0.2153E+3	0.3412E+6	0.3545E+6	0.3803E+6	0.4435E+6
0.4645E+3	0.2851E+6	0.2855E+6	0.3096E+6	0.3555E+6
0.1000E+4	0.1875E+6	0.2045E+6	0.2211E+6	0.2492E+6
0.2153E+4	0.1259E+6	0.1379E+6	0.1367E+6	0.1516E+6
0.4645E+4	0.7943E+5	0.8799E+5	0.7470E+5	0.8207E+5
0.1000E+5	0.5012E+5	0.5221E+5	0.3757E+5	0.4134E+5
0.2153E+5	0.2512E+5	0.2882E+5	0.1791E+5	0.1999E+5
0.4645E+5	0.1259E+5	0.1401E+5	0.8207E+4	0.9445E+4
0.1000E+6	0.6310E+4	0.7303E+4	0.3656E+4	0.4428E+4
0.2153E+6	0.3162E+4	0.3503E+4	0.1593E+4	0.2066E+4
0.4645E+6	0.1292E+4	0.1642E+4	0.6897E+3	0.9604E+3
0.1000E+7	0.7055E+3	0.6981E+3	0.3040E+3	0.4474E+3
0.2153E+7	0.3055E+3	0.2701E+3	0.1384E+3	0.2088E+3
0.4645E+7	0.9333E+2	0.9520E+2	0.6506E+2	0.9770E+2
0.1000E+8	0.3428E+2	0.3308E+2	0.3198E+2	0.4628E+2
0.2153E+8	0.1233E+2	0.1334E+2	0.1672E+2	0.2240E+2
0.4645E+8	0.6580E+1	0.6339E+1	0.6197E+1	0.1614E+2
Δ		0.2101E-2	0.2986E-1	0.1583E+ 0

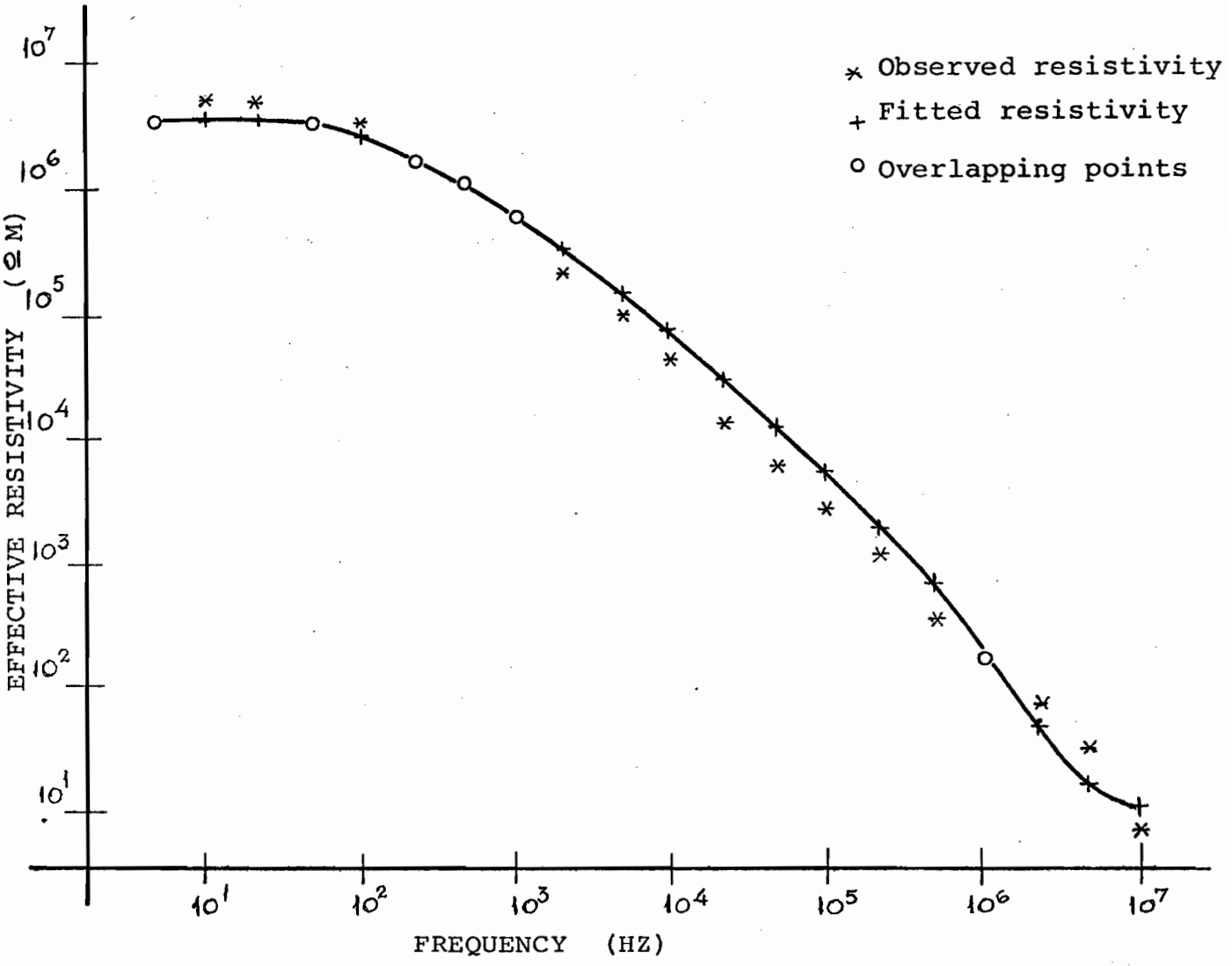

Figure 23. Effective resistivity versus frequency for natural clay permafrost at -27°C. (After Olhoeft, 1975). Note that Olhoeft uses the nomenclature real resistivity where we use effective resistivity. The field strength is 22V/cm.

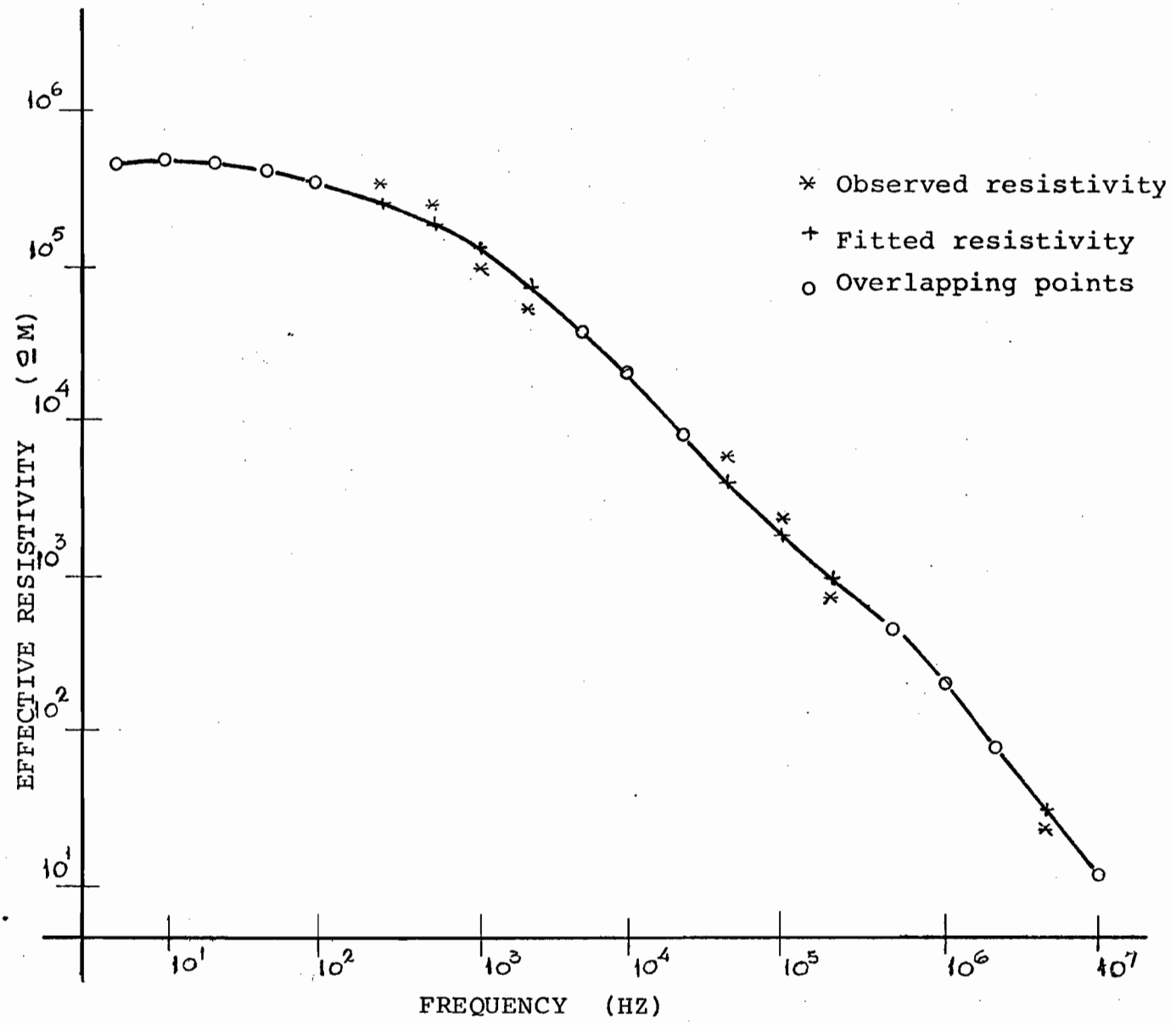

Figure 24. Effective resitivity versus frequency for natural clay permafrost at -10°C. (After Olhoeft, 1975). The field strength is 22V/cm.

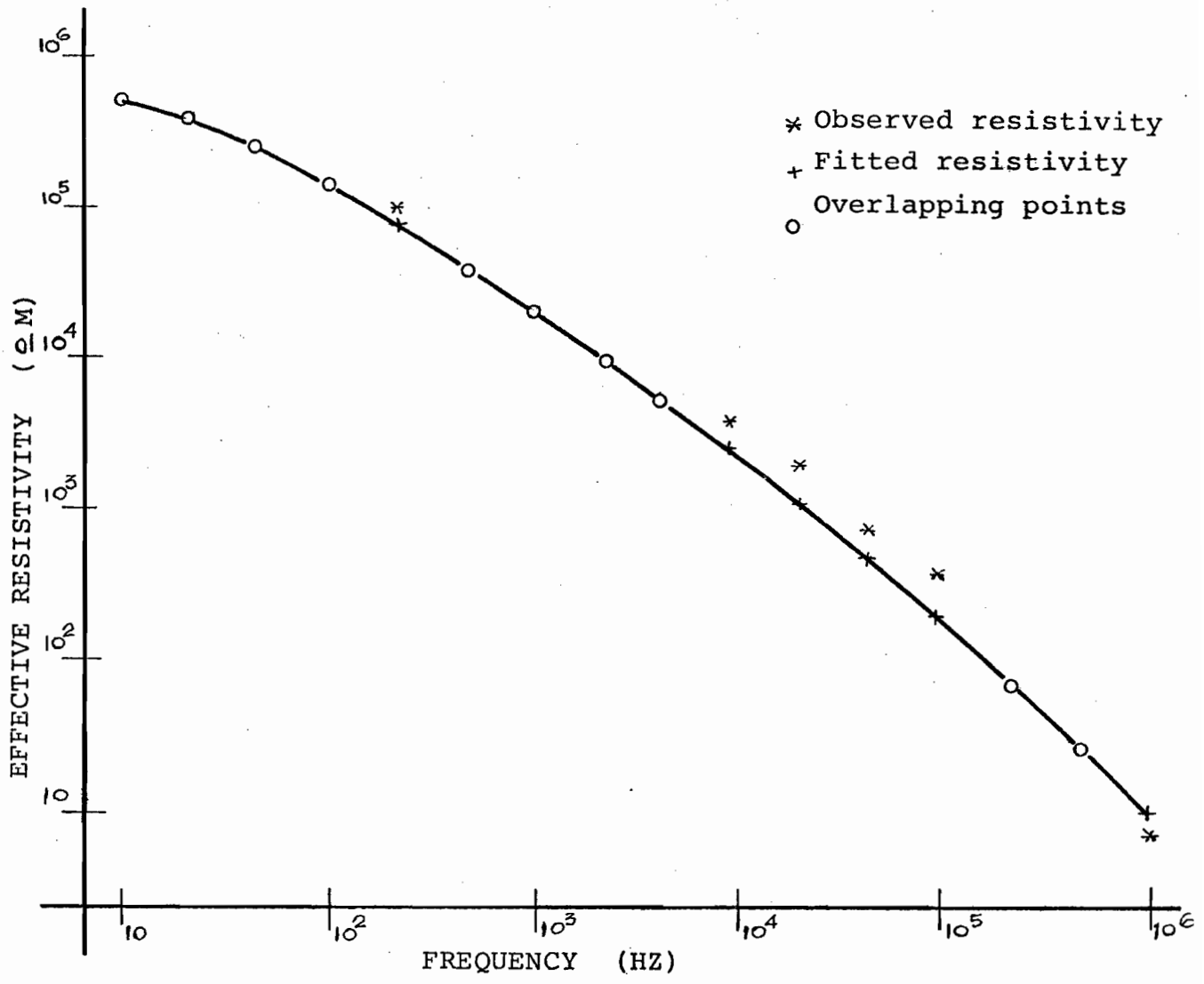

Figure 25. Effective resitivity versus frequency for natural ice core, at -27°C. (After Olhoeft, 1975). The field strength is 22V/cm.

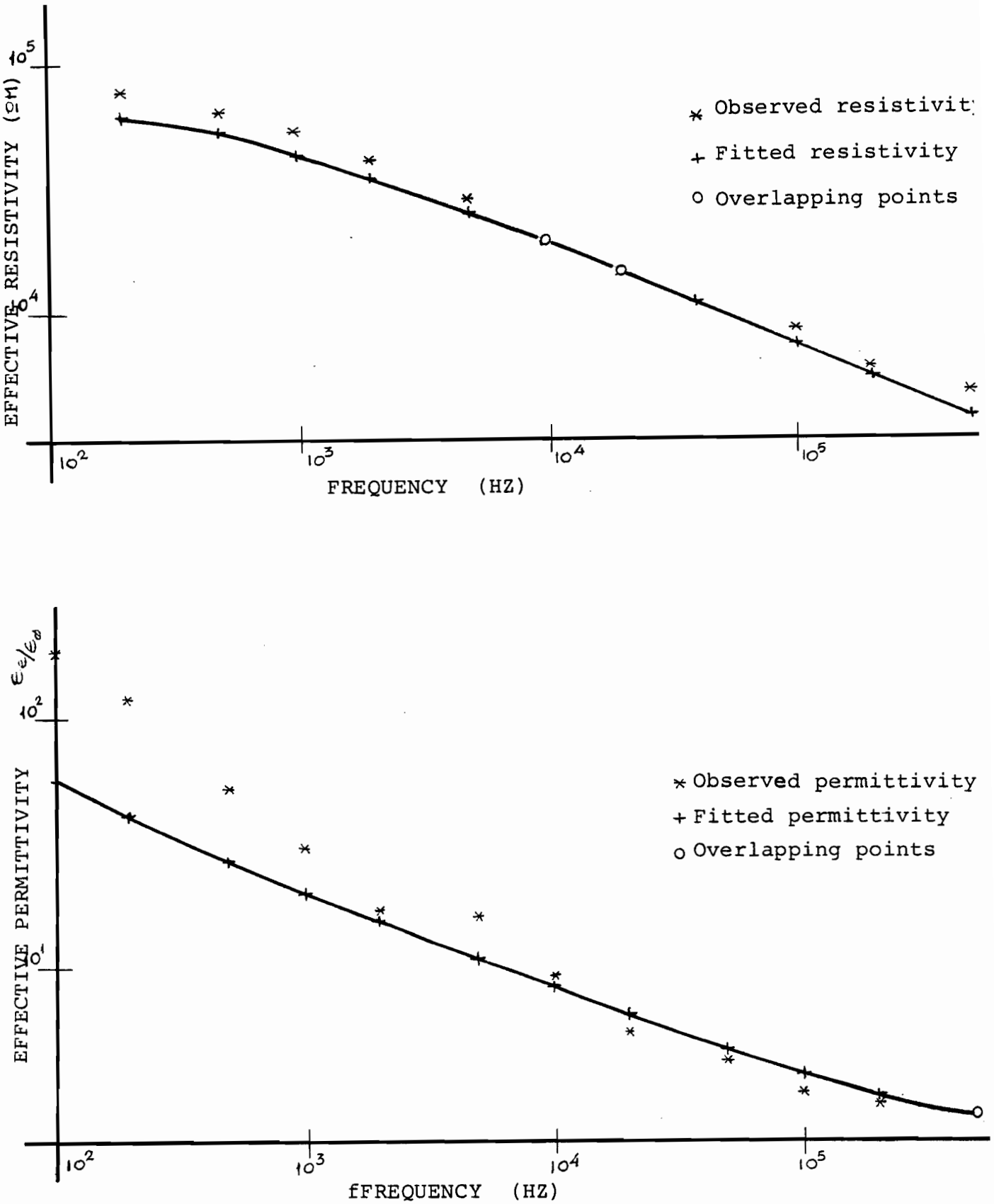

Figure 26. Fitted and observed effective resistivity and permittivity of serpentinite at 200°C, versus frequency. (After Carmichael, 1982). The above two curves were simultaneously inverted.

4.2 FORMATION FACTOR

One of the parameters calculated from rock properties is the so-called formation factor F. At VHF it is determined as (Sen et al., 1981)

$$F = \phi^{-m} = \frac{\epsilon''_w}{\epsilon''_o} \qquad 4\text{-}2\text{-}1$$

where ϕ is the porosity of the rock,

ϵ''_w is the imaginary part of the complex dielectric permittivity of a non-saturated salt-water solution,

ϵ''_o is the imaginary component of the complex dielectric permittivity of a salt-water saturated formation,

m is the cementation index which varies between 1.3 and 4. and is determined empirically.

At low frequencies, the equivalent measure is

$$F = \frac{\sigma_w}{\sigma} = \phi^{-m} \qquad 4\text{-}2\text{-}2$$

where σ_w is the dc conductivity of water and

σ is the conductivity.

The similarity of these two equations allows one to describe a more general, combined equaton for the formation

factor:

$$F = \phi^{-m} = \frac{[\epsilon''(\omega)+\sigma'(\omega)/\omega]_w}{[\epsilon''(\omega)+\sigma'(\omega)/\omega]_o} \qquad 4\text{-}2\text{-}3$$

where the subscript (o) stands for the measurement done for the sample and (w), the measurement for salt-water. Equation 4-2-3 reduces to equation 4-2-1 at VHF and to equation 4-2-2 at LF.

Archie's empirical law is

$$F \propto \phi^{-m} \qquad 4\text{-}2\text{-}4$$

and depending to the sample studied (see Sen et al.) it has been suggested to have the forms, $a\phi^{-m}$, $a(\phi-\phi_c)^{-m}$, $2\phi(3-\phi)^{-1}$, and also other forms can be encountered in the literature. The absence of the percolation threshold, $\phi_c = 0$, implies that the fluid phase remains essentially continuous to very low values of porosity and that pores are stongly interconnected. In general, the branching nature of the pore space in sedimentaty rocks is more complex than the simple networks usually assumed in theoretical models. There have been attempts to obtain formulae for the relationship between dielectric constants of a medium and its porosity which involves ellipsoidal particles and depolarization factors (Ziman, 1979 and Sen et al., 1981).

4.3 DIELECTRIC RESPONSE IN AN HETEROGENEOUS MEDIUM

Real data do not always show simple relaxation curves (Figure 27). To fit such measurements, more than one Cole-Cole dispersion must be considered. For example, let us consider a

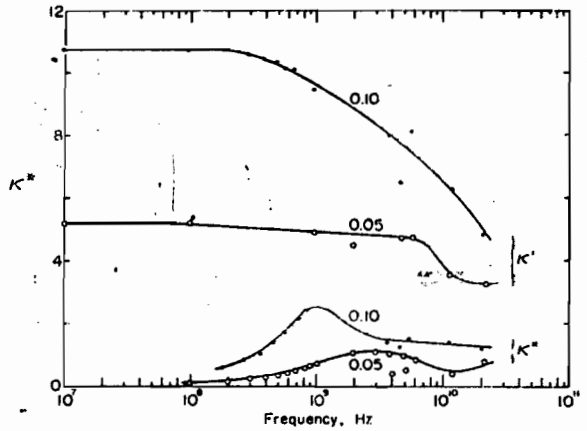

The complex dielectric constant of Goodrich clay at 24°C as a function of frequency at two water contents (g H_2O/g soil).

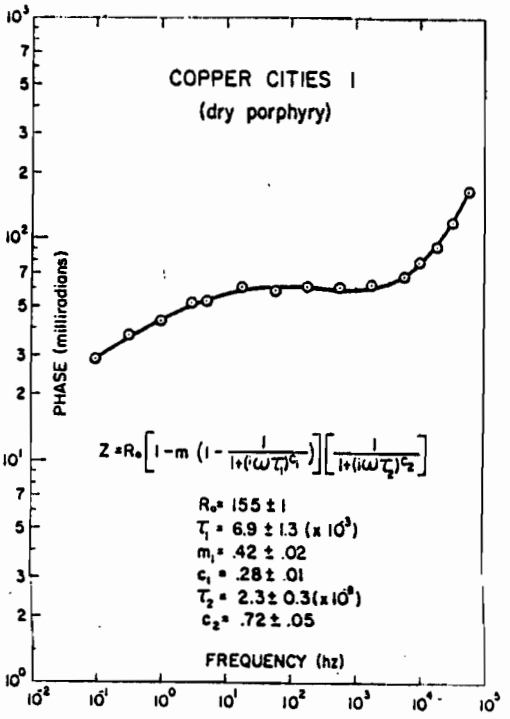

Phase angle spectra from the Copper Cities porphyry copper deposit in the Globe-Miami district of Arizona. Dipole-dipole array, $n = 1$, $x = 1$ m.

After Hoekstra and Delaney, 1974. After Pelton et al., 1976.

Figure 27.Permittivity and resistivity curves versus frequency do not always show simple Cole-Cole relationships.

porous rock matrix with permittivity ϵ_1^* and pores filled with water of permittivity ϵ_2^*. In such heterogeneous situations, the dielectric behavior of the system can be expected to show an average dielectric property ϵ_a^* plus a small difference from the average. In the solid-state physics of a disordered system, the exact field is computed in terms of multiple scattering theory in which these difference-fluctuations from the average medium are treated as perturbations. The combined dielectric constant ϵ^* computed from the macroscopic polarization of the system is found to be (Webman etal., 1977.)

$$\epsilon^* = \epsilon_a^* \left(1 + 2\sum_i f_i \frac{\epsilon_i^* - \epsilon_a^*}{\epsilon_i^* + 2\epsilon_a^*}\right)\left(1 - \sum_i f_i \frac{\epsilon_i^* - \epsilon_a^*}{\epsilon_i^* + 2\epsilon_a^*}\right), \qquad 4\text{-}3\text{-}1$$

where

ϵ^* = combined dielectric permittivity,

ϵ_a^* = dielectric permittivity of the equivalent homogeneous medium,

ϵ_i^* = local dielectric permittivity and

f_i = volume fraction of the i^{th} phase.

For a two-component system with a small concentration x of material ϵ_2^* imbedded as isolated spheres in ϵ_1^*, we can chose $\epsilon_a^* = \epsilon_1^*$ so that:

$$\frac{\epsilon^* - \epsilon_1^*}{\epsilon^* + 2\epsilon_1^*} = x\,\frac{\epsilon_2^* - \epsilon_1^*}{\epsilon_2^* + 2\epsilon_1^*} \qquad 4\text{-}3\text{-}2$$

or

$$\epsilon^* = \epsilon_1^*\,\frac{[\epsilon_2^*(1+2x) + 2\epsilon_1^*(1-x)]}{[\epsilon_1^*(1+2x) + \epsilon_2^*(1-x)]}\,, \qquad 4\text{-}3\text{-}4$$

This equation was derived by Bottcher (1952) and is called the "Average t-matrix Approximation", (ATA). Sen et al.,(1981) suggested a model they have called the "Coherent Potential Approximation", (CPA), in which the dielectric permittivity

of the medium is equal to that of the equivalent homogeneous model ϵ_o^* instead of being equal to that of the host rock ϵ_1^*. CPA treats all components symmetrically whereas ATA selects one as a host rock. Equation 4-3-4 for CPA obtains

$$\sum f_i \left[\frac{\epsilon_i^* - \epsilon^*}{[\epsilon_i^* + 2\epsilon^*]}\right] = 0. \qquad 4\text{-}3\text{-}5$$

Sen et al.,(1981) noted that the corrections for ϵ^* beyond CPA are 4th order in the transition matrix, while for ATA they are 2nd order. In practice CPA better agrees with experiments. The model Sen et al.,(1981) deal with describes large clusters of grains which are individually surrounded by water in which small separated grains exist. The model comprises large spheres coated with a water film containing small spheres (see Sen et al. ,1981 for details). The overall dielectric permittivity of such materials, is then

$$\frac{\epsilon_m^* - \epsilon^*}{\epsilon_m^* - \epsilon_w^*} \left(\frac{\epsilon_w^*}{\epsilon^*}\right)^{L_j} = \phi \qquad j = x, y, z \qquad 4\text{-}3\text{-}6$$

where L is the depolarizing factor associated with the i-axis along which the field is impressed,

ϵ^*_m is the dielectric permittivity of the grains and

ϵ^*_w is the dielectric permittivity of water.

The depolarizing factor depends upon the aspect ratio of the grains and is equal to 1/3 for spherical grains. The dielectric permittivity of the medium can be obtained given $_m$, $_w$ and . For the ATA model the equivalent equation becomes

$$\frac{\epsilon_w^* - \epsilon^*}{\epsilon_w^* - \epsilon_m^*} \left(\frac{\epsilon_m^*}{\epsilon^*}\right)^{L} = 1 - \phi \qquad 4\text{-}3\text{-}7$$

Although these two equations are similar, the former results in the following limiting cases

$$\omega \longrightarrow 0 \qquad \sigma = \sigma_w \phi^{1/2 L} \qquad 4\text{-}3\text{-}8$$

$$\omega \longrightarrow \infty \qquad \frac{\epsilon' - \epsilon'_m}{\epsilon'_w - \epsilon'_m} \left(\frac{\epsilon'_w}{\epsilon'}\right)^L = \phi \qquad 4\text{-}3\text{-}9$$

for $\epsilon'_m \ll \epsilon'_w \qquad \epsilon' = \epsilon_w \phi^{3/2} \qquad 4\text{-}3\text{-}10$

while the latter results in zero DC conductivity.

4.3.1 EXPERIMENTAL RESULTS

Figure 28 shows the low frequency (120 Hz), in-phase conductivity measurements for artificial rocks saturated with 10., 1, and 0.1 ≅ m NaCl solutions and is in agreement with equation 4-3-8. The value of drops as low as 2% and we dont have zero conductivity.

At 1.1 GHz, measurements (figure 29) of real and imaginary components of ϵ^* have been obtained for varying porosity. The agreement with the above mentioned theory is excellent. At high frequencies, the imaginary component is $\epsilon' + \sigma'/\omega$ while the real remains ϵ' since $\sigma''/\omega \ll \epsilon'$.

4.4 POROSITY, WATER CONTENT AND SALINITY

Poley et al. (1978), Katsube and Collett (1976), Pelton et al. (1978) carried out measurements of electrical properties of rocks over a wide range of frequencies. If a substance has a conductivity, this will mainly determine its electric behavior

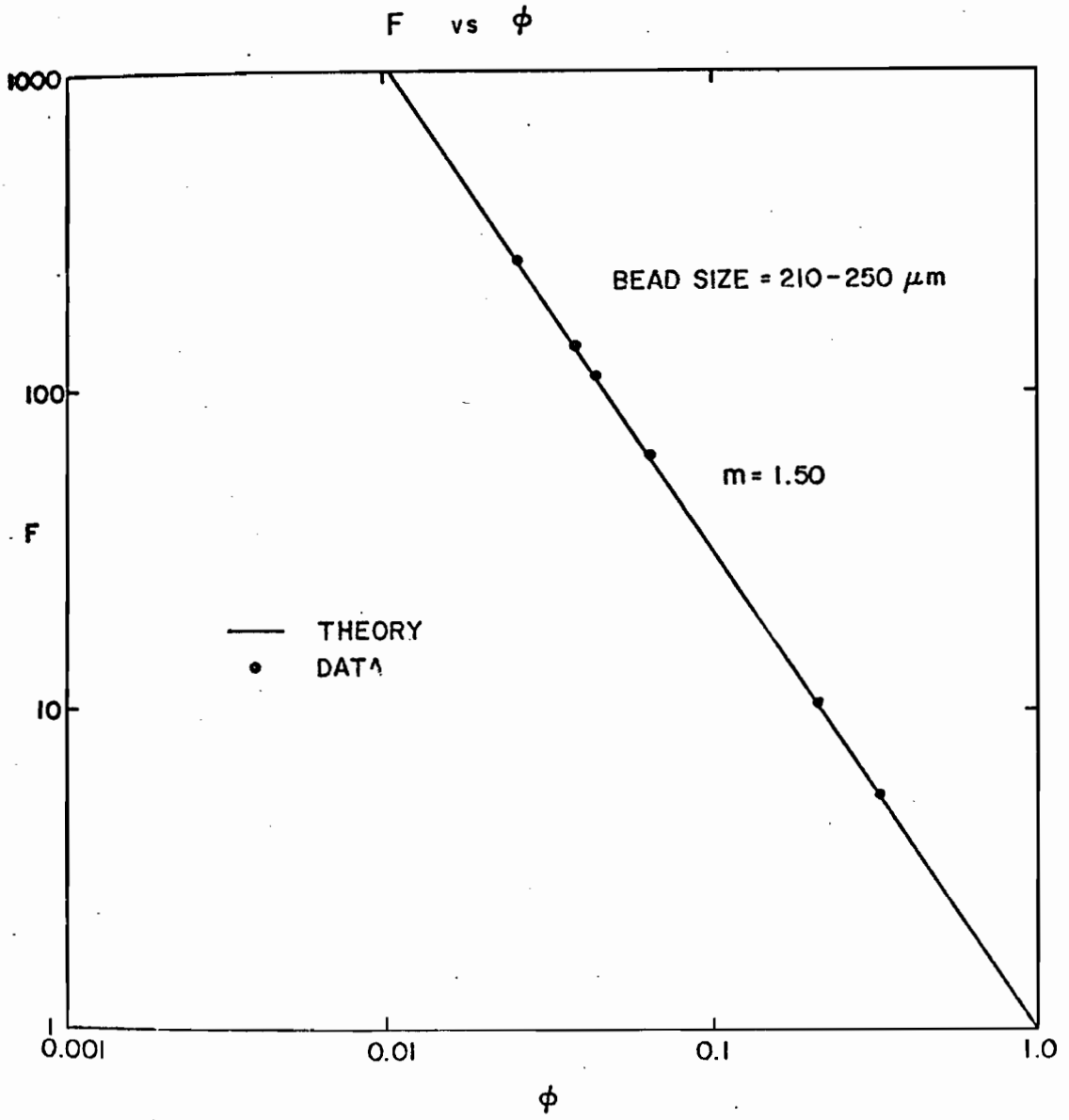

Conductivity of fused glass beads as a function of porosity showing $\sigma = \sigma_w \phi^{3/2}$ behavior. The size of grains in the self-similar model can all be the same (as here) or all different. Hanai Bruggeman formula would give $\sigma = 0$ for $\phi \simeq 0.5$.

Figure 28. (After Sen et al., 1981).

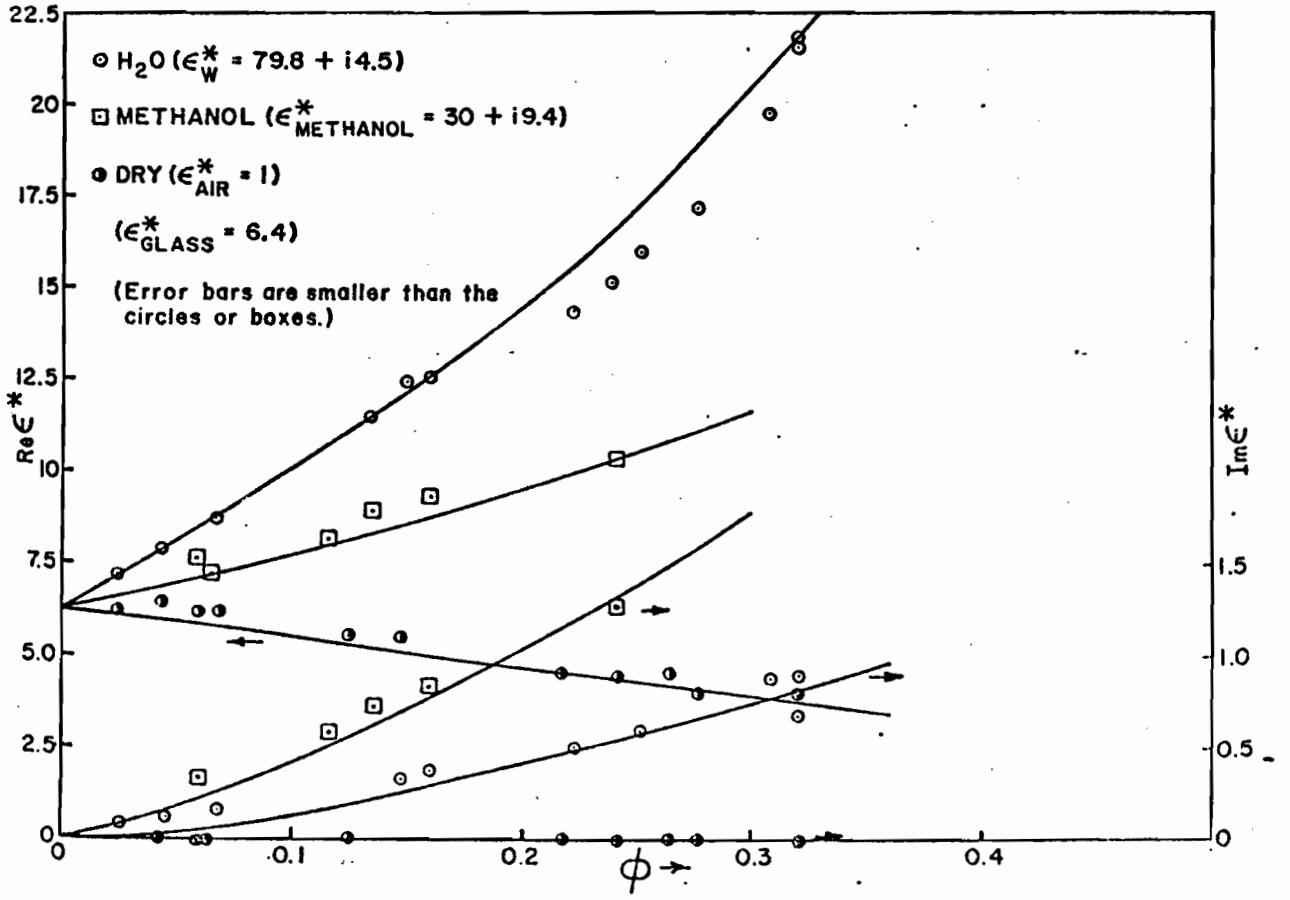

Real part ε' and imaginary part $\varepsilon'' + \sigma/\omega\varepsilon_0$ of the dielectric constant ε^* for fused glass beads at 1.1 GHz as a function of porosity aturated with distilled water, methanol, and air, respectively (measured by us). The lines are theoretical predictions. The dielectric con- of pure water and methanol at 1.1 GHz are (79.8 + *i*4.5) and (30 + *i*9.4), respectively. The value of ε'_m for glass is 6.4.

Figure 29. (After Sen et al., 1981).

at lower frequencies but this properties influence will decline rapidly toward high frequencies and the dielectric propertiy becomes significant beyond 10 KHz. By combining some logging data with VHF measurements of rock properties, fluid saturation, porosity, fluid salinity and formation factors might be deduced.

A series of sandstone and limestone samples with porosity of 6 to 26% were measured by Poley et al (1978) under various conditions of fluid saturation. These measurements showed that electrical parameters are strongly porosity dependent with real and imaginary dielectric permitivitties increasing with increasing porosity, while conductivity decreases with porosity (figure 30).

In water saturated porous formations, such as sandstone and volcanic rocks, the moisture content greatly affects the bulk dielectric permittivity since the DC dielectric constant of water is 80 ϵ_0. Furthermore, also the magnitude of ' generalyy increases with salinity. At VHF (above 10^8Hz), the real dielectric permittivity becomes virtually insensitive to salinity and thus insensitive to the nature of the water filling the pores and is dependent only upon the amount of water present. This is particularly important in geophysical mearurement since the water salinity is often unknown due to fresh water, CO_2 and chemical flooding. In water saturated formations at VHF ϵ' may serve as porosity indicator when the bulk permittivity of the rock matrix is known.

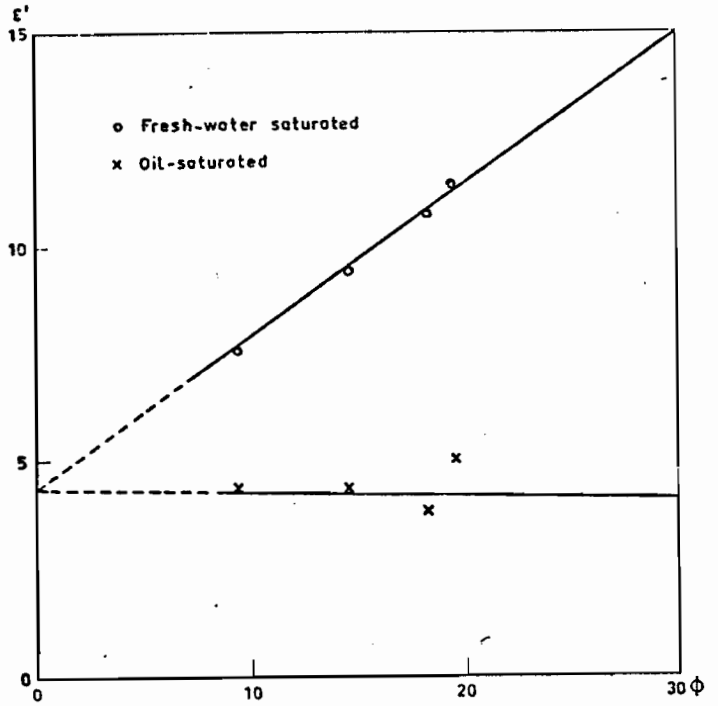

ϵ' Versus ϕ for Water-Saturated and Oil-Saturated Sandstones f = 1200 MHz

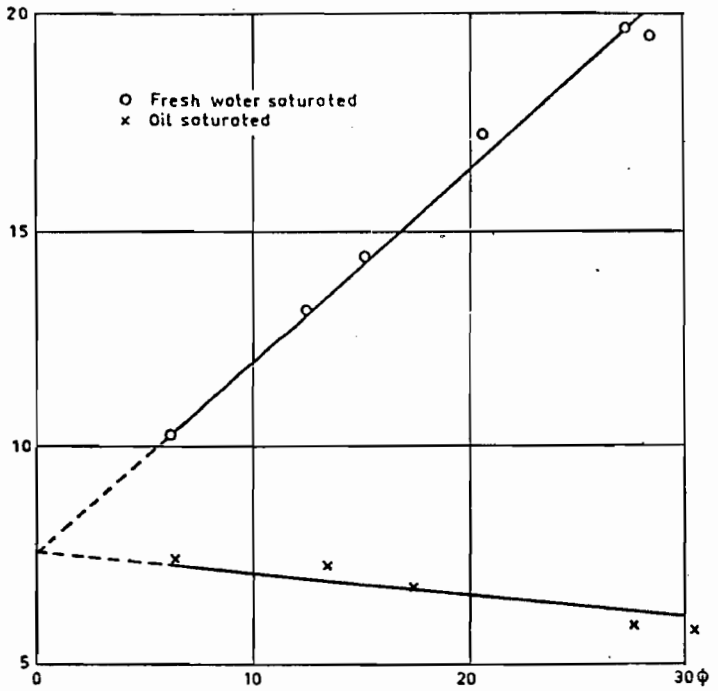

ϵ' Versus ϕ for Water-Saturated and Oil-Saturated Limestones (Calcites) f = 1200 MHz

Figure 30. (After Poley et al., 1978). ϵ' versus ϕ for water-saturated and oil-saturated limestones and sandstones at 1200 MHz.

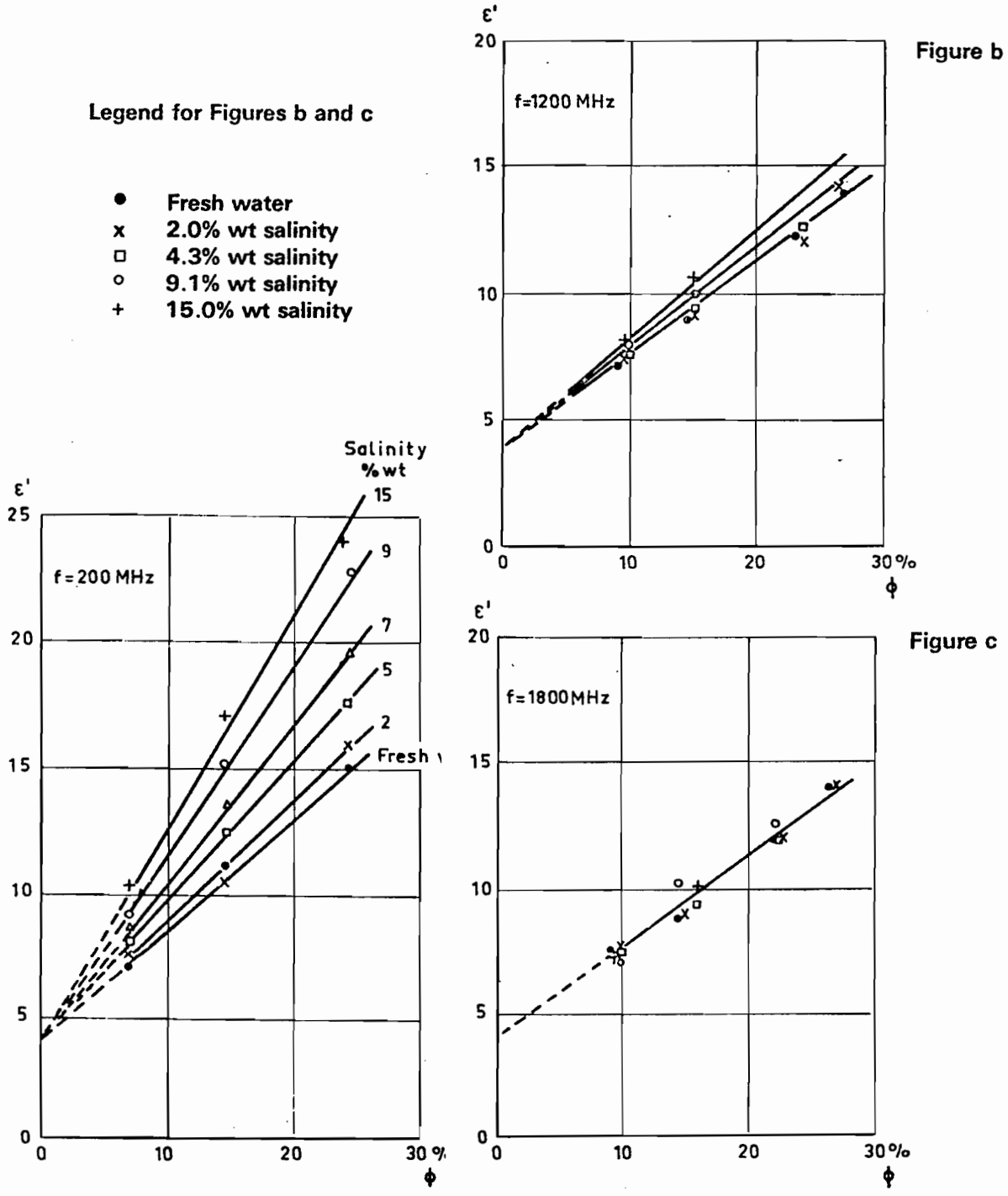

Figure 31. (After Poley et al., 1978).

Dependence of ε' on Porosity for Sandstones of Various Salinities

Figure 31 shows measurements of ϵ' for water saturated samples at different salinities for three frequencies. Figure 32 shows measurements of ϵ''-values at these same frequencies. From figure 33, we see that at 1800 Mhz, the ϵ'values are virtually independent of salinity while ϵ'' values show a small increase as a function of salinity with frequency. This is due to the basic conductivity contribution σ'/ω to the equivalent imaginary component of permittivity which in Poley's development is included directly in the imaginary permittivity. Thus when ϵ' and ϵ'' are measured together, ϵ" can be used as a salinity indicator.

In contrast to water, the dielectric permittivity of oil is only of the order of ϵ_0. In another experiment by Poley et al. (1978), measurements on completely oil-saturated (S_w=0) to completely water-saturated samples (S_w=1), at 250 MHz (figure 30). At VHF values of ϵ' and ϵ" are perhaps useful in differentiating between water and oil saturation.

4.5 ACCURACY OF MEASUREMENTS

Advances in HF time domain techniques made the measurement of dielectric permittivity possible up to 10^{12} Hz. EM-wave propagation borehole logging devices make measuremtns of phase shift, $\Delta\phi$, and attenuation, A, from which the composite dielectric properties can be calculated.

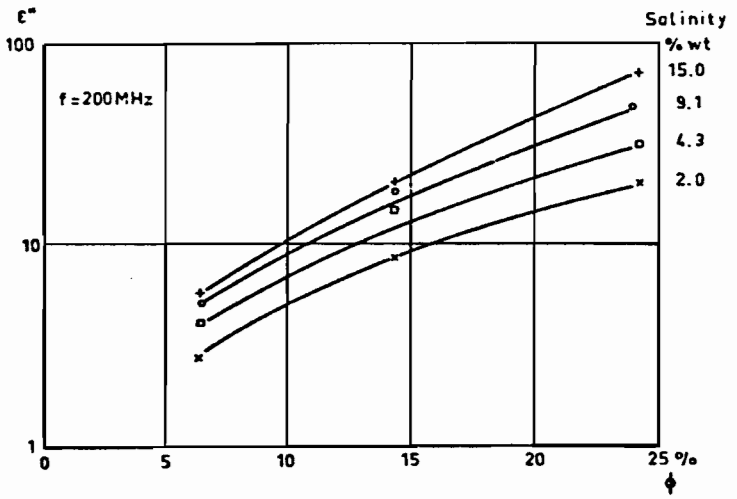

Figure a

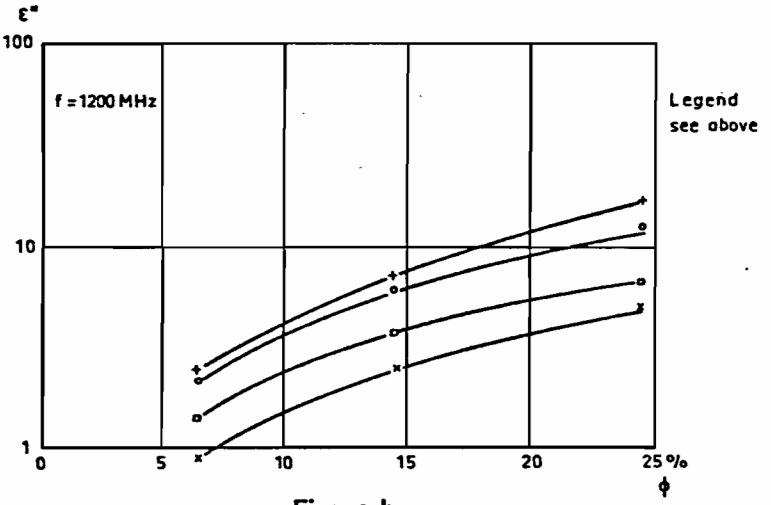

Figure b

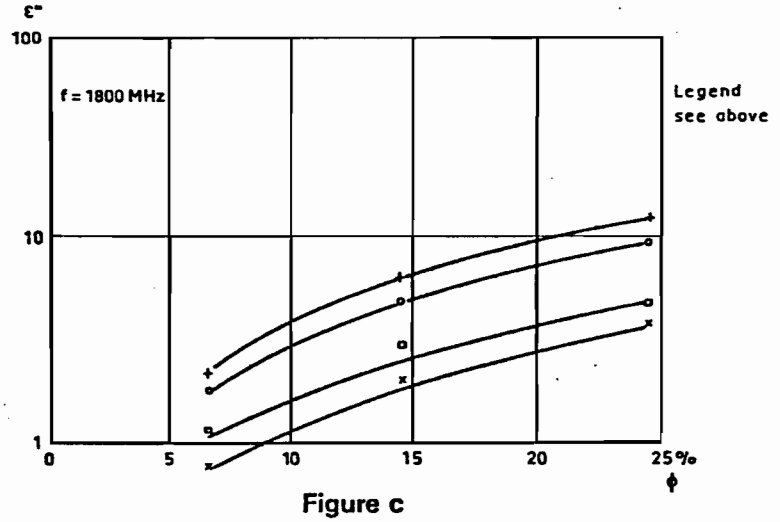

Figure c

Figure 32. (After Poley et al,, 1978).

Dependence of ϵ'' on Porosity for Sandstones Saturated with Water of Various Salinities

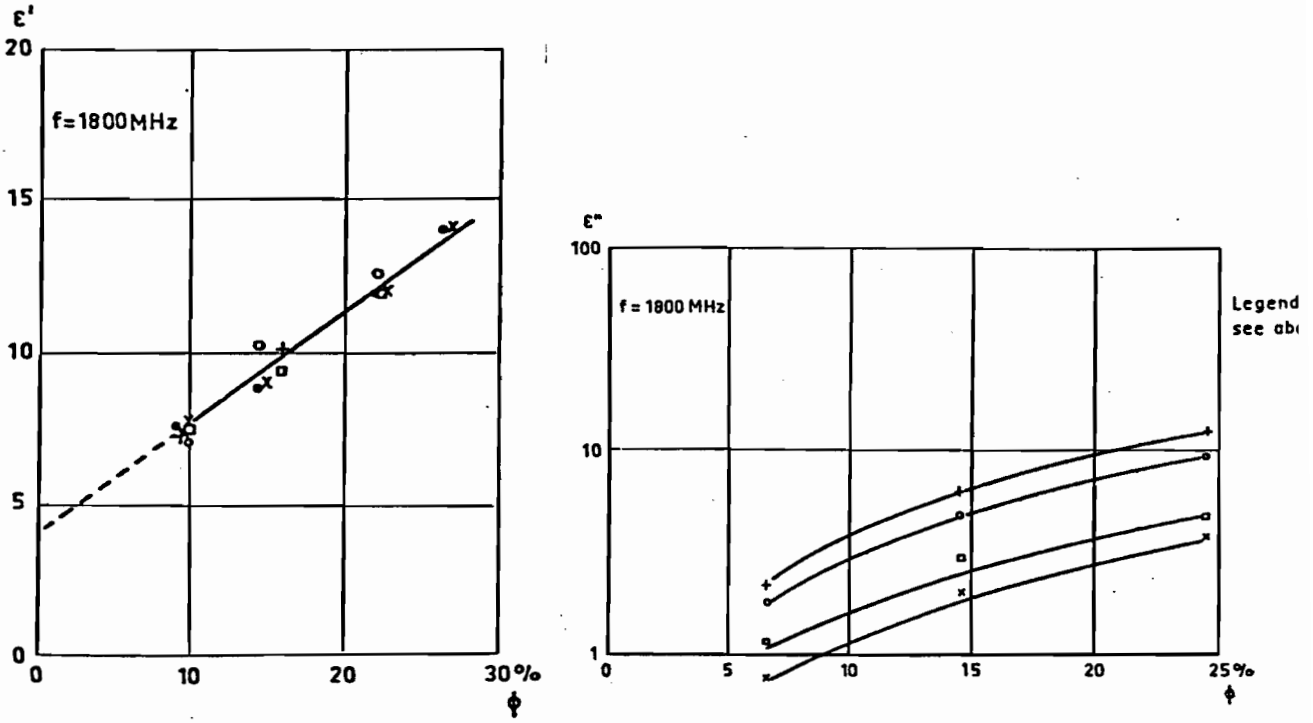

Figure 33. (After Poley et al., 1978). Measurements Of real and imaginary permittivity components for a water saturated sample at different salinities for 1800MHz. It can be seen that at 1800 MHz, the real permittivity is virtually independent of salinity while the imaginary component shows a small increase as a function of salinity.

Schlumberger introduced EM-wave travel time measurements which yield composite dielectric values. The travel time t_{pl} is the inverse phase velocity of EM wave propagating in an infinite homogeneous medium and has dimensions of inverse velocity. Theoretically it is defined by

$$t_{pl} = \left[\frac{\mu\epsilon_e}{2}\left((1+\tan^2\delta)^{1/2}+1\right)\right]^{1/2}. \qquad 4\text{-}5\text{-}1$$

The measured value t_{plc}, is the formation travel time versus wireline depth and is determined from a measured phase shift,

$$t_{plc} = \frac{\Delta\Phi}{2\pi L\omega}\ , \qquad 4\text{-}5\text{-}2$$

where L = distance between point receivers at x_1 and x_2 and ω = instrument (EPT) frequency.

The relative deviation of t_{plc} from t_{pl} has been investigated and found not to be more than 5%.

Let us consider a plane wave propagating along the x-axis. The E-field associated with this wave is:

$$E(x) = E_o\, e^{i(kx-\omega t)} \qquad 4\text{-}5\text{-}3$$

If we write the propagation constant as

$$k = \alpha - i\beta \qquad 4\text{-}5\text{-}4$$

one may evaluate the α and β corresponding to the EM-wave travel time. The phase shift, $\Delta\Phi$, of the electric field relative to two point receiver positions x_1 and x_2 is:

$$\Delta\phi = - \text{Im} \left[E(x_1)/E(x_2) \right] . \qquad 4\text{-}5\text{-}5$$

We consider equation 4-5-5 the exact expression for the phase shift. Schlumberger calculates α_c from the phase shift as

$$\alpha_c = \Delta\phi . (x_1 - x_2)^{-1} . \qquad 4\text{-}5\text{-}6$$

αc will be exact for a plane wave propagating through a half space.

The general attenuation in dB/m relative to the two point receivers is given by:

$$A = 8.686 . (x_1 - x_2)^{-1} . \text{Re} \{ \ln[E(x_1)/E(x_2)] \} . \qquad 4\text{-}5\text{-}7$$

Thus β_c is in terms of A, as suggested by Schlumberger, for plane waves is obtained according to

$$\beta_c = \frac{A - A_s}{8.686} = (x_2 - x_1)^{-1} \text{Re} \left\{ \ln \left[E(x_1)/E(x_2) \right] \right\} - A_s/8.686 , \qquad 4\text{-}5\text{-}8$$

where A_s is the attenuation in dB/m arising from spreading losses which are dependent on the properties of the medium which difficult to determine. the approximation procedure used to evaluate A_s is to replace it by the value of attenuation in air where $\beta_{air} = \emptyset$. Schlumberger also introduce a second travel time:

$$t_{po} = \left(\frac{\alpha^2 + \beta^2}{\omega^2} \right)^{1/2} \qquad 4\text{-}5\text{-}9$$

or

$$t_{pl} = \left(t_{po}^2 - \beta^2/\omega^2 \right)^{1/2} \qquad 4\text{-}5\text{-}10$$

then deduce the following equation for t_{pl}

$$t_{pl} = \phi S_{xo} t_{p\omega} + \phi (1 - S_{xo}) t_{ph} + (1 - \phi) t_{pma}$$

Using this form, provided accurate values of t_{pw}, t_{ph}, t_{pma} are available by laboratory experiments, water and oil saturation and porosity can be deduced.

In frequencies between 10-40 MHz, the real dielectric constant ϵ' of a water - oil - saturated matrix is consistent with the following equation (Meador and Cox, 1975):

$$\epsilon'^{c} = [\phi S_w \epsilon'^{c}_{w} + \phi (1-S_w) \epsilon'^{c}_{oi} + (1-\phi) \epsilon'^{c}_{ma}] \qquad 4\text{-}5\text{-}11$$

where S_w = water saturation

ϵ'_w = real dielectric permittivity of water,

ϵ'_{oi} = real dielectric permittivity of oil, and

ϵ'_{ma} = real dielectric permittivity of rock matrix,

ϕ = porosity, and

c = an empirical factor between 0 and 2 which depends upon the porosity, grain size, shape and orientation.

Freedmann and Vorgiatzis (1979) suggested that if c=1/2 and if we multiply equation 4-5-11 by $\mu^{1/2}$ we obtain

$$t_{po} = \phi S_w t_{pow} + \phi (1-S_w) + t_{poh} + (1-\phi) t_{poma}, \qquad 4\text{-}5\text{-}12$$

where t_{pw}, t_{poh} and t_{poma} are travel times for the water hydrocarbons and rock matrix and

$$t_{pox} = [\mu \epsilon'_x]^{1/2} \qquad 4\text{-}5\text{-}13$$

which is essentially the same as the equation used by Schlumberger because the correction term β^2/ω^2 is relatively small.

Freedman and Vorgiatzis consider a model of a half space (layer 1.) in which there is a layer (2) of mudcake of uniform thickness d and in which is located a transmitting antenna at x = Ø with two receiving antennae at x_1 and x_2. The electric field due to the boundary conditions of the model has just a z-component (Figure 34). The phase shift and the attenuation can be determined by equations 4-5-5 and 4-5-7 for point receivers, but practically for finite receivers $\Delta\phi$ and A are position-dependent vary over the area of the receivers. Provided the receivers measure averaged electric field at their locations, we can still use equations 4-5-5 and 4-5-7 but we must use equation 2-2-36 to describe the E-field in terms of the near field Hertz vector. Considering the boundary conditions, Freedman and Vorgiatzis (1979) obtain the following equation for E:

$$E(r) = 2(ip/4\pi\epsilon_\emptyset)\int_0^\infty \left[\frac{\lambda^3 J_\alpha(\lambda r) e^{-i\gamma_1 d}(\gamma_1 k_2^2 - \gamma_2 k_1^2)\, d\lambda}{\gamma_1(\gamma_2 k_1^2(e^{i\gamma_1 d} + e^{-i\gamma_1 d}) - \gamma_1 k_2^2(e^{i\gamma_1 d} - e^{-i\gamma_1 d})}\right]$$

$$-p/4\pi\epsilon_\emptyset \; e^{ik_1 r}/r^3 \,(1 - ik_1 r - (k_1 r)^2)$$

They performed computer calculations for various values of the two media from phase shift and attenation and compared them to the measured values and found that, in the absence of mudcake, the error in t_{plc} was between Ø.7 and 4.3%, t_{plc} being always less than t_{pc}. With mudcake the error was of the order of Ø.1 to 11.4%. The attenuation was a monotonically increasing function of the mudcake thickness; the phase shift increased with the effective permittivity of the medium. The formation dielectric properties calculated in this way are properly apparent

rather than true. For qualitative purposes however, this method is acceptable. It is also possible to construct departure curves which enable one to obtain true formation properties from apparent values.

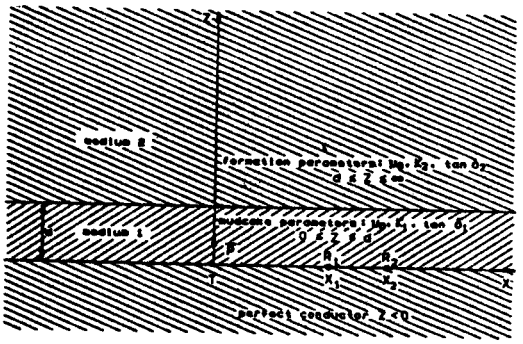

A schematic view of the theoretical model.

Figure 34. (After Freedman and Vorgiatzis, 1979).

CHAPTER V

5.1 ALTERNATING CURRENT SOUNDING

Sommerfeld (1936) has developed the theory of alternating current EM-sounding for very simple configurations of antennas; i.e. vertical and horizontal dipoles over a plane homogeneous half-space. Although in practice the antenna design is very critical, for our present mathematical development of the theory we will idealize the transmitter and receiver and treat them as electrical and magnetic dipoles. In EM exploration, frequency plays a dominant role. Multifrequency EM sounding is known as the parametric sounding.

The Sommerfeld theory attracted little geophysical interest because of its technical and practical limitations until two decades ago, when elaborate multifrequency instruments were developed. The ability to make measurements stimulated continuing development of the theory for various transmitter receiver configurations (Patra and Mallick 1980, Frischknecht 1966, 1967, etc...).

Parallel with the development of the theory digital filters for the numerical evaluation of the required Hankel transforms have been developed (Anderson 1977, 1978). These filters very closely approximate the Hankel transforms and are a powerful tool in the evaluation of these integrals. In the recent

literature, the asymptotic solutions for large kr terms have been developed by several workers (Mittra et al., 1979, Kuo and Mei 1978). These yield more rapid solutions, closely approximating the potential vector.

In general, the objective of these AC soundings is either to determine the variations of the earth's electrical parameters with depth (parametric sounding) or to recognize lateral inhomogeneities (geometric sounding). Our objective here is rather to describe the frequency dependence of the electrical parameters of a homogeneous half-space. The Hertz vector was described by Sommerfeld (1936) and has been used to derive EM-field components while dealing with the electric current flow. Magnetic dipoles which are represented by frame antennas have an analogous magnetic current flow which relates to another vector, similar to the Hertz vector, the Fitzgerald vector F. The general form of these two vectors is:

$$\vec{\Pi} = A\int_0^\infty K(\lambda)\, J_n(\lambda r)\, d\lambda \qquad 5\text{-}1\text{-}1$$

where

A = dimensionaless scaling factor,

J_n = Bessel function of order Ø or 1 and

K = Kernel function, either

$$k(\lambda) = \frac{e^{-h\mu + z\mu_E}}{\mu k_E + k\mu_E} \quad \text{or} \quad \frac{e^{-h\mu + z\mu_E}}{\mu_E + \mu}$$

h = height of antenna above the assumed half-space,

z = depth of measurement,

$k = \omega^2 \mu \epsilon_0$

k_ϵ = propagation constant of the half-space

$$k_\epsilon = -i\omega^2 \mu (\epsilon\omega + i\sigma)$$

The Kernel of these equations must be decreasing functions with λ, which will always be the case if we chose the negative real part of the exponents. Due to the oscillatory nature of the Bessel functions $J_n(\lambda r)$, there is a further cancellation of terms which enhances the convergence of the integrals.

The major contribution to these integral transformations derives primarely from small values of λ. It must be noted that those integrals with the denominators $\mu_\epsilon k^2 + \mu k_\epsilon^2$ have a pair of simple poles $\lambda = \pm\lambda_p$ where

$$\lambda_p = \pm (1+n^2)^{-1/2} \qquad 5\text{-}2$$

The poles do not lie normally in the integration path because n is a complex constant, but if otherwise, must be avoided by the path of integration. This theory has been used to evaluate E- and H-field for several different transmitter configurations and also to determine the impedance of a loop-loop and a loop and wire configuration Using the appropriate Cole-Cole resistivity and dielectric permittivity parameters.

Since there is a similarity between vertical electric dipole and horizontal magnetic loop antenna, let us discuss these two cases in parallel. In the following development, antenna dimensions to be considered small with respect to the wavelength and some distance above the halfspace surface boundary.

An alternating field is imposed on the halfspace by a loop or a long wire antenna. These source EM fields are the primary excitations; the secondary stimulation is produced by currents induced within the halfspace. A receiver coil or rod can then measure the perturbation of the normal field due to subsurface induced currents. For geophysical sounding from the surface the sum of the primary and secondary fields must be considered. In geophysical prospecting, it is the stimulation in the ground due to the secondary field which is of essential interest.

5.2 A VERTICAL ELECTRIC DIPOLE ANTENNA ABOVE A DISSIPATIVE EARTH

The E- and H-field for the vertical electric antenna are obtained as (Sommerfeld, 1936)

$$\vec{E} = -k_\epsilon^2 \vec{\Pi} + \nabla(\nabla \cdot \vec{\Pi}) \qquad 5\text{-}3$$

$$\vec{H} = \frac{k_\epsilon^2}{i\omega\mu_0} \nabla \times \vec{\Pi} \qquad 5\text{-}4$$

where

$$\vec{\Pi} = \vec{\Pi}(\omega, r, \phi, z)$$

in cylindrical coordinates. The z-axis coincides with the antenna axis and $z = 0$ is the air-ground interface. A harmonic time dependence of $e^{-i\omega t}$ has been suppressed throughout. The Hertz vector direction is that of the antenna current that is:

$$\vec{\Pi} = \vec{\Pi}_z$$

and because of cylindrical symmetry around the antenna Π_z is independent of ϕ, thus $\frac{\partial}{\partial \phi} = 0$ and

$$\vec{\Pi}_z = \vec{\Pi}_z(r, z, \omega) \qquad 5\text{-}5$$

Inserting equation 5-5 in 5-4 and 5-3 we obtain

$$\vec{E}_\phi = \vec{H}_r = 0 \qquad 5\text{-}6$$

and

$$E_r = A\frac{\partial}{\partial r}\left(\frac{\partial}{\partial z}\Pi_z\right) \qquad 5\text{-}7$$

and

$$H_\phi = -\frac{k^2 A}{i\omega\mu}\frac{\partial \Pi_z}{\partial r} \qquad 5\text{-}8$$

where A is the dimensionality factor, and we are going to absorb it into the Π_z term,

$$A = \frac{I\,dx}{4\pi\omega\epsilon_0}, \qquad 5\text{-}9$$

with

I = current in antenna,

dx = element of length of the antenna,

ω = angular frequency and

ϵ_0 = permittivity of free space.

Avoiding the details, we consider the following case:

At the air-ground interface boundary conditions are:

$$E_{r1} = E_{r2}$$

and

$$H_{\phi 1} = H_{\phi 2},$$

Without applying any specific properties of the parameters of the media, the Hertz vector has the form

$$\vec{\Pi}_z = A\int_0^\infty \frac{2\lambda}{n^2\gamma+\gamma_\varepsilon} e^{-\gamma h+\gamma_\varepsilon z} J_0(\lambda r)\,d\lambda \qquad 5\text{-}10$$

where

$$n^2 = k_\varepsilon^2/k^2.$$

By taking the appropriate derivatives (Sommerfeld) we get, for E_r and H_ϕ respectively,

$$\vec{E}_r = -2Ak^2 \int \gamma_\varepsilon \lambda^2 \frac{e^{\gamma_\varepsilon z-\gamma h}}{k_\varepsilon^2\gamma + k^2\gamma_\varepsilon} J_1(\lambda r)\,d\lambda \qquad 5\text{-}11$$

and

$$\vec{H}_\phi = -2iAk_\varepsilon^2 \omega\epsilon_\phi \int \lambda^2 \frac{e^{\gamma_\varepsilon z-\gamma h}}{k^2\gamma_\varepsilon + k_\varepsilon^2\gamma} J_1(\lambda r)\,d\lambda \qquad 5\text{-}12$$

At the origin, necessarily

$$\vec{E}_r(r=0) = \vec{H}_\phi(r=0) = 0 \ . \qquad 5\text{-}13$$

5.3 HORIZONTAL MAGNETIC ANTENNA OVER AN ARBITRARY EARTH

In the case of a magnetic dipole source the Fritzgerald vector $\vec{F}$ is used instead of $\vec{\Pi}$, and

$$\vec{E} = -i\omega\gamma_\cdot \nabla \times \vec{F} \qquad 5\text{-}14$$

$$\vec{H} = -k^2 \vec{F}_z + \nabla^2 \vec{F} \qquad 5\text{-}15$$

Insulated electric current loops (i.e. magnetic dipole) have considerable value as antennas for electromagnetic probing. The basic model used now is a small loop source, carrying an alternating current, oriented in the z-direction. In cylindrical coordinates, we will have one Fitzgerald potential vector component in the z-direction, $\vec{F}_z$. This vector is symme-

tric in ϕ. Taking the appropriate derivatives through equations 5-14 and 5-15 above, our horizontal field components become

$$\vec{E}_\phi = i\omega\gamma \frac{\partial}{\partial r}\vec{F}_z \ , \qquad 5\text{-}16$$

$$\vec{H}_r = \frac{\partial}{\partial z}\left(\frac{\partial}{\partial r}\vec{F}_z\right) \ , \qquad 5\text{-}17$$

and

$$\vec{E}_r = \vec{H}_\phi = \emptyset . \qquad 5\text{-}18$$

The vertical magnetic component becomes

$$\vec{H}z = i\omega\gamma_0\left[\frac{1}{r}\frac{\partial}{\partial r}\left(r\frac{\partial F}{\partial r}\right)\right] . \qquad 5\text{-}19$$

Using the appropriate boundary conditions we find the Fritzgerald vector

$$\vec{F}_z = A\int \frac{2\lambda}{\gamma+\gamma_E} e^{-\gamma h+\gamma_E z} J_0(\lambda r)\,d\lambda \qquad 5\text{-}20$$

and inserting this form into equations 5-17, 5-18, 5-19 above, the horizontal field component becomes

$$\vec{E}_\phi = -2i\omega\gamma_\cdot A\int_0^\infty \frac{\lambda^2}{\gamma+\gamma_E} e^{\gamma_E z-\gamma h} J_1(\lambda r)\,d\lambda \qquad 5\text{-}21$$

$$\vec{H}_r = -2A\int_0^\infty \frac{\gamma_E\lambda^2}{\gamma+\gamma_E} e^{\gamma_E z-\gamma h} J_1(\lambda r)\,d\lambda \qquad 5\text{-}22$$

and the vertical component,

$$\vec{H}_z = -2iA\omega\gamma_\cdot\int_0^\infty \lambda^3 \frac{e^{\gamma_E z-\gamma h}}{\gamma+\gamma_E} J_0(\lambda r)\,d\lambda . \qquad 5\text{-}23$$

At the origin

$$E_\phi(r=\emptyset) = H_r\ (r=\emptyset) = \emptyset .$$

The field component $\vec{E}_\phi$ can be measured using a transversely oriented pair of ground potential probes; $\vec{H}_z$ can be measured

with a horizontal coil of few turns. There are some special difficulties in measuring the H_r-components. All six integrals above can be evaluated by numerical integration with the help of Anderson's (1978) digital filters. The Kernels of these integrals are generally complicated terms, involving roots of complex values in both the exponent and denominator. Several approximations must be made in order to evaluate these integrals: for example, for measurements at the surface (z=Ø), we considered that:

$$k_o^2 \longrightarrow 0 \ (\text{i.e.} \sqrt{\lambda^2 - k^2} \longrightarrow \lambda)$$

and consequently, at the surface, the Kernels

$$\frac{e^{\gamma_e^2 - \gamma h}}{\gamma_e k^2 + \gamma k_e^2} \qquad \text{and} \qquad \frac{e^{\gamma_e^2 - \gamma h}}{\gamma_e + \gamma}$$

reduce to

$$\frac{e^{-\lambda h}}{k_e^2 \lambda} \qquad \text{and} \qquad \frac{e^{-\lambda \gamma}}{\lambda + \gamma_e}$$

These assumptions are only appropriate at "low" frequencies and can not be generalized. The major contribution to these integrals is from small k_r's, where at high frequencies k_o is not small compared to λ. At large distances, the assymptotic solutions of the above integrals are often used in replacement. As we have seen above, many geophysical parameters are involved in the determination of the EM-field components. Let us recall these parameters which appear directly in the field equations;

λ = variable of integration

$\gamma = \sqrt{\lambda^2 - k_o^2}$ where $k_o^2 = \omega^2 \mu_o \epsilon_o$

$\gamma_E = \sqrt{\lambda^2 - k_E^2}$ where $k_E^2 = \omega \mu_o (\omega \epsilon_e - i\sigma_e)$

$A = A(I, \omega)$ = dimensionless scaling term.

The Kernels of the Hankel integrals are dependent on frequency and also on the propagation constants in both media. We are especially interested in the propagation vector in the ground halfspace which is definitely determined by the geophysical ground properties. Since ke appears in the exponent of integration, small changes in k_E can appreciably modify the magnitude of the EM-fields.

By measuring, then, these fields at several frequencies (at least 8 frequencies are required to overdetermine the solutions) we may determine by inversion the propagation constant of the homogeneous ground and from this constant, the geophysical properties of the ground. Let us now determine the form of these fields as a function of different parameters.

5.4 VARIATION WITH DEPTH

We here consider the E_r and H_ϕ fields of the vertical electric dipole. For all other antenna configurations, similar conclusions with respect to the kernels of the Hankel integrals can be drawn. We shall keep the frequency constant thus k_o and k_E and A remain contant. The height of the dipole is first

arbitrarily fixed to be one wave length in the following examples. The horizontal position of measurement is taken to be some substantial distance away from the antenna since just beneath the antenna, fields are nul. A unit current will drive the antenna: fields are evaluated as functions of depth. For H_ϕ, the essential factor in the integral containing the depth is $e^{-z\gamma_E}$ where

$$z\gamma_E = z\gamma_R + iz\gamma_I$$

As expected, fields decrease exponentially with depth while oscillating due to the sinusoidal form of $e^{iz\mu_I}$.

The corresponding integral factor for the E_r field is $\gamma_E e^{-z\gamma_E}$. The behavior of this field will show some minimum value at the surface reaching a maximum at some depth and then continue decreasing (but less rapidly than exponential) toward larger depths. In Figure 35 the two curves show E_r and H_ϕ fields for a homogeneous half-space of the clay permafrost at -27°C (Olhoeft) in chapter IV, section 4.1.1 with depth. Once we know the character of variation of the fields with depth, we shall fix henceforth, the depth at once skin depth for the subsequent examples.

5.5 VARIATION WITH HEIGHT OF ANTENNA

The effect of increasing the height of the antenna also provides an exponential decrease on H_ϕ-field (Figure 36). The term responsible for this effect is $e^{-h\gamma}$. For

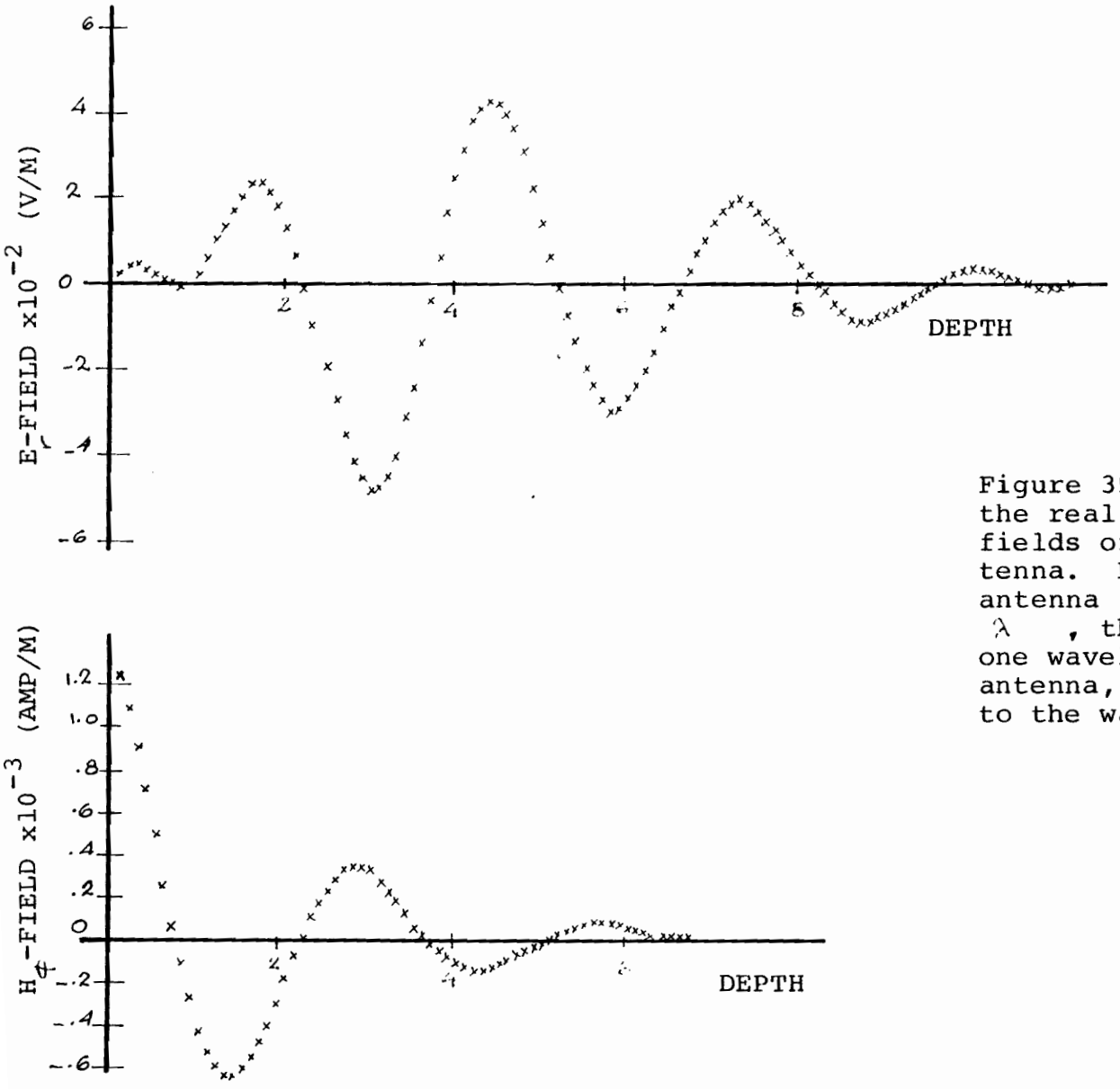

Figure 35. Variation with depth of the real components of E_r- and H_ϕ-fields of a vertical transmitting antenna. Frequency = 10^7Hz, length of antenna = $\lambda/4$, height above ground = λ, the distance of measurement is one wavelength from the transmitting antenna, and the depth is normalized to the wavelength.

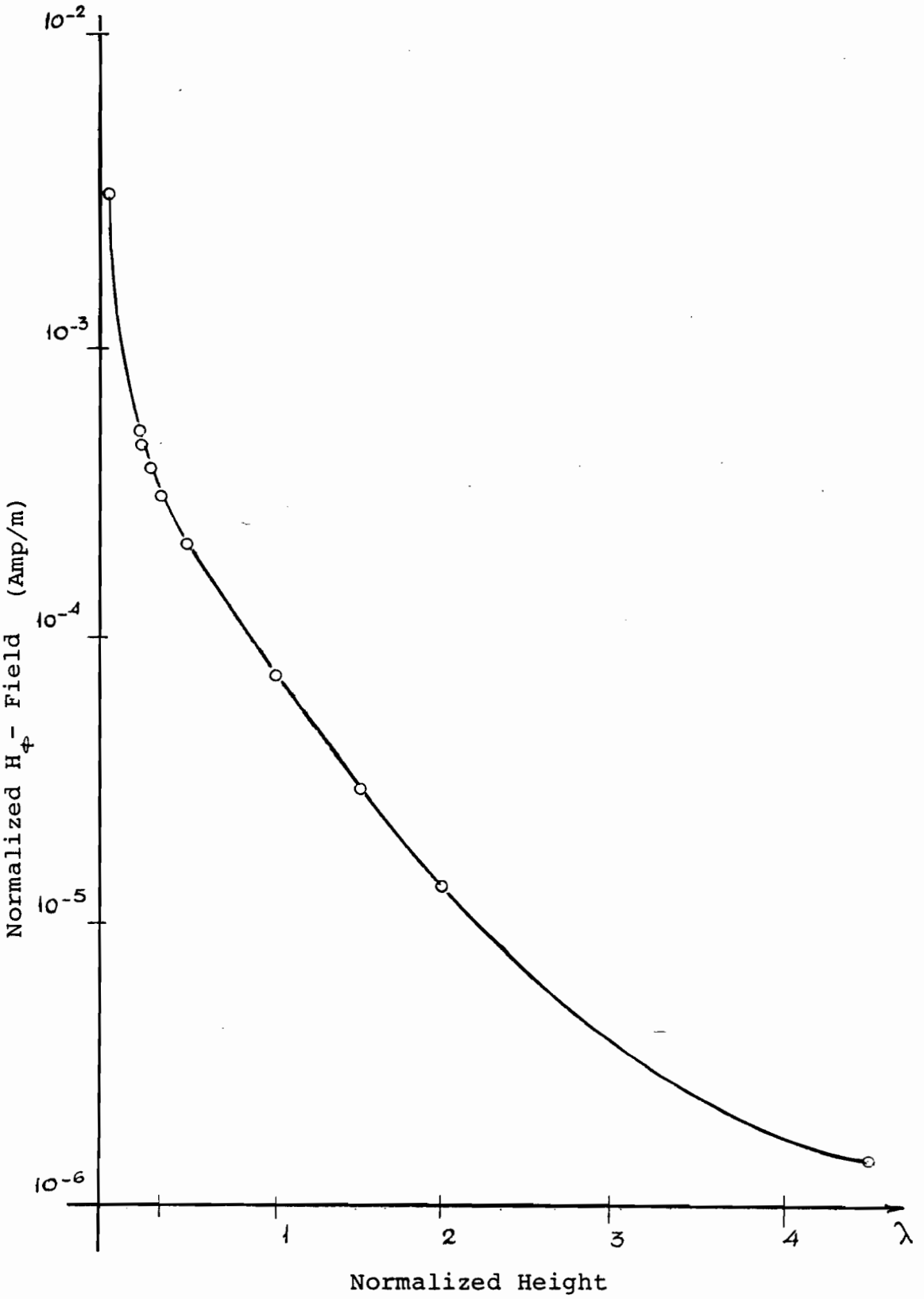

Figure 36. Variation of normalized H -field with height, for the example of the clay permafrost of Chapter IV, section 4.1.1. The wavelength is 3 m., the antenna length $\lambda/4$ and the depth is equal to one skin depth.

the term $e^{-h_1 u}$ is purely oscillatory, while for

$$0 \leq \lambda < k_0$$

this term is purely negative exponetially. In the transform integral, this second form dominates so that there will be an exponential decrease with increasing height. Let us now set the height again at one wavelength and consider the variation of fields with the horizontal axis at for several frequencies. Here we will see the effect of the propagation constant.

5.6 FREQUENCY VARIATION

As seen in figures (37 - 42), the major effects on the field occurs within a radius of about one wavelength; beyond this range, the fields die off rapidly. A more important effect is the variation of the maximum amplitude of the field with frequency. At some particular frequency, we find a maximum field amplitude for any particular height due to the choice of the Cole-Cole models which determine the propagation constant of the halfspace ground medium.

5.7 RADIATION ENERGY

The quadratic quantity of energy flow is determined by the amplitude of Poynting's vector

$$S = [EH]. \qquad 5\text{-}24$$

averaged over all time and space. Due to the orthogonality of the eigenfunctions, the Bessel functions cancel in this product and the total energy flow integrated over a horizontal plane reduces to

$$S = \int S_z \, d\sigma = \int [E_r . H_\phi - E_\phi . H_r] \, d\sigma. \qquad 5\text{-}25$$

All energy which enters the Earth is effectively transformed into Joule heat so that $-S_-$ is the total thermal absorption of Earth per unit time. S_+ is the total radiation is air above the halfspace. The energy input to the antenna per unit time (i.e. the radiative power) is:

$$W = S_+ - S_-$$

For the vertical magnetic loop integral 5-24 is obtained in Appendix E. For the vertical dipole and horizontal dipole, the mathematical development was done by Sommerfeld (1936). The results for the three antenna configurations are summarized:

i - Vertical electric antenna:

$$W = \frac{2\pi k^5}{\gamma_0 \omega} \left(\frac{1}{3} + \frac{2\sin J - J\cos J}{J^3} + U \right) \qquad 5\text{-}26$$

where

$$U = \frac{1}{k^5} R_e \left\{ i \int_0^\infty \frac{2\gamma_1}{n_1^2 \gamma_0 + \gamma_1} e^{-2\gamma h} \frac{\lambda^3}{\gamma} \, d\lambda \right\} \qquad 5\text{-}27$$

ii - Horizontal electric antenna:

$$W = \frac{2\pi k^5}{\gamma_0 \omega}\left(\frac{2}{3} - \frac{\sin\zeta}{\zeta} + \frac{\zeta\sin\zeta - \zeta\cos\zeta}{\zeta^3} + L\right)$$

where

$$L = \frac{1}{k^3} Re\left(i\int_0^\infty e^{-2\gamma h}\left(\frac{2\gamma\gamma_E - \lambda^2}{n^2\gamma + \gamma_E}\right)\lambda\, d\lambda\right)$$

iii - Vertical magnetic loop:

$$W = \frac{2\pi k^5}{\gamma_0 \omega}\left(\frac{2}{3} + \frac{\sin\zeta}{\zeta} - \frac{\sin\zeta - \zeta\cos\zeta}{\zeta^3} + V\right)$$

where

$$V = \frac{1}{k^3} Re\left(i\int_0^\infty e^{-2\gamma^* h}\frac{\gamma_E^*}{n^{*2}\gamma + \gamma_E^*}\left(\frac{\lambda^2 - 2k}{\gamma^*}\right)\lambda\, d\lambda\right)$$

and

$$\zeta = 2\,kh.$$

We see that the first part of the contribution to the power is due simply to geometrical factors the frequency, and only the second part, that is the integral part, involves the ground geophysical parameters. These integrals have been numerically evaluated by the computer and have never shown a contribution larger than about 5% of the first part. Hence, independently of the range of the geophysical parameters, the power input to the antennas can be computed on the basis of the frequency and the geometrical factors of the antenna alone.

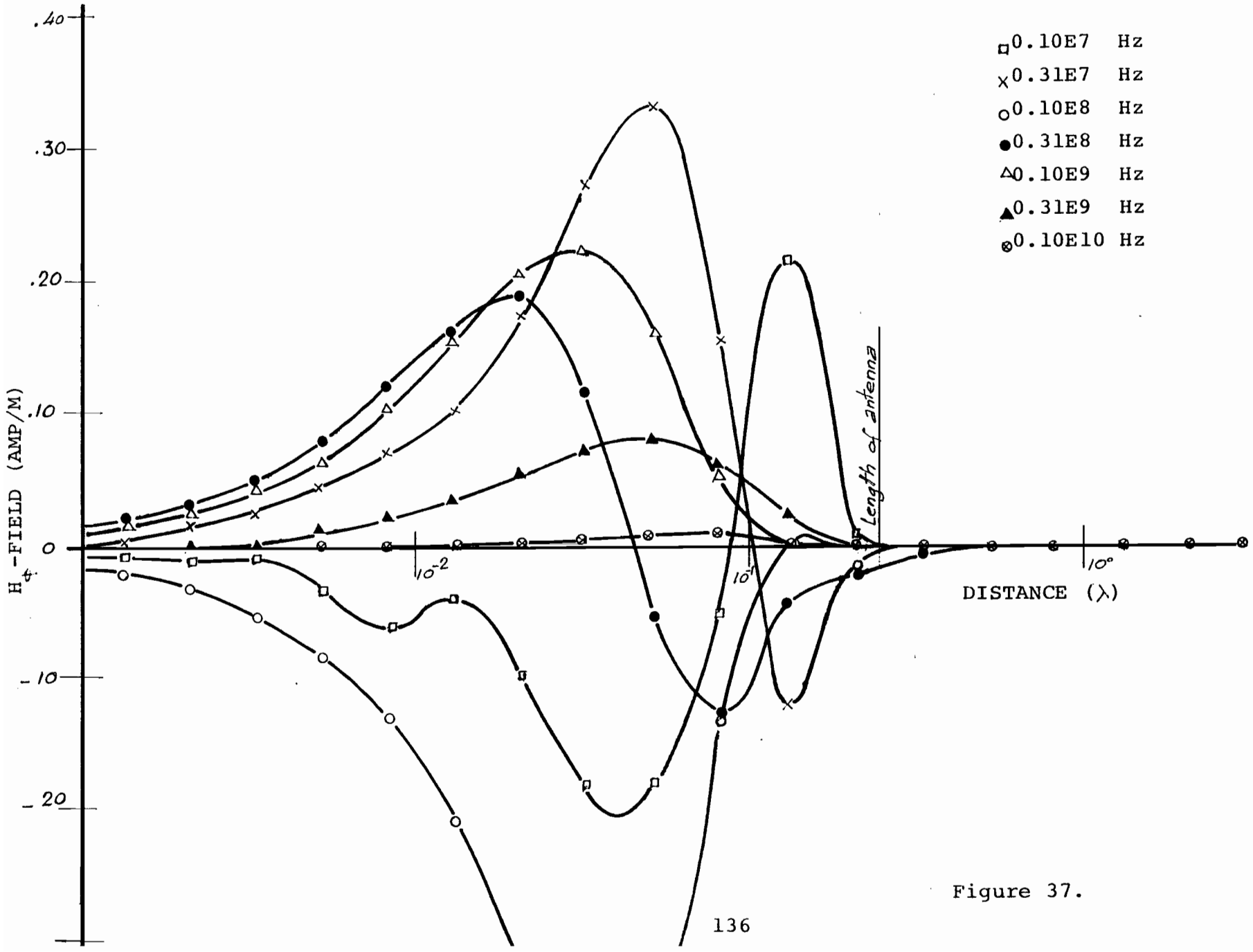
.40
.30
.20
.10
0
-.10
-.20
H -FIELD (AMP/M)
0.10E7 Hz
0.31E7 Hz
0.10E8 Hz
0.31E8 Hz
0.10E9 Hz
0.31E9 Hz
0.10E10 Hz
Length of antenna
10^{-2}
10^{-1}
10^{0}
DISTANCE (λ)

Figure 37.

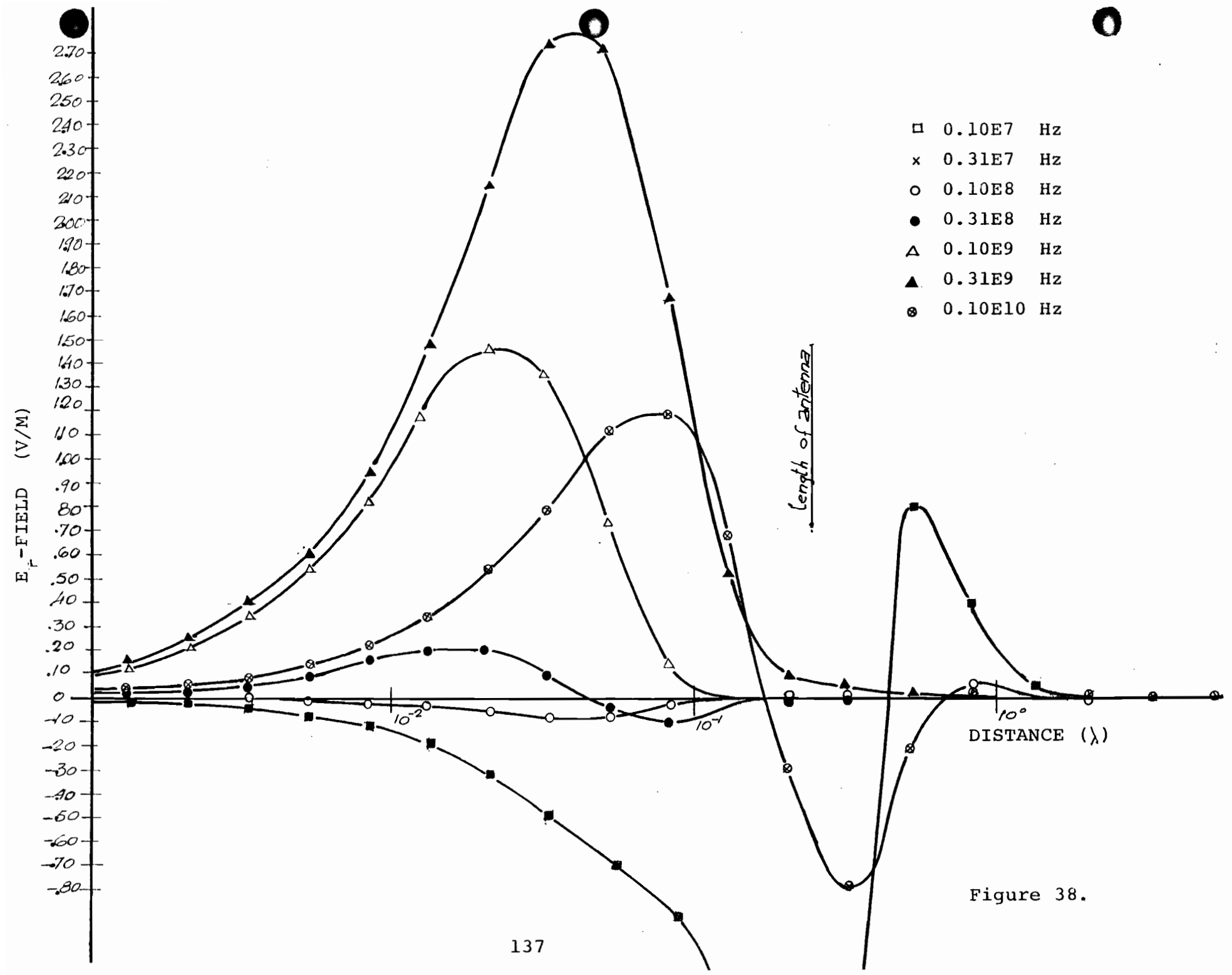
0.10E7 Hz
0.31E7 Hz
0.10E8 Hz
0.31E8 Hz
0.10E9 Hz
0.31E9 Hz
0.10E10 Hz
E_r-FIELD (V/M)
270
260
250
240
230
220
210
200
190
180
170
160
150
140
130
120
110
100
90
80
70
60
50
40
30
20
10
0
-10
-20
-30
-40
-50
-60
-70
-80
length of antenna
10^-2
10^-1
10^0
DISTANCE (λ)

Figure 38.

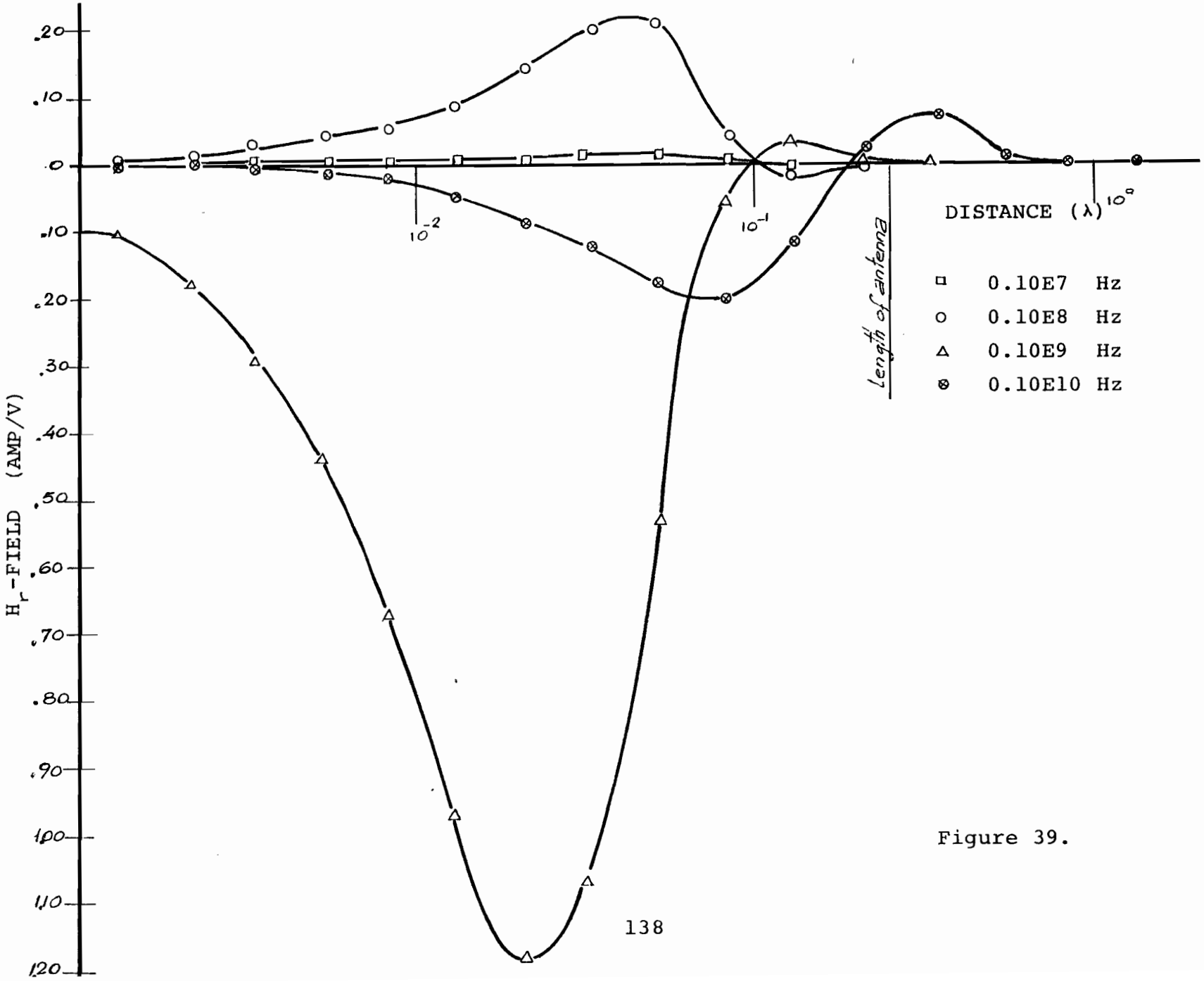
.20
.10
0
.10
.20
.30
.40
.50
.60
.70
.80
.90
1.00
1.10
1.20
H_r-FIELD (AMP/V)
10^{-2}
10^{-1}
10^{0}
DISTANCE (λ)
Length of antenna
0.10E7 Hz
0.10E8 Hz
0.10E9 Hz
0.10E10 Hz

Figure 39.

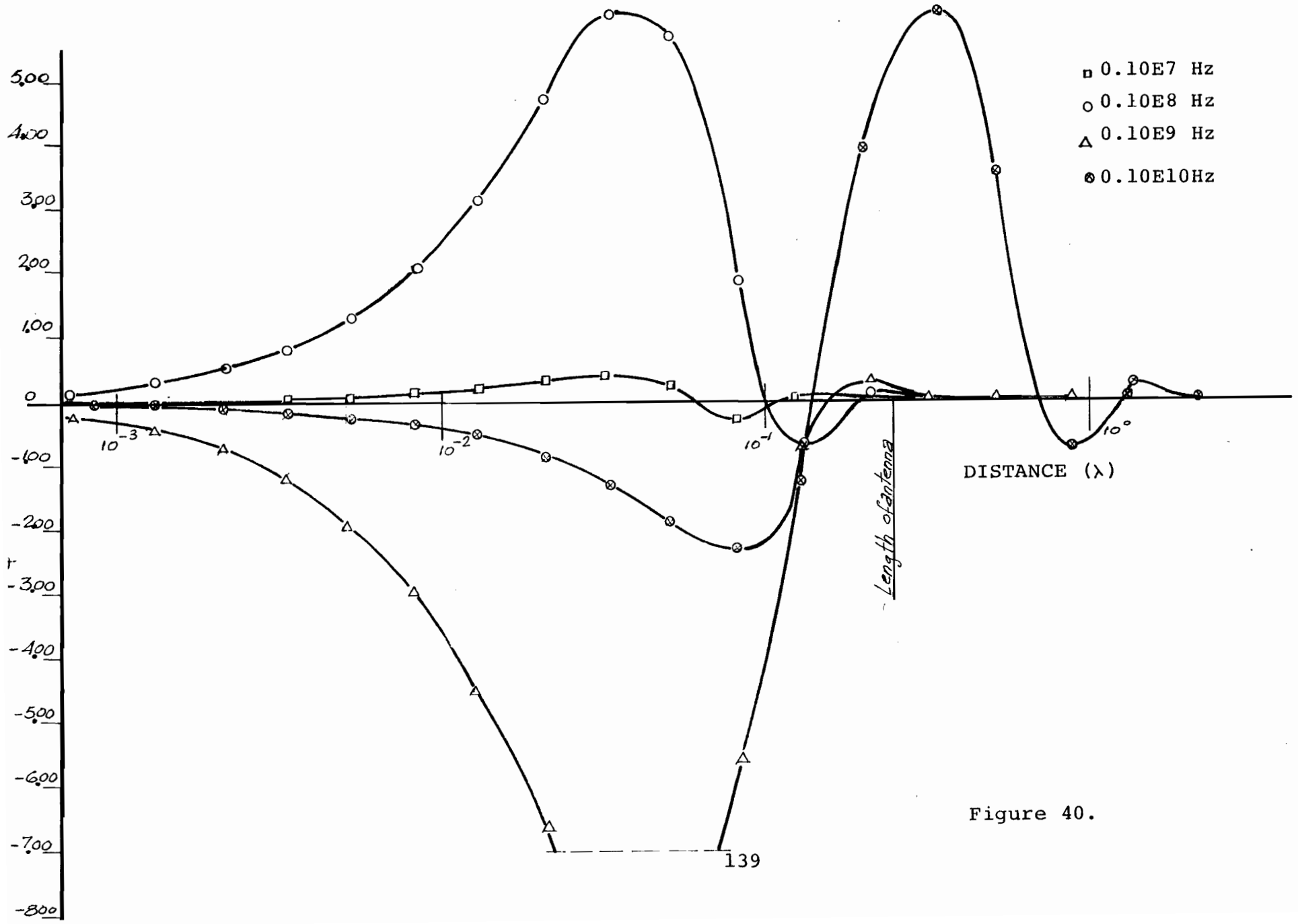
0.10E7 Hz
0.10E8 Hz
0.10E9 Hz
0.10E10Hz
5.00
4.00
3.00
2.00
1.00
0
-1.00
-2.00
-3.00
-4.00
-5.00
-6.00
-7.00
-8.00
10^{-3}
10^{-2}
10^{-1}
10^{0}
DISTANCE (λ)
Length of antenna

Figure 40.

Figure 37. Real component of secondary H_ϕ-field for a vertical transmitting dipole antenna, at various frequencies. The electrical parameters used to create these spectra are those of a half-space of clay permafrost at -27°C, as obtained in section 4.1.1. The current of the transmitter is equal to unity, the horizontal distance is in terms of the wavelength, the length of the antenna is equal to $\lambda/4$, and the depth of measurement is equal to one skin depth. It should be noted that the purpose of these plots is to show the aspect of the secondary field at various frequencies, due to frequency-dependent electrical parameters of the half-space. The maximum field occurs at 10^7 Hz.

Figure 38. Real component of the secondary E_r-field for a vertical transmitting dipole antenna, at various frequencies. Parameters are all the same as in figure 37. The maximum field occurs at 10^7 Hz.

Figure 39. Real component of the secondary H_r-field for a magnetic transmitting antenna, at various frequencies. Same parameters as above are used. The maximum field occurs at 10^8 Hz.

Figure 40. Real component of the secondary E_ϕ-field for a magnetic transmitting antenna, at various frequencies. Same parameters as above are used. The maximum field occurs at 10^8 Hz.

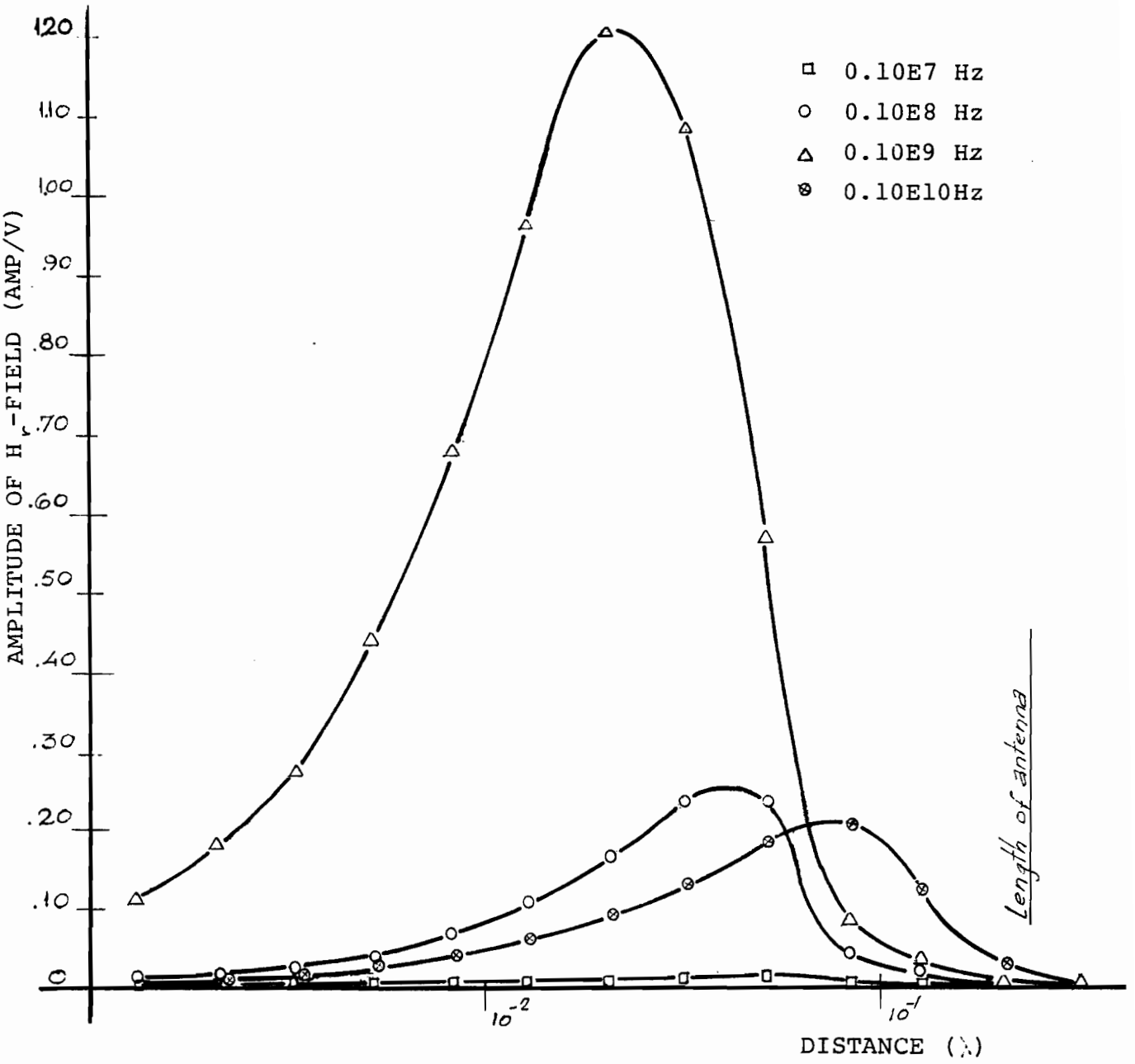

Figure 41. Amplitude of secondary H_r-field, of a horizontal magnetic antenna at various frequencies. Maximum frequency occurs at 10^8Hz. All parameters are as previously.

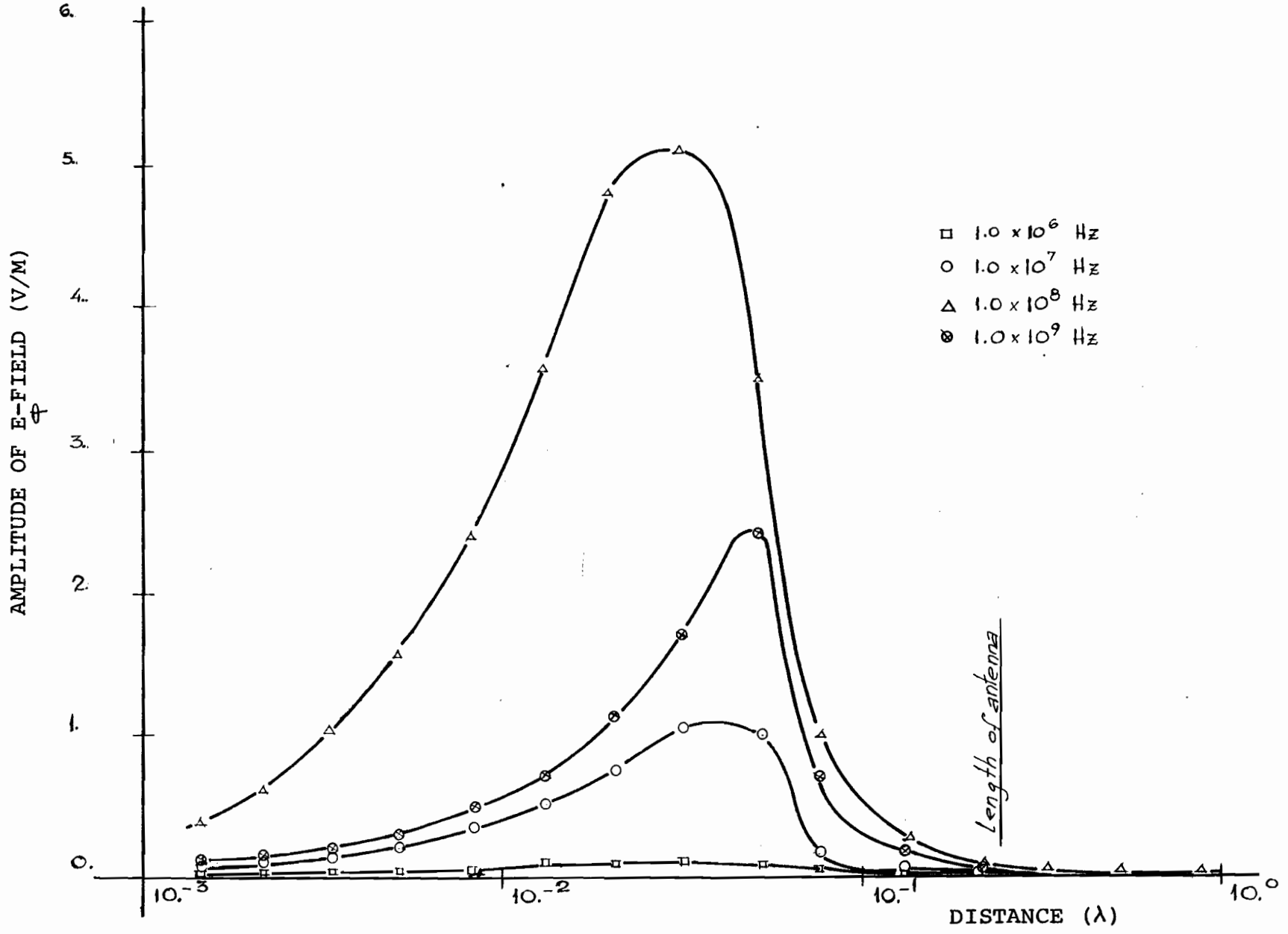

Figure 42. Amplitude of secondary E_ϕ-field, of a horizontal magnetic antenna at various frequencies

CHAPTER VI

CONCLUSIONS

6.1 SUMMARY OF THE THESIS AND DISCUSSION OF RESULTS

The original intention of the research project and this thesis which derives from it was to obtain an elaborated geophysical theory of electromagnetic fields and waves. The present work has concentrated, mainly, on the near-field induction problem for very-high and ultra-high frequency fields generated by idealized dipole antennas in proximity to a ground halfspace. The major, and largely original, contribution of this research has been to allow for geophysically reasonable models of a halfspace in which the basic electromagnetic parameters are complex-valued and frequency-dependent. In spite of the fact of a lacking solid-state physical theoretical explanation for the Cole-Cole model of complex conductivity, permittivity and permeability, we chose to employ this model because it is of considerable contemporary interest in geophysics and because it is relatively simple mathematically while corresponding closely to the Kirkwood-Fuoss physical permittivity model.

The electromagnetic theory has been described in parallel in both the time and frequency domains. In attempting to

describe complex frequency dependent parameters, the details of this parallelism are especially important because it must be shown, for example, that models are reasonable. That is, we must always ensure that the parametric models employed are physically realizable: stable, causal and perhaps of minimum phase (or delay). For the Cole-Cole permittivity models, Jain (1981) and here, for the equivalent conductivity model (cf. Pelton et al. (1978)) the time-domain equivalents have been derived. In the case of the audio-frequency conductivity measurements as obtained in contemporary IP (induced polarization) surveying, this parallelism is of considerable importance. As very-high and ultra-high frequency electromagnetic methods become more used in geophysical surveying, the parallelism of the permittivity models will be similarly topical.

Olhoeft's (1975) published data for permafrozen clay soils and Carmichael's data for serpentinite have been inverted using various Cole-Cole models of material conductivity and permittivity. Olhoeft had recognized the need for describing permafrozen materials with complex-valued permittivities which contribute to an additional apparent conductivity-like loss at frequencies beyond a few hertz. The inversions for these same data presented above yield much lower error bounds when the frequency-dependent Cole-Cole models are used in replacement of Olhoeft's constant complex permittivity assumption.

The thesis offers a substantial review of contemporary models of geophysical electromagnetic parameters which are known to be dependent upon such various conditions as temperature, salinity, porosity, electrochemistry, mineral grain size and shape, etc.. The newest of these models can contribute to the better understanding of high-frequency induced polarization effects and ultra-high frequency induction effects which can now be observed with modern geophysical prospecting and surveying instruments.

6.2 SUGGESTIONS FOR FURTHER WORK

In continuation of the developments of an elaborated geophysical electromagnetic theory, it would be useful to consider the similar problems concerning a grounded current electric dipole at high freqency and HF-to-UHF wave propagation phenomena in presence of the complex-valued, frequency dependent geophysical materials. Solution of the former problem could offer an essential theoretical description of the IP phenomena which are now so much used in base-metal geophysical prospecting and which show promise for petroleum exploration. Solution of the latter problem could extend the geophysical application of surface wave impedance measurements into the very-high to ultra-high frequency range.

It now remains to demonstrate that in practical geophysical prospecting and surveying, these elaborations of the description of electromagnetic phenomena will lead to improved interpretations of geological structures. That task is best

accomplished in the industrial environment of geophysical surveying and prospecting. We hope that this research will be of interest to the broader community of pure and applied geophysicists.

GENERAL REFERENCE

ABRAMOWITZ M. and STEGUN I. A. (1968)
Handbook of mathematical functions with formulaes, graphs and mathematical tables. pp 228-251 and 295-309. US Government Printing Office, Washington DC.

ALVAREZ R. (1973).
Complex dielectric permittivity in rocks: A method for its measurment and analysis: Geophysics, Vol. 38, No. 5, 1973, pp. 920-940.

ANDERSON L. W. (1979)
Computer program. Numerical integration of related Hankel transforms of orders 0 and 1 by adaptive digital filtering: Geophysics, Vol. 44, No. 7, 1979, pp. 1287-1305.

ARCONE S. A. (1980)
Distortion of model subsurface radar pulse in complex dielectrics: Radio Science, Vol. 16, No. 5, 1980, pp. 855-864.

ARFKEN G. (1970)
Mathematical methods for physicists, Sec. Edition. Academic Press N.Y. pp. 346-373

BANOS A. (1966)
Dipole radiation in the presence of conducting half space, Pergamon Press. N.Y.

BOTTCHER C. J. F. (1952)
Theory of electric polarization: Elsevir Publishing Co. Amsterdam, Houston, London, N.Y., pp. 363-438.

BUSELLI G. (1982)
The effect of near-surface superparamagnetic material on electromagnetic measurements: Geophysics, Vol. 47, No. 9, 1982, pp. 1315-1324.

CARMICHAEL R. (1982)
Handbook of physical properties of rocks, Vol. 1., pp. 217-290. CRC Inc. Boca Raton, Florida.

CHANG D. C. and FISHER R. J. (1974)
A unified theory on radiation of a vertical electric dipole above a dissipative earth: Radio Science, Vol. 9, No. 12, pp. 1129-1138.

COLE K. S. and COLE R. H. (1942)
Dispersion and absorption in dielectrics II. Direct current characteristics: Journal of Chemical Physics, Vol. 10, 1942, pp. 98-105.

COLE K. S. and COLE R. H. (1941)
Dispersion and absorption in dielectrics I. Alternating current characteristics: Journal of Chemical Physics, Vol. 9, 1941, pp. 341-353.

COLLETT L. S. and KATSUBE T. J. (1973)
Electrical parameters of rocks in developing geophysical techniques: Geophysics, Vol. 38, No. 1, 1973, pp. 76-91.

COON A., FULLER J.C. and SCHAFERS C. J. (1981)
Experimental uses of short pulseradar in coal seams: Geophysics, Vol. 46, No. 8, 1981, pp. 1163-1168.

CROSSLEY D. J. (1982)
The theory of EM surface wave impedance measurements: Geophysical Applications of Surface Wave Impedance Measurements, Edited by Collett and Jensen, Paper 81-15, 1982, pp. 1-13.

DEBYE P. (1929)
Polar molecules: pp. 77-124. Chemical Catalog Co. Inc. Dover publications, Inc. N.Y.

FOSTER R. M. (1931)
Mutual impedance of grounded wires lying on the surface of the earth: Bell System Technical Journal, Vol. 10, 1931, pp. 408-419.

FREEDMAN B. and VORGIATZIS J. P. (1979)
Theory of microwave dielectric constant logging using the electromagnetic wave propagation method: Geophysics, Vol. 44, No. 5, 1979, pp. 969-986.

FULLER J. A. and WAIT J. R. (1972)
High-frequency electromagnetic coupling between small coplanar loops over an inhomogeneous ground: Geophysics, Vol. 37,No. 6, 1972, pp. 997-1004.

FULLER B. D. and WARD S. H. (1970)
Linear system description of the electrical parameters of rocks: IEEE transactions on Geoscience electronics, Vol. GE8, No. 1, 1970, pp.7-18.

GALT J. K. (1952)
Motiom of a ferromagnetic domain wall in Fe_3O_4: Physical Rev., Vol. 85, p. 664.

GRAY A. and MATHEWS G. B. (1966)
A treatise on Bessel functions and their applications to physics: Second edition prepared by Gray and MacRobert, Dover Publications Inc. N.Y.

GUPTASARMA D. (1983)
Effect of surface polarization on resistivity modeling: Geophysics, Vol. 48,No. 1, 1983, pp. 98-106.

GUPTASARMA D. (1982)
Computation of time domain response of a polarizable ground: Geophysics, Vol. 47,No. 1, 1982, pp. 1574-1576.

HOEKSTRA P. and DELANEY A. (1974)
Dielectric properties of soils at UHF and microwave frequencies: Journal of Geophysical Research, Vol 79, No. 1, 1974, pp. 1699-1708.

HANNEKEN J. W., GARNES J. G. and VANFHULL L. L. (1976)
The frequency dependence of the viscous component of the magnetic susceptibility of lunar rock and soil samples: Earth and Planetary Science Letters, Vol. 32, 1976, pp. 45-50.

JAIN S. C. (1981)
Master curves for derivation of Cole-Cole parameters from multichannel time-domain: Project no. IND/74/012, Report No. IND/74/012-20.

KATSUBE T. J. and COLLETT L.S. (1973)
Measuring techniques for rocks with high permittivity and high loss: Geophysics, Vol. 38, No. 1, 1973, pp. 92-103.

KING R. W., WU T. T. and SHEN L. C. (1974)
The horizontal wire antenna over a conducting or dielectric half space; Current and admittance: Radio Science, Vol. 9, No. 7, 1974, pp. 701-709.

KLEIN J. D. and SILL W. R. (1982)
On the electrical properties of Clay-bearing Sandstone: Personnal communication

KIRKWOOD J. G. and FUOSS R. M. (1941)
Anomalous dispersion and dielectric loss in polar polymers: Journal of Chemical Physics,vol. 9, 1941, pp. 329-340.

KITTEL C. (1958)
Introduction to solid state physics, Fifth Edition. John Wiley and Sons inc. N.Y., London, Sydney. Chap. 7.

KUO W. C. and MEI K. K. (1978)
Numerical approximations of the Sommerfeld integral for fast convergence: Radio Science, Vol. 13, No. 3, 1978, pp. 407-415.

KUO W. C. (1975)
Numerical treatment of Sommerfeld's integrals and its application to antenna and scattering problems: Ph.D. thesis, Department of Electrical Eng. and Computer Sciences, University of California, Berkley, Clifornia.

LAFLECHE P. (1984)
Field report on the McGill University VLF/UHF geophysical imaging system at the big nickel mine. Sudbury, Ontario: Unpublished.

LANDAU L. D. and LIFSHITZ E. M. (1969)
Statistical physics, Addison-Wesley Publishing Co., Section 125.

LANDAU L. D. and LIFSHITZ E. M. (1960)
Electrodynamics of continuous media, Pergamon Press, pp. 251-283.

LANGMUIR R. V. (1961)
Electromagnetic fields and waves, McGraw-Hill, N.Y., Toronto, London, Chap. 3,5-7,11.

LORRAIN P. and CORSON D. (1970)
Electromagnetic fields and waves, W. H. Freeman and company, San Francisco. Chap. 3,7-13.

MADDEN T. R. and CANTWELL T. (1967)
Induced polarization, a review: Mining Geophysics, Vol. 2, Tulsa, SEG, pp. 373-400.

MADDEN T. R. and MARSHALL D. J. (1959)
Induced polarization; a study of its causes and magnenitude in geologic materials: AEC Report RME-3169.

MEADOR R. A. and COX P. T. (1975)
Dielectric constant logging, a salinity independent estimation of formation water volume, Presented at the annual meetting of SPE, October 1975, Dallas TX.

MEGAW H. D. (1957)
Ferroelectricity in crystals. Chap. 1 and 4. Methuen Co. Ltd., London.

MILLET F. B. (1967)
Electomagnetic coupling of colinear dipoles on a uniform halfspace: Mining Geophysics, Vol. 2, Tulsa, SEG, PP.401-419.

MITTRA R., PARHAMI P. and RAHMAT-SAMII Y. (1979)
Solving the current element problem over lossy half space without Sommerfeld integrals: IEEE Transactions on Antennas and Propagation, Vol. AP27, No. 6, 1979, pp. 778-782.

SEN P. N., SCALA C. and COHEN M. H. (1981)
A self-similar model for sedimentary rocks with application to the dielectric constant of fused glass beads: Geophysics, Vol. 46, No. 5, 1981, pp. 781-795.

SHUEY R. T. and JOHNSON M. (1973)
On the phenomenology of electrical relaxation in rocks: Geophysics, Vol. 38, No. 1, 1973, pp. 37-48.

SIEGEL M. and KING P. W. (1970)
Electromagnetic fields in a dissipative half-space. A numerical approach: J. Appl. Phys., Vol. 41, 1970, pp. 2415-2423.

SMYTH C. P. (1955)
Dielectric behavior and structure, McGraw Hill N.Y., Toronto, London, pp. 17-104.

SOMMERFELD A. (1949)
Partial differential equations in physics, Academic Press, N.Y.

STRANGWAY D. W. (1967)
SEG - Mining Geophysics Vol. II pp. 437-445.

STRATTON J. A. (1941)
Electromagnetic Theory, McGraw Hill N.Y.

TELFORD W. M., GELDART L. P., SHERIFF R. E. and KEYS D. A. (1976)
Applied Geophysics, Cambridge University Press, Cambridge, London N.Y., Melbourne, pp. 442-457, 500-512.

TOMBS J. M. C. (1979)
A study of induced polarization decay curves: Report #102, Natural Environment Research Council, Institute of Geological Sciences, Applied geophysics Unit.

ULRYCH T. J. and LASSERE M. (1966)
Minimum phase: Journal of the Can. Soc. of Explo. Geo., Vol. 2, No. 1, 1966, pp. 22-32.

VAN BEEK L. K. H. (1967)
Dielectric behavior of heterogeneous systems: Progress in Dielectrics, Vol. 7, 1967, pp. 69-109.

VAN VOORHIS G. D., NELSON P. H. and DRAKE T. L. (1973)
Complex resistivity spectra of porphory copper mineralization: Geophysics, Vol. 38, No. 1, 1973, pp.49-60.

VINCENZ S. A.(1965)
Frequency dependence of magnetic susceptibility of rocks in weak alternating fields: Journal of Geophysical Research, Vol. 7, No. 6, 1965, pp. 1371-1377.

MOFFAT D. L. and PUSKAR R. J. (1976)
A subsurface electromagnetic pulse radar: Geophysics, Vol. 41, No. 3, 1976, pp. 506-518.

NEEL L. (1955)
Some theoretical aspects of rock magnetism: Advances in Physics, Vol. 4, 1955, pp. 191-243.

OLHOEFT G. R. and STRANGWAY D. W. (1974)
Magnetic relaxation and the electromagnetic response parameter: Geophysics, Vol. 39, No. 3, 1974, pp. 302-311.

OLHOEFT G. R. (1975)
The electrical properties of permafrost: Ph.D. thesis, Dept. of Physics, University of Toronto.

PATRA H. P. and MALLICK K. (1980)
Geosounding principles, 2: Time varying geoelectric soundings. Chap. 4 and 5, pp. 47-73.

PELTON W. H., RIJO L. and SWIFT C. M. (1978)
Inversion of 2-dimensional resistivity and IP data: Geophysics, Vol.43, No. 4, 1978, pp. 788-803.

PELTON W. H., WARD S. H., MALLOF P. G., SILL W. R. and NELSON P. H. (1976)
Mineral discrimination and removal of inductive coupling with multifrequency IP: Geophysics, Vol. 43, No. 3, 1976, pp. 588-609.

POLEY J. Ph., NOOTEBOOM J. J. and WAAL P. J. (1978)
Use of VHF dielectric measurements for borehole formation analysis: Log Analyst, pp. 8-30.

POWELL B. W. (1978)
Radiohm mapping of permafrost: M.Sc. thesis, Dep. of Minning and Metallurgical Eng., McGill University.

TOMBS J. M. C. (1979)
A study of induced polarization decay curves: Project No. 102, Report No. 046-79-1 MPP UK.

RYU J., WARD S. H., NASH W. P. and BUZZEL D. (1972)
K and tan spectra of dry lunar analog measured by various techniques: Geophysics, Vol. 38, No. 1, 1972, pp. 125-134.

SAKAR T. K. (1976)
Computer program descriptions: IEEE Transactions on Antennas and Propagation, Vol. AP24, No. 4, 1976, pp. 544-545.

SEARS F. W. (1951)
Electricity and magnetism, Addison-Wesley Publishing Co., Massachusetts.

SEN P. N., SCALA C. and COHEN M. H. (1981)
A self-similar model for sedimentary rocks with application to the dielectric constant of fused glass beads: Geophysics, Vol. 46, No. 5, 1981, pp. 781-795.

SHUEY R. T. and JOHNSON M. (1973)
On the phenomenology of electrical relaxation in rocks: Geophysics, Vol. 38, No. 1, 1973, pp. 37-48.

SIEGEL M. and KING P. W. (1970)
Electromagnetic fields in a dissipative half-space. A numerical approach: J. Appl. Phys., Vol. 41, 1970, pp. 2415-2423.

SMYTH C. P. (1955)
Dielectric behavior and structure, McGraw Hill N.Y., Toronto, London, pp. 17-104.

SOMMERFELD A. (1949)
Partial differential equations in physics, Academic Press, N.Y.

STRANGWAY D. W. (1967)
SEG - Mining Geophysics Vol. II pp. 437-445.

STRATTON J. A. (1941)
Electromagnetic Theory, McGraw Hill N.Y.

TELFORD W. M., GELDART L. P., SHERIFF R. E. and KEYS D. A. (1976)
Applied Geophysics, Cambridge University Press, Cambridge, London N.Y., Melbourne, pp. 442-457, 500-512.

TOMBS J. M. C. (1979)
A study of induced polarization decay curves: Report #102, Natural Environment Research Council, Institute of Geological Sciences, Applied geophysics Unit.

ULRYCH T. J. and LASSERE M. (1966)
Minimum phase: Journal of the Can. Soc. of Explo. Geo., Vol. 2, No. 1, 1966, pp. 22-32.

VAN BEEK L. K. H. (1967)
Dielectric behavior of heterogeneous systems: Progress in Dielectrics, Vol. 7, 1967, pp. 69-109.

VAN VOORHIS G. D., NELSON P. H. and DRAKE T. L. (1973)
Complex resistivity spectra of porphory copper mineralization: Geophysics, Vol. 38, No. 1, 1973, pp.49-60.

VINCENZ S. A.(1965)
Frequency dependence of magnetic susceptibility of rocks in weak alternating fields: Journal of Geophysical Research, Vol. 7, No. 6, 1965, pp. 1371-1377.

Appendix A

Program SVD.P1 inverts an effective resistivity curve and yields in the cole-cole electrical parameters.

```
LIST SVD.P1

C-------------------------------------------------
C  INVERTING OF WAVE-IMPEDANCE
C  DATA: AC10.D  AC27.D  BC10.D  BC27.D
C  RHO COLE ONLY
C  SVD.P1
C-------------------------------------------------
      INTEGER NO,NP,M
      REAL FRQ(20),ORES(20),CRES(20),DRES(20),DELX(6),S1(20),
     *     S2(20),E1(20),E2(20),X1(4),X2(4),PI,EPSI,
     *     X(6),XEP(4),D1(20),D2(20),EPS1,OMEGA(20)
      REAL*8 D(6),DELTA(20),WR(416),A(20,6),TITLE
      LOGICAL ALTERN,ACOLE
      DATA PI,EPS0/3.1415927,.885E-11/,IDGT/1/
C-----------------------------------------READING IN
      READ(5,230) TITLE
        READ(5,200) TEMP
      READ(5,220) NO,NP
      READ(5,200)(FRQ(I),ORES(I),I=1,NO)
      NP2=NP/2
      READ(5,200)(X1(I),I=1,NP2)
      READ(5,200)(X2(I),I=1,NP2)
      READ(5,200) EPS1
C-----------------------------------------WRITING OUT
      WRITE(6,300)
      WRITE(6,240) TITLE,TEMP
      WRITE(6,300)
      WRITE(6,320)
      WRITE(6,210)(FRQ(I),ORES(I),I=1,NO)
C-----------------------------------------DEFINING PARAMETERS
C     WRITE(6,250)
C     WRITE(6,330)(X1(I),I=1,NP2)
C     WRITE(6,260)
C     WRITE(6,330)(X2(I),I=1,NP2)
C     WRITE(6,300)
      DO 10 I=1,NO
      ORES(I)=ALOG10(ORES(I))
 10   OMEGA(I)=FRQ(I)*2.*PI*EPS0
      NI=1
      RHOI=2.92
      EPS=43.1
       X2(4)=.958
       X2(3)=.214E+5
      X2(1)=.4736E+6
      EPSI=ALOG10(1.01)
C-----------------------------------------FORMING COLOMN DELTA
      ACOLE=.FALSE.
 20   CALL COLE(S1,S2,X2,ACOLE,FRQ,PI,NO)
C     CALL RHO(E1,E2,S1,S2,OMEGA,CRES,RZERO,EPS0,ALTERN,NO)
       SSS=0.0
      WRITE(6,*) EPS,X2(1),X2(2),X2(3),X2(4)
      DO 30 I=1,NO
           Y=1./(S1(I)+OMEGA(I)*EPS)
        CRES(I)=Y+RHOI
      WRITE(6,*) CRES(I)
      CRES(I)=ALOG10(CRES(I))
         DRES(I)=RHOI*1.01+Y
       DRES(I)=ALOG10(DRES(I))
      DELTA(I)=ORES(I)-CRES(I)
      A(I,6)=(DRES(I)-CRES(I))/EPSI
      SSS=SSS+DELTA(I)*DELTA(I)
 30   CONTINUE
      SSS=SSS/NO
      WRITE(6,*) SSS
      WRITE(6,*)( DELTA(J),J=1,NO)
C-----------------------------------------FORMING MATRIX A
C     CALL PLOT2(DRES,ORES,CRES,20,60)
      DO 50 I=1,4
      X2(I)=X2(I)*1.01
      CALL COLE(D1,D2,X2,ACOLE,FRQ,PI,NO)
      DO 40 J=1,NO
        Z=RHOI+(1./(D1(J)+OMEGA(J)*EPS))
      DRES(J)=ALOG10(Z)
40    A(J,I)=(DRES(J)-CRES(J))/EPSI
50     X2(I)=X2(I)/1.01
       EPS=EPS*1.01
      DO 60 J=1,NO
      Z=RHOI+(1./(S1(J)+OMEGA(J)*EPS))
```

```
      DRES(J)=ALOG10(Z)
   )  A(J,5)=(DRES(J)-CRES(J))/EPSI
      DO 61 I=1,NO
   61   WRITE(6,310)(A(I,J),J=1,6)
      WRITE(6,1)
    1 FORMAT(' I AM AT INVERTING')
      NNN=6
      DO 70 I=1,4
   70 X(I)=X2(I)
      X(5)=EPS/1.01
      X(6)=RHOI
      CALL SVD(A,X,DELTA,DELX,D,WR,EPS1,NO,NNN)
      WRITE(6,300)
      NI=NI+1
        DO 129 I=1,NP2
  129  X2(I)=X(I)
      EPS=X(5)
      RHOI=X(6)
      IF(NI.LT.5) GO TO 20
      DO 140 I=1,NP2
   140 DELX(I)=10.**(DELX(I))
C     WRITE(6,270)(X(I),DELX(I),I=1,6)
      WRITE(6,300)
C     WRITE(6,*)(E1(I),I=1,20)
C     DO 135 I=1,NP2
C135   DELX(I)=DELX(I+NP2)
C     WRITE(6,260)
C     WRITE(6,270)(X2(I),DELX(I),I=1,NP2)
    199 STOP
    200 FORMAT(4G10.4)
    210 FORMAT(2G10.4)
    220 FORMAT(2I6)
    230 FORMAT(A7)
    240 FORMAT(/,' CASE OF',A7,'AT ',F10.2,'C',/)
    250 FORMAT(/'  COLE-COLE PERMITTIVITY PARAMETERS',/,
   *'    EPSI-ZERO    EPSI-INFINITY       TAU        ALFA'/)
    260 FORMAT(/,'  COLE-COLE CONDUCTIVITY PARAMETERS',/,
   *'    SIGMA-ZERO    SIGMA-INFINITY       TAU      ALFA',/)
    270 FORMAT(G12.4,'ERR',G12.4)
    300 FORMAT('-------------------------------------------')
    310 FORMAT(8G10.3)
    320 FORMAT(/,15X,'INPUT DATA',/,4X,'FREQUENCY',4X,'RESISTIVITY',/)
    330 FORMAT(3X,G10.4,7X,3G10.4)
      END
C-------------------------------------COLE-COLE COMPLEX CURVES
      SUBROUTINE COLE(Z1,Z2,X,ACOLE,FRQ,PI,NO)
      REAL Z1(1),Z2(1),X(1),FRQ(1),ZERO,LMT,TAU,ALFA,Y,A,
     *       AR,PI,F,B
      LOGICAL ACOLE
      ZERO=X(1)
      LMT=X(2)
      TAU=1./X(3)
      ALFA=X(4)
      Y=ALFA*PI/2.
      A=COS(Y)
      B=SIN(Y)
      IF(.NOT.ACOLE) GO TO 5
      A=SIN(Y)
      B=COS(Y)
      ALFA=1.-ALFA
    5 DO 10 I=1,NO
      Y=(FRQ(I)*TAU)**ALFA
      F=Y**2.+2.*A*Y+1.
      F=(ZERO-LMT)/F
      Z1(I)=(1.+Y*A)*F+LMT
C     Z2(I)=B*Y*F
   10 CONTINUE
      IF(ACOLE) GO TO 30
      DO 20 I=1,NO
      AR=Z1(I)*Z1(I)+Z2(I)*Z2(I)
      Z1(I)=Z1(I)/AR
C     Z2(I)=Z2(I)/AR
   20 CONTINUE
   30 CONTINUE
```

```
      RETURN
      END
C-----------------------------------------------SVD
      SUBROUTINE SVD(A,X,B,DELX,D,WR,EPS1,NO,NP)
      REAL*8 B(1),D(1),A(NO,1),WR(1),SUM
      REAL X(1),DELX(1)
      CALL LSVDF(A,NO,NO,NP,B,NO,1,D,WR,IER)
      WRITE(6,1)
    1 FORMAT(' SINGULAR VALUES')
      WRITE(6,50) (D(I),I=1,6)
      DO 20 I=1,NP
      SUM=0.0
      IF(D(I).NE.0.0) SUM=B(I)/((D(I)*D(I)+EPS1)/D(I))
   20 B(I)=SUM
      DO 40 I=1,NP
      SUM=0.0
      DO 30 J=1,NP
   30 SUM=SUM+A(I,J)*B(J)
      X(I)=ALOG10(X(I))
      IF(10**(X(I)).GT.4.*10**(X(I)+SUM)) GO TO 35
      IF(10**(X(I)).LT.10**(X(I)+SUM)/4.) GO TO 35
      X(I)=X(I)+SUM
   35 X(I)=10.**X(I)
   40 DELX(I)=SUM
      WRITE(6,60)
      WRITE(6,50) (X(I),I=1,6)
   50 FORMAT(4G12.4)
   60 FORMAT('  PARAMETERS AFTER CORRECTION')
      RETURN
      END
```

Appendix B

Program SVD.P simultaneously inverts effective resistivity and permittivity curves and yields in the corresponding Cole-Cole electrical parameters.

```
C-------------------------------------------------
C  INVERTION OF RESISTIVITY AND DIELECTRIC PERMITTIVITY
C   SERPENTINITE DATA
C-------------------------------------------------
      INTEGER NO,NP,M
      REAL FRQ(24),ORES(24),CAL(24),DER(24),DELX(8),OBS(24),
     *     S2(24),E1(24),E2(24),X1(4),X2(4),PI,EPSI,S1(24),
     *     X(8),XEP(4),D1(24),D2(24),EPS1,OMEGA(24),ODIEL(24)
      REAL*8 D(8),DELTA(24),WR(1024),A(24,8),TIT,LE
      LOGICAL ACOLE
      DATA PI,EPSO/3.1415927,.8841941E-11/,IDGT/1/
C-----------------------------------------READING IN
      READ(5,230) TIT,LE
      READ(5,200) TEMP
      READ(5,220) NO,NP
      READ(5,210)(FRQ(I),ORES(I),ODIEL(I),I=1,NO)
      NP2=NP/2
      NO2=NO*2
      READ(5,200)(X1(I),I=1,NP2)
      READ(5,200)(X2(I),I=1,NP2)
      READ(5,200) EPS1
C-----------------------------------------WRITING OUT
      WRITE(6,290)
      WRITE(6,300)
      WRITE(6,240) TIT,LE,TEMP
      WRITE(6,300)
      WRITE(6,320)
      WRITE(6,280)(FRQ(I),ORES(I),ODIEL(I),I=1,NO)
C-----------------------------------------DEFINING PARAMETERS
      WRITE(6,250)
      WRITE(6,330)(X1(I),I=1,NP2)
      WRITE(6,260)
      WRITE(6,330)(X2(I),I=1,NP2)
      WRITE(6,300)
      DO 10 I=1,NO
      OBS(I+NO)=ALOG10(ORES(I))
      OBS(I)=ALOG10(ODIEL(I))
 10   OMEGA(I)=FRQ(I)*2.*PI
      NI=1
      DO 15 I=1,NP2
      X(I)=X1(I)
 15   X(I+NP2)=X2(I)
C-----------------------------------------FORMING COLOMN DELTA
 20   RZERO=X2(1)
      ACOLE=.FALSE.
      CALL COLE(S1,S2,X2,ACOLE,FRQ,PI,NO)
      ACOLE=.TRUE.
      CALL COLE(E1,E2,X1,ACOLE,FRQ,PI,NO)
      CALL RHO(E1,E2,S1,S2,OMEGA,CAL,RZERO,EPSO,NO)
      WRITE(6,200) CAL
      DEL=0.0
      DO 40 I=1,NO2
      CAL(I)=ALOG10(CAL(I))
      DELTA(I)=OBS(I)-CAL(I)
 40   DEL=DEL+DELTA(I)
      DEL=DEL/NO2
      WRITE(6,*) DEL
C-----------------------------------------FORMING MATRIX A
      M=1
      ACOLE=.TRUE.
 60   CALL DERIV(X1,XEP,EPSI,NP2,M)
      CALL COLE(D1,D2,XEP,ACOLE,FRQ,PI,NO)
      CALL RHO(D1,D2,S1,S2,OMEGA,DER,RZERO,EPSO,NO)
      CALL MATRIX(DER,CAL,A,EPSI,NO2,NP2,M)
      M=M+1
      IF(M.LE.NP2) GO TO 60
       M1=1
      ACOLE=.FALSE.
 70   CALL DERIV(X2,XEP,EPSI,NP2,M1)
      RZERO=XEP(1)
      CALL COLE(D1,D2,XEP,ACOLE,FRQ,PI,NO)
      CALL RHO(E1,E2,D1,D2,OMEGA,DER,RZERO,EPSO,NO)
      CALL MATRIX(DER,CAL,A,EPSI,NO2,NP2,M)
      M=M+1
       M1=M1+1
      IF(M.LE.NP) GO TO 70
      M=M-1
      DO 61 I=1,24
C 61     WRITE(6,310)(A(I,J),J=1,8)
      WRITE(6,1)
      WRITE(6,300)
 1    FORMAT(' I AM AT INVERTING')
```

```
      CALL SVD(A,X,DELTA,DELX,D,WR,EPS1,NO2,NP)
      NI=NI+1
        DO 80 I=1,NP2
       X1(I)=X(I)
 80    X2(I)=X(I+NP2)
      IF(NI.LT.2) GO TO 20
      ACOLE=.FALSE.
      CALL COLE(S1,S2,X2,ACOLE,FRQ,PI,NO)
      ACOLE=.TRUE.
      CALL COLE(E1,E2,X1,ACOLE,FRQ,PI,NO)
      CALL RHO(E1,E2,S1,S2,OMEGA,CAL,RZERO,EPSO,NO)
      WRITE(6,200) CAL
      WRITE(6,240) TIT,LE,TEMP
      DO 140 I=1,NP
 140  DELX(I)=10.**(DELX(I))
      WRITE(6,270)(X(I),DELX(I),I=1,NP)
      WRITE(6,300)
 199  STOP
200   FORMAT(4G10.4)
210   FORMAT(3G10.4)
220   FORMAT(2I6)
230   FORMAT(4X,2A8)
240   FORMAT(/,' CASE OF ',2A8,' AT ',F10.2,'C')
250   FORMAT(/'  COLE-COLE PERMITTIVITY PARAMETERS',/,
     *'    EPSI-ZERO    EPSI-INFINITY       TAU        ALFA'/)
260   FORMAT(/,'  COLE-COLE CONDUCTIVITY PARAMETERS',/,
     *'    RESIS-ZERO    RESIS-INFINITY       TAU      ALFA',/)
270   FORMAT(G12.4,'ERR',G12.4)
 280  FORMAT(2G14.4,G17.4)
 290  FORMAT(1H1)
300   FORMAT('-----------------------------------------------')
310   FORMAT(8G10.3)
 320  FORMAT(/,15X,'INPUT DATA',/,4X,'FREQUENCY',4X,'RESISTIVITY',4X,
     &'DIELECTRIC PERM.'/)
 330  FORMAT(3X,G10.4,7X,3G10.4)
      END
C-----------------------------------------COLE-COLE COMPLEX CURVES
      SUBROUTINE COLE(Z1,Z2,X,ACOLE,FRQ,PI,NO)
      REAL Z1(1),Z2(1),X(1),FRQ(1),ZERO,LMT,TAU,ALFA,Y,A,
     *       AR,PI,F,B
      LOGICAL ACOLE
      ZERO=X(1)
      LMT=X(2)
      TAU=1./X(3)
      ALFA=X(4)
      Y=ALFA*PI/2.
      A=COS(Y)
      B=SIN(Y)
      IF(.NOT.ACOLE) GO TO 5
      A=SIN(Y)
      B=COS(Y)
      ALFA=1.-ALFA
   5  DO 10 I=1,NO
      Y=(FRQ(I)*TAU)**ALFA
      F=Y**2.+2.*A*Y+1.
      F=(ZERO-LMT)/F
      Z1(I)=(1.+Y*A)*F+LMT
 10   Z2(I)=B*Y*F
      IF(ACOLE) GO TO 30
      DO 20 I=1,NO
      AR=Z1(I)*Z1(I)+Z2(I)*Z2(I)
      Z1(I)=Z1(I)/AR
 20   Z2(I)=Z2(I)/AR
  30  CONTINUE
C     WRITE(6,40) Z1,Z2
      RETURN
 40   FORMAT(12G7.1)
      END
C-----------------------------------------DERIVATIVE OF PARAMTERS
      SUBROUTINE DERIV(X,XEP,EPSI,NP,M)
      REAL X(1),XEP(1),EPSI
      DO 10 I=1,NP
 10   XEP(I)=X(I)
      EPSI=0.01*X(M)
      XEP(M)=XEP(M)+EPSI
      EPSI=ALOG10(XEP(M))-ALOG10(X(M))
      RETURN
      END
C-----------------------------------------FORMING THE MATRIX A
      SUBROUTINE MATRIX(DER,CRES,A,EPSI,NO,NP,M)
      REAL DER(1),CRES(1),EPSI
      REAL*8 A(NO,NP)
```

```
      DO 10 I=1,NO
      DER(I)=ALOG10(DER(I))
   10 A(I,M)=(DER(I)-CRES(I))/EPSI
      RETURN
      END
C-----------------------------------------------RESISTIVITY
      SUBROUTINE RHO(E1,E2,S1,S2,OMEGA,CRES,RZERO,EPSO,NO)
      REAL E1(1),E2(1),S1(1),S2(1),OMEGA(1),CRES(1),RZERO
      DO 10 I=1,NO
      CRES(I)=E1(I)+S2(I)/OMEGA(I)/EPSO
      SE=S1(I)+OMEGA(I)*E2(I)*EPSO
 10   CRES(I+NO)=1./SE
 30   RETURN
      END
C-----------------------------------------------SVD
      SUBROUTINE SVD(A,X,B,DELX,D,WR,EPS1,NO,NP)
      REAL*8 B(1),D(1),A(NO,1),WR(1),SUM
      REAL X(1),DELX(1)
      CALL LSVDF(A,NO,NO,NP,B,NO,1,D,WR,IER)
      WRITE(6,1)
   1  FORMAT(' SINGULAR VALUES')
      WRITE(6,50) (D(I),I=1,8)
      DO 20 I=1,NP
      SUM=0.0
      IF(D(I).NE.0.0) SUM=B(I)/((D(I)*D(I)+EPS1)/D(I))
 20   B(I)=SUM
      DO 40 I=1,NP
      SUM=0.0
      DO 30 J=1,NP
 30   SUM=SUM+A(I,J)*B(J)
      X(I)=ALOG10(X(I))
      IF(10**(X(I)).GT.4.*10**(X(I)+SUM)) GO TO 35
      IF(10**(X(I)).LT.10**(X(I)+SUM)/4.) GO TO 35
      X(I)=X(I)+SUM
 35   X(I)=10.**X(I)
      IF(X(4).GT.1.0) X(4)=0.99
  40  DELX(I)=SUM
      IF(X(8).GT.1.0)X(8)=0.99
      WRITE(6,60)
      WRITE(6,50) (X(I),I=1,8)
 50   FORMAT(4G12.4)
 60   FORMAT('  PARAMETERS AFTER CORRECTION')
      RETURN
      END
```

Appendix C

Program HORANT.P given the electrical parameters at a certain frequency, calculates the E- and H-fields of a horizontal magnetic loop transmitting antenna versus distance over a homogeneous dissipative half-space.

```
LIST HORANT.P

C-------------------------------------------------------
C         HORIZONTAL ANTENNA OVER ARBITRARY EARTH
C
C   EARTH IS CONSIDERED TO BE HALF-SPACE.
C   A HORIZONTAL CONFIGUTATION OF A ROD ANTENNE IS  CONSIDERED.
C   THE ANTENNA IS POSITIONNED ONE WAVELENGHT ABOVE THE GROUND.
C   THE ANTENNA  LENGTH IS TAKEN  TO  BE EQUAL TO WAVELENGHT/4.
C   DEPTH OF MEASURMENT IS INITIALLY  EQUAL TO ONE  SKIN DEPTH.
C   FIELDS  ARE COMPUTED PER UNIT CURRENT,  BEING LINEAR IN IT.
C   THE VERTICAL CONFIGURATION  OF A FRAME ANTENNA CAN ALSO BE
C   COMPUTED FROM THIS PROGRAM BY INTERCHANGING E & H WITH H &
C   -E, AND EPSI & MU WITH MU & EPSI.
C
C   IFC  GIVES US THE  DIRECTION  OF THE HORIZONTAL  AXIS WITH
C   RESPECT TO THE DIRECTION OF THE ANTENNA,  BEING IT SELF IN
C   THE X-DIRECTION.
C   IFC=1   X-AXIS. (WE HAVE THE MAXIMUM FIELD VALUE HERE)
C   IFC=2   THE INDEPENDENT VARIABLE IS NORMALIZED WITH RESPECT
C           OF THE WAVELENGTH. X-AXIS CONSIDERED ONLY
C   IFC=3   AXIS MAKES 45 DEGREES WITH X-AXIS.
C   IFC=4   Y-AXIS. (WE HAVE THE MINIMUM FIELD HERE)
C
C   THIS PROGRAM USES ANDERSONS HANKEL TRANSFORM
C------------------------------------------- MAIN VARIABLES
      REAL FRQ,PI,CMU,EPSO,ANTLN,HGHT,DPTH,TOL,R(22),RNORM(22)
      REAL*8 K2,HF,EF
      COMPLEX COMP,ZHANKS,HX,HY,EX(22),EY(22),HYN(22),COEF1,COEF2,
     &        Z1,Z2,Z3,Z4,Z5,Z6
      COMPLEX*16 KE2,XX
      INTEGER NN,N,IFC
      EXTERNAL C1,C2,C3,C4,C5,C6
      COMMON/PARMTR/KE2,K2,DPTH,HGHT
      DATA PI,EPSO,CMU/3.1415927,8.841941E-12,1.25664E-6/,NN/21/
      DATA HF/'H-FIELD'/,EF/'E-FIELD'/
      READ(5,210) FRQ,K2,KE2
      READ(5,210) RR,TOL
      READ(5,220) MULT,IFC
C-----------------------------------------PARAMETERS
      C=10.**0.2
      RN=(1./3.)*1.E-3
      COMP=CMPLX(0.0,1.0)
      SL=EPSO*CMU
      SL=SQRT(SL)
C -------------------------------------------------ANTENNA LENGHT
      ANTLN=1./SL/4./FRQ
      HGHT=ANTLN*4.*MULT
      COEF1=COMP*ANTLN/PI/2.
      COEF2=ANTLN*FRQ*CMU/KE2
      XX=CDSQRT(KE2)
      DPTH=ABS(AIMAG(XX))
      DPTH=1./DPTH
      WRITE(6,320)
      WRITE(6,260)
      WRITE(6,230)
      WRITE(6,250) HGHT,ANTLN
      WRITE(6,240) DPTH
      WRITE(6,310) FRQ
      WRITE(6,260)
      WRITE(6,270)
C=----------------------------------------ANDERSON'S FILTER
      WRITE(6,280) HF
      WRITE(6,290)
      HX=0.0
      DO 80 I=1,NN
      CI=C**I
      N=INT(I/5.)
      TOLI=TOL/10.**N
      RI=RR*CI
      R(I)=RI
      RNORM(I)=RI/ANTLN/4.
      GO TO (20,30,30,40),IFC
 20   RNORM(I)=RN*CI
      RI=RNORM(I)*ANTLN*4.
      R(I)=RI
C-----------------------------------------INTEGRAL 2
 30   Z2=ZHANKS(1,RI,C2,TOLI,NF,1)
      CALL SAVER(1,1)
C-----------------------------------------INTEGRAL 5
      Z5=ZHANKS(0,RI,C5,TOLI,NF,0)
      Z5=Z5-Z2/RI
```

```
C-----------  ----------------------------------INTEGRAL 3
      Z3=ZHANKS(1,RI,C3,TOLI,NF,1)
       CALL SAVER(1,1)
C-------------------------------------------------INTEGRAL 4
       Z4=ZHANKS(1,RI,C4,TOLI,NF,0)
      Z4=Z4-Z3/RI
C-------------------------------------------------INTEGRAL 1
 40   Z1=ZHANKS(0,RI,C1,TOLI,NF,1)
      Z1=Z1*KE2
C-------------------------------------------------INTEGRAL 6
      Z6=ZHANKS(0,RI,C6,TOLI,NF,1)
      EY(I)=0.0
      GO TO(70,70,50,60), IFC
 50   HX=Z5*COEF1/2.
      HY=-COEF1*(Z6+Z5/2.)
      EX(I)=COEF2*(Z1+Z5/2.)
      EY(I)=-COEF2*Z4/2.
      GO TO 80
 60   HY=-COEF1*Z6
      EX(I)=COEF2*Z1
      GO TO 80
 70   HY=-COEF1*(Z6+Z5)
      EX(I)=COEF2*(Z1+Z4)
 80   WRITE(6,300) RI,RNORM(I),HX,HY
      WRITE(6,260)
      WRITE(6,280) EF
      WRITE(6,290)
C ---------------------------------------------WRITING OUT E-FIELD
       DO 110 I=1,NN
 110  WRITE(6,300) R(I),RNORM(I),EX(I),EY(I)
      GO TO 200
C     IF(IFC.NE.3) GO TO 200
C     WRITE(6,260)
C     WRITE(6,330)
C     WRITE(6,350)
C     DO 120 I=2,NN
C120  WRITE(6,340)RNORM(I),HYN(I),EEX(I)
 200   STOP
 210  FORMAT(4G10.4)
 220  FORMAT(2I6)
 230  FORMAT(' HORIZONTAL ANTENNA OVER AN ARBITRARY EARTH WITH'/)
 240  FORMAT(9X,' DEPTH=',G12.4,' M')
 250  FORMAT(8X,' HEIGHT=',G12.4,' M',/,' ANTENNA LENGTH=',G12.4,' M')
 260  FORMAT('-------------------------------------------------',/)
 280  FORMAT(' ANDERSON FILTER IS USED FOR FIELD EVALUATION',//)
 280  FORMAT(6X,'R        R/L',27X,A8)
 290  FORMAT(34X,'X',26X,'Y'//)
 300  FORMAT(2G10.4,2X,2('(',G11.5,'+I',G12.5,')')/)
 310  FORMAT(5X,' FREQUENCY=',G12.4,' HZ'/)
 320  FORMAT(1H1)
 330  FORMAT(/34X,' NORMALIZED FIELDS  ',/)
 340  FORMAT(6X,G10.4,6X,2('(',G11.5,'+I',G12.5,')')/)
 350  FORMAT(9X,'R/L',19X,'HY-FIELD',16X,'EX-FIELD'//)
      END
C------------------------------------------------- KERNEL 1
      COMPLEX FUNCTION C1(G)
      COMPLEX*16 KE2,C,B,E
      REAL*8 K2,AMDA,AMD,A,DPTH,HGHT
      COMMON/PARMTR/KE2,K2,DPTH,HGHT
      AMD=DBLE(G)
      AMDA=AMD*AMD
      A=AMDA-K2
      A=DSQRT(DABS(A))
      C=AMDA-KE2
      B=CDSQRT(C)
      IF(DREAL(B).LT.0.0) B=-B
      C=B*DPTH+A*HGHT
      E=1.0
      IF(DREAL(C).LT.150.) GO TO 100
      C1=0.0
      GO TO 200
 100  IF(DREAL(C).GE.0.1E-6)E=1./CDEXP(C)
      C1=AMD*E/(A+B)
      CR=REAL(C1)
      CI=AIMAG(C1)
      IF(ABS(CR).LT.0.1E-20) CR=0.0
      IF(ABS(CI).LT.0.1E-20) CI=0.0
      C1=CMPLX(CR,CI)
 200  RETURN
      END
C------------------------------------------------- KERNEL 2
```

```
C------------------------------------------------ KERNEL 2
      COMPLEX FUNCTION C2(G)
      COMPLEX*16 KE2,C,B,E
       REAL*8 K2,AMDA,A,DPTH,HGHT
      COMMON/PARMTR/KE2,K2,DPTH,HGHT
      AMDA=DBLE(G)
      AMDA=AMDA*AMDA
      A=AMDA-K2
      A=DSQRT(DABS(A))
      C=AMDA-KE2
      B=CDSQRT(C)
      IF(DREAL(B).LT.0.0) B=-B
      C=B*DPTH+A*HGHT
      E=1.0
      IF(DREAL(C).LT.170) GO TO 100
      C2=0.0
      GO TO 200
  100 IF(DREAL(C).GE.0.1E-6) E=1./CDEXP(C)
      C2=AMDA*(A-B)*E/(KE2*A+K2*B)
      CR=REAL(C2)
      CI=AIMAG(C2)
      IF(ABS(CR).LT.0.1E-20) CR=0.0
      IF(ABS(CI).LT.0.1E-20) CI=0.0
      C2=CMPLX(CR,CI)
  200 RETURN
      END
C------------------------------------------------ KERNEL 3
      COMPLEX FUNCTION C3(G)
      COMPLEX*16 KE2,C,B,E
       REAL*8 K2,AMDA,A,DPTH,HGHT
      COMMON/PARMTR/KE2,K2,DPTH,HGHT
      AMDA=DBLE(G)
      AMDA=AMDA*AMDA
      A=AMDA-K2
      A=DSQRT(DABS(A))
      C=AMDA-KE2
      B=CDSQRT(C)
      IF(DREAL(B).LT.0.0) B=-B
      C=B*DPTH+A*HGHT
      E=1.0
       IF(DREAL(C).LT.150.) GO TO 100
      C3=0.0
      GO TO 200
  100 IF(DREAL(C).GE.0.1E-3) E=1./CDEXP(C)
      C3=AMDA*E*(B*(A-B)/(KE2*A+K2*B)+1./(A+B))
      CR=REAL(C3)
      CI=AIMAG(C3)
      IF(ABS(CR).LT.0.1E-20) CR=0.0
      IF(ABS(CI).LT.0.1E-20) CI=0.0
      C3=CMPLX(CR,CI)
  200 RETURN
      END
C------------------------------------------------ KERNEL 4
      COMPLEX FUNCTION C4(G)
      COMPLEX*16 KE2,C,B,E
      REAL*8 K2,AMDA,AMD,A,DPTH,HGHT
      COMMON/PARMTR/KE2,K2,DPTH,HGHT
      AMD=DBLE(G)
      AMDA=AMD*AMD
      A=AMDA-K2
      A=DSQRT(DABS(A))
      C=AMDA-KE2
      B=CDSQRT(C)
      IF(DREAL(B).LT.0.0) B=-B
      C=B*DPTH+A*HGHT
      E=1.0
       IF(DREAL(C).LT.150.) GO TO 100
      C4=0.0
      GO TO 200
  100 IF(DREAL(C).GE.0.1E-6) E=1./CDEXP(C)
      C4=AMD*AMDA*E*(1./(A+B)+B*(A-B)/(KE2*A+K2*B))
      CR=REAL(C4)
      CI=AIMAG(C4)
      IF(ABS(CR).LT.0.1E-20) CR=0.0
      IF(ABS(CI).LT.0.1E-20) CI=0.0
      C4=CMPLX(CR,CI)
  200 RETURN
      END
C------------------------------------------------ KERNEL 5
```

```
C------------------------------------------------ KERNEL 5
      COMPLEX FUNCTION C5(G)
      COMPLEX*16 KE2,C,B,E
       REAL*8 K2,AMDA,AMD,A,DPTH,HGHT
      COMMON/PARMTR/KE2,K2,DPTH,HGHT
      AMD=DBLE(G)
      AMDA=AMD*AMD
      A=AMDA-K2
      A=DSQRT(DABS(A))
      C=AMDA-KE2
      B=CDSQRT(C)
      IF(DREAL(B).LT.0.0) B=-B
      C=B*DPTH+A*HGHT
      E=1.0
       IF(DREAL(C).LT.170.) GO TO 100
      C5=0.0
      GO TO 200
  100 IF(DREAL(C).GE.0.1E-6) E=1./CDEXP(C)
      C5=AMD*AMDA*(A-B)*E/(KE2*A+K2*B)
      CR=REAL(C5)
      CI=AIMAG(C5)
      IF(ABS(CR).LT.0.1E-20) CR=0.0
      IF(ABS(CI).LT.0.1E-20) CI=0.0
      C5=CMPLX(CR,CI)
  200 RETURN
      END
C------------------------------------------------ KERNEL 6
      COMPLEX FUNCTION C6(G)
      COMPLEX*16 KE2,C,B,E
      REAL*8 K2,AMDA,AMD,A,DPTH,HGHT
      COMMON/PARMTR/KE2,K2,DPTH,HGHT
      AMD=DBLE(G)
      AMDA=AMD*AMD
      A=AMDA-K2
      A=DSQRT(DABS(A))
      C=AMDA-KE2
      B=CDSQRT(C)
      IF(DREAL(B).LT.0.0) B=-B
      C=B*DPTH+A*HGHT
      E=1.0
      IF(DREAL(C).LT.170) GO TO 100
      C6=0.0
      GO TO 200
  100 IF(DREAL(C).GE.0.1E-6) E=1./CDEXP(C)
      C6=B*AMD*E/(A+B)
      CR=REAL(C6)
      CI=AIMAG(C6)
      IF(ABS(CR).LT.0.1E-20) CR=0.0
      IF(ABS(CI).LT.0.1E-20) CI=0.0
      C6=CMPLX(CR,CI)
  200 RETURN
      END
C-----------------------------------------HANKEL FILTER
      COMPLEX FUNCTION ZHANKS(N,B,FUN,TOL,NF,NEW)
      COMPLEX FUN,C,CMAX,FSAVE,KE2
      COMMON/SAVE/FSAVE(283),GSAVE(283),NSAVE
      COMMON/PARMTR/KE2,K2,DPTH,HGHT
      DOUBLE PRECISION E,ER,Y1,Y
      DIMENSION T(2),TMAX(2)
      DIMENSION WT0(283),WA0(76),WR0(76),WC0(76),WD0(55),
     *          WT1(283),WA1(76),WB1(76),WC1(76),WD1(55)
      EQUIVALENCE (WT0(1),WA0(1)),(WT0(77),WB0(1)),(WT0(153),WC0(1)),
     *            (WT0(229),WD0(1)),(WT1(1),WA1(1)),(WT1(77),WB1(1)),
     *            (WT1(153),WC1(1)),(WT1(229),WD1(1))
      EQUIVALENCE (C,T(1)),(CMAX,TMAX(1))
C-----------------------------------------E=DEXP(.2D0, ER=1./E
      DATA E/1.2214027581601698340/,ER/.81873075307798185900/
      DATA WA0/
     * 2.1969101E-11, 4.1201161E-09,-6.1322980E-09, 7.2479291E-09,
     *-7.9821627E-09, 8.5778983E-09,-9.1157294E-09, 9.6615250E-09,
     *-1.0207546E-08, 1.0796633E-08,-1.1393033E-08, 1.2049873E-08,
     *-1.2708789E-08, 1.3446466E-08,-1.4174300E-08, 1.5005577E-08,
     *-1.5807160E-08, 1.6747136E-08,-1.7625961E-08, 1.8693427E-08,
     *-1.9650840E-08, 2.0869789E-08,-2.1903555E-08, 2.3305308E-08,
     *-2.4407377E-08, 2.6033678E-08,-2.7186773E-08, 2.9094334E-08,
     *-3.0266804E-08, 3.2534013E-08,-3.3672072E-08, 3.6408936E-08,
```

```
*-3.7425022E-08, 4.0787921E-08,-4.1543242E-08, 4.5756842E-08,
*-4.6035233E-08, 5.1425075E-08,-5.0893896E-08, 5.7934897E-08,
*-5.6086570E-08, 6.5475248E-08,-6.1539913E-08, 7.4301996E-08,
*-6.7117043E-08, 8.4767837E-08,-7.2583120E-08, 9.7366568E-08,
*-7.7553611E-08, 1.1279873E-07,-8.1416723E-08, 1.3206914E-07,
*-8.3217217E-08, 1.5663185E-07,-8.1482581E-08, 1.8860593E-07,
*-7.3963141E-08, 2.3109673E-07,-5.7243707E-08, 2.8867452E-07,
*-2.6163525E-08, 3.6808773E-07, 2.7049871E-08, 4.7932617E-07,
* 1.1407365E-07, 6.3720626E-07, 2.5241961E-07, 8.6373487E-07,
* 4.6831433E-07, 1.1916346E-06, 8.0099716E-07, 1.6696015E-06,
* 1.3091334E-06, 2.3701475E-06, 2.0803829E-06, 3.4012978E-06/
 DATA WBO/
* 3.2456774E-06, 4.9240402E-06, 5.0005198E-06, 7.1783540E-06,
* 7.6367633E-06, 1.0522038E-05, 1.1590021E-05, 1.5488635E-05,
* 1.7510398E-05, 2.2873836E-05, 2.6368006E-05, 3.3864387E-05,
* 3.9610390E-05, 5.0230379E-05, 5.9397373E-05, 7.4612122E-05,
* 8.8951409E-05, 1.1094809E-04, 1.3308026E-04, 1.6511335E-04,
* 1.9895671E-04, 2.4587195E-04, 2.9728181E-04, 3.6629770E-04,
* 4.4402013E-04, 5.4589361E-04, 6.6298832E-04, 8.1375348E-04,
* 9.8971624E-04, 1.2132772E-03, 1.4772052E-03, 1.8092022E-03,
* 2.2045122E-03, 2.6980811E-03, 3.2895354E-03, 4.0238764E-03,
* 4.9080203E-03, 6.0010999E-03, 7.3216878E-03, 8.9489225E-03,
* 1.0919448E-02, 1.3340696E-02, 1.6276399E-02, 1.9873311E-02,
* 2.4233627E-02, 2.9555699E-02, 3.5990069E-02, 4.3791529E-02,
* 5.3150319E-02, 6.4341372E-02, 7.7506720E-02, 9.2749987E-02,
* 1.0980561E-01, 1.2791555E-01, 1.4525830E-01, 1.5820085E-01,
* 1.6058576E-01, 1.4196085E-01, 8.9781222E-02,-1.0238278E-02,
*-1.5083434E-01,-2.9059573E-01,-2.9105437E-01,-3.7973244E-02,
* 3.8273717E-01, 2.2014118E-01,-4.7342635E-01, 1.9331133E-01,
* 5.3839527E-02,-1.1909845E-01, 9.9317051E-02,-6.6152628E-02,
* 4.0703241E-02,-2.4358316E-02, 1.4476533E-02,-8.6198067E-03/
 DATA WCO/
* 5.1597053E-03,-3.1074602E-03, 1.8822342E-03,-1.1456545E-03,
* 7.0004347E-04,-4.2904226E-04, 2.6354444E-04,-1.6215439E-04,
* 9.9891279E-05,-6.1589037E-05, 3.7996921E-05,-2.3452250E-05,
* 1.4479572E-05,-8.9417427E-06, 5.5227518E-06,-7.4114252E-06,
* 2.1074101E-06,-1.3019229E-06, 8.0433617E-07,-4.9693681E-08,
* 3.0702417E-07,-1.8969219E-07, 1.1720069E-07,-3.2412496E-08,
* 4.4740283E-08,-2.7643004E-08, 1.7079403E-08,-1.0552634E-08,
* 6.5200311E-09,-4.0284597E-09, 2.4890232E-09,-1.5378695E-09,
* 9.5019040E-10,-5.8708696E-10, 3.6273937E-10,-2.2412348E-10,
* 1.3847792E-10,-8.5560821E-11, 5.2865474E-11,-3.2664392E-11,
* 2.0182948E-11,-1.2470979E-11, 7.7057678E-12,-4.7611713E-12,
* 2.9415274E-12,-1.8170081E-12, 1.1221034E-12,-6.9271067E-13,
* 4.2739744E-13,-2.6344388E-13, 1.1697105E-13,-9.9147443E-14,
* 6.0487998E-14,-3.6973097E-14, 2.2817964E-14,-1.4315547E-14,
* 9.1574735E-15,-5.9567236E-15, 3.9209969E-15,-2.5911739E-15,
* 1.6406939E-15,-8.8248590E-16, 3.0195409E-16, 2.2622634E-17,
*-8.0942556E-17,-3.7172363E-17, 1.9299542E-16,-3.3388160E-16,
* 4.6174116E-16,-5.8627358E-16, 7.2227767E-16,-8.7972941E-16,
* 1.0211793E-15,-1.0940039E-15, 1.0789555E-15,-9.7089814E-16/
 DATA WDO/
* 7.4110927E-16,-4.1700094E-16, 8.5977184E-17, 1.3396469E-16,
*-1.7838410E-16, 4.8975421E-17, 1.9398153E-16,-5.0046989E-16,
* 8.3280985E-16,-1.1544640E-15, 1.4401527E-15,-1.6637066E-15,
* 1.7777129E-15,-1.7322187E-15, 1.5247247E-15,-1.1771155E-15,
* 6.9747910E-16,-1.2088956E-16,-4.8382957E-16, 1.0408292E-15,
*-1.5220450E-15, 1.9541597E-15,-2.4107448E-15, 2.9241438E-15,
*-3.5176475E-15, 4.2276125E-15,-5.0977851E-15, 6.1428456E-15,
*-7.3949962E-15, 8.8597601E-15,-1.0515959E-14, 1.2264584E-14,
*-1.3949870E-14, 1.5332490E-14,-1.6146782E-14, 1.6084121E-14,
*-1.4962523E-14, 1.2794804E-14,-9.9286701E-15, 6.8825809E-15,
*-4.0056107E-15, 1.5965079E-15,-7.2732961E-18,-4.0433218E-16,
*-6.5679655E-16, 3.3011866E-15,-7.3545910E-15, 1.2394851E-14,
*-1.7947697E-14, 2.3774303E-14,-3.0279168E-14, 3.9252831E-14,
*-5.5510504E-14, 9.0505371E-14,-1.7064873E-13/
 DATA WA1/
*-4.2129715E-16, 5.3667031E-15,-7.1183962E-15, 8.9478500E-15,
*-1.0767891E-14, 1.2362265E-14,-1.3371129E-14, 1.3284178E-14,
*-1.1714302E-14, 8.4134738E-15,-3.7726725E-15,-1.4263879E-15,
* 6.1279163E-15,-9.1102765E-15, 9.9696405E-15,-9.3649955E-15,
* 8.6009018E-15,-8.9749846E-15, 1.1153987E-14,-1.4914821E-14,
* 1.9314024E-14,-2.3172388E-14, 2.5605477E-14,-2.6217555E-14,
* 2.5057768E-14,-2.2485539E-14, 1.9022752E-14,-1.5198084E-14,
* 1.1422464E-14,-3.9323958E-15, 4.8421406E-15,-2.1875032E-15,
*-3.2177842E-17, 1.8637565E-15,-3.3683643E-15, 4.6132219E-15,
*-5.6209538E-15, 6.4192841E-15,-6.8959928E-15, 6.9895792E-15,
```

```
     *-6.5355935E-15, 5.6125163E-15,-4.1453931E-15, 2.6358827E-15,
     *-9.5104370E-16, 1.4600474E-16, 5.6166519E-16, 8.2899246E-17,
     * 5.0032100E-16, 4.3752205E-16, 2.1052293E-15,-9.5451973E-16,
     * 6.4004437E-15,-2.1926177E-15, 1.1651003E-14, 5.8415433E-16,
     * 1.8044664E-14, 1.0755745E-14, 3.0159022E-14, 3.3506138E-14,
     * 5.8709354E-14, 8.1475200E-14, 1.2530006E-13, 1.8519112E-13,
     * 2.7641786E-13, 4.1330823E-13, 6.1506209E-13, 9.1921659E-13,
     * 1.3698462E-12, 2.0447427E-12, 3.0494477E-12, 4.5501001E-12,
     * 6.7870250E-12, 1.0126237E-11, 1.5104976E-11, 2.2536053E-11/
      DATA WB1/
     * 3.3617368E-11, 5.0153839E-11, 7.4818173E-11, 1.1161804E-10,
     * 1.6651222E-10, 2.4840923E-10, 3.7058109E-10, 5.5284353E-10,
     * 8.2474468E-10, 1.2303750E-09, 1.8355034E-09, 2.7382502E-09,
     * 4.0849867E-09, 6.0940898E-09, 9.0913020E-09, 1.3562651E-08,
     * 2.0233058E-08, 3.0184244E-08, 4.5029477E-08, 6.7176304E-08,
     * 1.0021488E-07, 1.4950371E-07, 2.2303208E-07, 3.3272689E-07,
     * 4.9636623E-07, 7.4049804E-07, 1.1046805E-06, 1.6480103E-06,
     * 2.4585014E-06, 3.6677163E-06, 5.4714550E-06, 8.1626422E-06,
     * 1.2176782E-05, 1.8166179E-05, 2.7099223E-05, 4.0428804E-05,
     * 6.0307294E-05, 8.9971508E-05, 1.3420195E-04, 2.0021123E-04,
     * 2.9860417E-04, 4.4545291E-04, 6.6423156E-04, 9.9073275E-04,
     * 1.4767050E-03, 2.2016806E-03, 3.2788147E-03, 4.8837292E-03,
     * 7.2596811E-03, 1.0788355E-02, 1.5973323E-02, 2.3612041E-02,
     * 3.4655327E-02, 5.0608141E-02, 7.2827752E-02, 1.0337889E-01,
     * 1.4207357E-01, 1.8821315E-01, 2.2996815E-01, 2.5088500E-01,
     * 2.0334626E-01, 6.0665451E-02,-2.0275683E-01,-3.5772336E-01,
     *-1.8280529E-01, 4.7014634E-01, 7.2991233E-03,-3.0614594E-01,
     * 2.4781735E-01,-1.1149185E-01, 2.5985386E-02, 1.0850279E-02,
     *-2.2830217E-02, 2.4644647E-02,-2.2895284E-02, 2.0197032E-02/
      DATA WC1/
     *-1.7488968E-02, 1.5057670E-02,-1.2953923E-02, 1.1153254E-02,
     *-9.6138436E-03, 8.2952090E-03,-7.1628361E-03, 6.1882910E-03,
     *-5.3482055E-03, 4.6232056E-03,-3.9970542E-03, 3.4560118E-03,
     *-2.9883670E-03, 2.5840861E-03,-2.2345428E-03, 1.9323046E-03,
     *-1.6709583E-03, 1.4449655E-03,-1.2495408E-03, 1.0805480E-03,
     *-9.3441130E-04, 8.0803899E-04,-6.9875784E-04, 6.0425624E-04,
     *-5.2253532E-04, 4.5186652E-04,-3.9075515E-04, 3.3790861E-04,
     *-2.9220916E-04, 2.5269019E-04,-2.1851585E-04, 1.8896332E-04,
     *-1.6340753E-04, 1.4130796E-04,-1.2219719E-04, 1.0567099E-04,
     *-9.1379828E-05, 7.9021432E-05,-6.8334412E-05, 5.9092726E-05,
     *-5.1100905E-05, 4.4189914E-05,-3.8213580E-05, 3.3045496E-05,
     *-2.8576356E-05, 2.4711631E-05,-2.1369580E-05, 1.8479514E-05,
     *-1.5980307E-05, 1.3819097E-05,-1.1950174E-05, 1.0334008E-05,
     *-8.9364160E-06, 7.7278366E-06,-6.6827083E-06, 5.7789251E-06,
     *-4.9973715E-06, 4.3215167E-06,-3.7370660E-06, 3.2316575E-06,
     *-2.7946015E-06, 2.4166539E-06,-2.0898207E-06, 1.8071890E-06,
     *-1.5627811E-06, 1.3514274E-06,-1.1686576E-06, 1.0106056E-06,
     *-8.7392952E-07, 7.5573750E-07,-6.5353002E-07, 5.6514528E-07,
     *-4.8871388E-07, 4.2261921E-07,-3.6546333E-07, 3.1603732E-07/
      DATA WD1/
     *-2.7329579E-07, 2.3633470E-07,-2.0437231E-07, 1.7673258E-07,
     *-1.5283091E-07, 1.3216174E-07,-1.1428792E-07, 9.8831386E-08,
     *-8.5465227E-08, 7.3906734E-08,-6.3911437E-08, 5.5267923E-08,
     *-4.7793376E-08, 4.1329702E-08,-3.5740189E-08, 3.0906612E-08,
     *-2.6726739E-08, 2.3112160E-08,-1.9986424E-08, 1.7283419E-08,
     *-1.4945974E-08, 1.2924650E-08,-1.1176694E-08, 9.6651347E-09,
     *-8.3580023E-09, 7.2276490E-09,-6.2501673E-09, 5.4048822E-09,
     *-4.6739154E-09, 4.0418061E-09,-3.4951847E-09, 3.0224895E-09,
     *-2.6137226E-09, 2.2602382E-09,-1.9545596E-09, 1.6902214E-09,
     *-1.4616324E-09, 1.2639577E-09,-1.0930164E-09, 9.4519327E-10,
     *-8.1736202E-10, 7.0681930E-10,-6.1122713E-10, 5.2856342E-10,
     *-4.5707937E-10, 3.9526267E-10,-3.4180569E-10, 2.9557785E-10,
     *-2.5560176E-10, 2.2103233E-10,-1.9113891E-10, 1.6528994E-10,
     *-1.4294012E-10, 1.2361991E-10,-8.2740936E-11/
C
      NONE=0
      IF(NEW.EQ.0) GO TO 100
      NSAVE=0
      Y1=.735885266147979446D0/DBLE(B)
  100 ZHANKS=CMPLX(0.0,0.0)
      CMAX=CMPLX(0.0,0.0)
      NF=0
      Y=Y1
      ASSIGN 110 TO M
      I=131
```

```
      Y=Y*E
      GO TO 200
  110 TMAX(1)=AMAX1(ABS(T(1)),TMAX(1))
      TMAX(2)=AMAX1(ABS(T(2)),TMAX(2))
      I=I+1
      Y=Y*E
      IF(I.LE.149) GO TO 200
      IF(TMAX(1).EQ.0.0.AND.TMAX(2).EQ.0.0) NONE=1
      CMAX=TOL*CMAX
      ASSIGN 120 TO M
      GO TO 200
  120 IF(ABS(T(1)).LE.TMAX(1).AND.ABS(T(2)).LE.TMAX(2)) GO TO 130
      I=I+1
      Y=Y*E
      IF(I.LE.283) GO TO 200
  130 Y=Y1
      ASSIGN 140 TO M
      I=130
      GO TO 200
  140 IF(ABS(T(1)).LE.TMAX(1).AND.ABS(T(2)).LE.TMAX(2).AND.
     *NONE.EQ.0) GO TO 190
      I=I-1
      Y=Y*ER
      IF(I.GT.0) GO TO 200
  190 ISAVE=1
      ZHANKS=ZHANKS/B
      RETURN
  200 G=SNGL(Y)
      IF(NEW) 300,210,300
  210 IF(ISAVE.GT.NSAVE) GO TO 300
      ISAVE0=ISAVE
  220 IF(G.EQ.GSAVE(ISAVE)) GO TO 240
      ISAVE=ISAVE+1
      IF(ISAVE.LE.NSAVE) GO TO 220
      ISAVE=ISAVE0
      GO TO 300
  240 C=FSAVE(ISAVE)
      ISAVE=ISAVE+1
      IF(N) 270,260,270
  260 C=C*WT0(I)
      GO TO 280
  270 C=C*WT1(I)
  280 ZHANKS=ZHANKS+C
      GO TO M,(110,120,140)
  300 NSAVE=NSAVE+1
      C=FUN(G)
      NF=NF+1
      FSAVE(NSAVE)=C
      GSAVE(NSAVE)=G
      GO TO 250
  400 RETURN
      END
C-----------------------------------------SUBPROGRAM SAVER
      SUBROUTINE SAVER(I,J)
      COMPLEX FSAVE
      COMMON/SAVE/FSAVE(283),GSAVE(283),NSAVE
      DO 1 K=1,NSAVE
    1 FSAVE(K)=(GSAVE(K)**I)*(FSAVE(K)**J)
      RETURN
      END
```

Appendix D

Program VERANT.P, given the electrical parameters at a certain frequency, calculates the E- and H-fields of a vertical transmitting dipole antenna versus distance, over a homogeneous dissipative half-space.

```
LIST VERANT.P

VAX PROGRESS
C-----------------------------------------------------------
C         VERTICAL ANTENNA OVER ARBITRARY EARTH
C
C   EARTH IS CONSIDERED TO BE HALF-SPACE.
C   A VERTIAL  CONFIGUTATION  OF A ROD  ANTENNA IS CONSIDERED.
C   THE ANTENNA IS POSITIONNED MULT X WAVELENGHT ABOVE GROUND.
C   GROUND.
C   THE ANTENNA LENGHT IS TAKEN TO BE EQUAL TO WAVELENGHT/4.
C   THE DEPTH OF  MEASUREMENT IS  EQUAL  TO  ONE  SKINDEPTH.
C   FIELDS ARE COMPUTED PER UNIT CURRENT,  BEING LINEAR IN IT
C   THE HORIZONTAL CONFIGURATION OF A FRAME  ANTENNA CAN ALSO
C   BE COMPUTED FROM THIS PROGRAM BY INTERCHANGING E & H WITH
C   H & -E, AND EPSI, MU WITH MU,EPSI.
C
C   IFC=0  INDEPENDENT VARIABLE NORMALIZED
C   IFC=1  INDEPENDENT VARIABLE AS AN ABSOLUTE MEASURE
C
C   THIS PROGRAM USES ANDERSONS HANKEL TRANSFORM
C-----------------------------------------------------------  MAIN VARIABLES
      REAL OMEGA,EPSO,PI,ANTLN,HGHT,FRQ,R,TOL,CMU,DPTH,SIGR(1),SIGI(1),
     ¥     RNORM(25),COLP(4)
      REAL*8 K2,HF,EF,XS
      COMPLEX COMP,Z,ZHANKS,E,H,HN(25)
      COMPLEX*16 KE2,XX
      INTEGER NN
      LOGICAL ACOLE
      ACOLE=.FALSE.
      EXTERNAL C1,C2
      COMMON/PARMTR/KE2,K2,DPTH,HGHT
      DATA HF/'H-FIELD'/,EF/'E-FIELD'/
      DATA PI,EPSO,CMU/3.1415927,.8841941E-11,.125664E-5/,NN/20/
C     READ(5,210) FRQ,K2,KE2
      READ(5,210) FRQ
      READ(5,210) COLP
      READ(5,210) R,TOL
      READ(5,220) MULT,IFC
C-----------------------------------------------------PARAMETERS
      OMEGA=2.*PI*FRQ
      C=10.**0.2
      RN=(1./3.)*1.E-03
       SL=EPSO*CMU
      K2=OMEGA*OMEGA*SL
      SL=SQRT(SL)
      COMP=CMPLX(0.0,1.0)
      CALL COLE(SIGR,SIGI,COLP,ACOLE,FRQ,PI,1)
      XX=CMPLX(SIGR(1),-SIGI(1))
      KE2=OMEGA*CMU*XX
C-----------------------------------------------SET ANTENNA LENGHT
      ANTLN=1./SL/4./FRQ
      HGHT=ANTLN*4.*MULT
      XX=CDSQRT(KE2)
      DPTH=ABS(AIMAG(XX))
      DPTH=1./DPTH
      WRITE(6,310)
      WRITE(6,260)
      WRITE(6,230)
      WRITE(6,240) DPTH
      WRITE(6,250) HGHT, ANTLN
       WRITE(6,290) FRQ
      WRITE(6,350) MULT
      WRITE(6,260)
      WRITE(6,270)
      WRITE(6,260)
      WRITE(6,340) KE2,K2
C-----------------------------------------------ANDERSON'S FILTER
      WRITE(6,280) HF,EF
      DO 370 I=1,NN
      CI=C**I
      N=INT(I/5.)
```

```
      TOLI=TOL/10.**N
      IF(IFC.EQ.0) GO TO 10
      CI=R*CI
      RNORM(I)=SL*RI*RQ
      GO TO 20
   10 RNORM(I)=RN*CI
      RI=RNORM(I)*ANTLN*4.
C-----------------------------------------------------INTEGRAL 1
C                                                H=2.*PARM*K2*KE2*Z/MU/OMEGA
   20 Z=ZHANKS(1,RI,C1,TOLI,NF,1)
      H=-COMP*ANTLN*KE2*Z/PI/2.
      IF(IFC.EQ.0) HN(I)=H/OMEGA
C-----------------------------------------------------INTEGRAL 2
C                                                    E=-2.*I*K2*Z*PARM
C     Z=ZHANKS(1,RI,C2,TOLI,NF,1)
C     E=-FRQ*CMU*ANTLN*Z
      WRITE(6,300) RI,RNORM(I),H,E
  170 CONTINUE
      IF(IFC.NE.0) GO TO 200
      WRITE(6,260)
      WRITE(6,320)HF
      WRITE(6,330)(RNORM(I),HN(I),I=1,NN)
  200  STOP
  210 FORMAT(4G10.4)
  220 FORMAT(2I6)
  230 FORMAT(' VERTICAL ANTENNA OVER AN ARBITRARY EARTH W)TH'/)
  240 FORMAT(' DEPTH',T16,'=',G10.3,'M')
  250 FORMAT(' HEIGHT',T16,'=',G10.3,'M',/
     *,' ANTENNA LENGTH',T16,'=',G10.3,'M')
  260 FORMAT('-------------------------------------------------',/)
  270 FORMAT(' ANDERSON FILTER IS USED FOR FIELD EVALUATION ')
  280 FORMAT(5X,'R',8X,'R/L',14X,A8,20X,A8,/,4X,'(M)',24X,
     &'(AMP/M)',22X,'(V/M)',//)
  290 FORMAT(' FREQUENCY',T16,'=',G12.4,'HZ')
  300 FORMAT(2G10.4,2X,2('(',G10.4,'+I',G12.4,')')/)
  310 FORMAT(1H1)
  320 FORMAT('    NORMALIZED H-FIELD  (AMP/M/FRQ)',/,T3,'R/L',T20,A8)
  330 FORMAT(G10.4,2X,'(',G10.4,'+I',G12.4,')'/)
  340 FORMAT(' KE2=',T16,2G14.5,/' K2=',T16,G14.5)
C 350  FORMAT(/' THE DEPTH OF MEASUREMENT IS ',I5,' X SKINDEPTH ',
  350 FORMAT(/' THE ANTENNA IS POSITIONNED ',G10.4,' X WAVELENGTH ',
     &'ABOVE GROUND')
C     &'BELOW  GROUND')
      END
C-------------------------------------------------- KERNEL 1
      COMPLEX FUNCTION C1(G)
      COMPLEX*16 KE2,C,B
      REAL*8 K2,AMDA,DPHT,A,E,HGHT,AMD
      COMMON/PARMTR/KE2,K2,DPTH,HGHT
      AMD=DBLE(G)
      AMDA=AMD*AMD
      A=AMDA-K2
      A=DSQRT(DABS(A))
      C=AMDA-KE2
      B=CDSQRT(C)
      IF(DREAL(B).LT.0.0) B=-B
      C=B*DPTH+A*HGHT
      E=1.0
      IF(DREAL(C).LT.170.) GO TO 100
      C1=0.0
      GO TO 200
  100 IF(DREAL(C).GE.0.1E-6) E=1./CDEXP(C)
      C1=AMDA*E/(KE2*A+K2*B)
      CR=REAL(C1)
      CI=AIMAG(C1)
      IF(ABS(CR).LT.0.1E-20) CR=0.0
      IF(ABS(CI).LT.0.1E-20) CI=0.0
      C1=CMPLX(CR,CI)
      WRITE(6,10) AMD,A,B,C1
  200 RETURN
   10 FORMAT(6G12.5)
      END
```

```
C-----------------------------------------------------------------[illegible]
      COMPLEX FUNCTION C2(G)
      COMPLEX*16 KE2,C,B
      REAL*8 K2,AMDA,DPTH,A,E,HGHT
      COMMON/PARMTR/KE2,K2,DPTH,HGHT
      AMDA=DBLE(G)
      AMDA=AMDA*AMDA
      A=AMDA-K2
      A=DSQRT(DABS(A))
      C=AMDA-KE2
      B=CDSQRT(C)
      IF(DREAL(B).LT.0.0) B=-B
      C=B*DPTH+A*HGHT
      E=1.0
       IF(DREAL(C).LT.170.) GO TO 100
       C2=0.0
      GO TO 200
100   IF(DREAL(C).GE.0.1E-6) E=1./CDEXP(C)
      C2=AMDA*B*E/(KE2*A+K2*B)
      CR=REAL(C2)
      CI=AIMAG(C2)
      IF(ABS(CR).LT.0.1E-20) CR=0.0
      IF(ABS(CI).LT.0.1E-20) CI=0.0
      C2=CMPLX(CR,CI)
200   RETURN
      END
C------------------------------------------------HANKELCFILTER
      COMPLEX FUNCTION ZHANKS(N,B,FUN,TOL,NF,NEW)
      COMPLEX FUN,C,CMAX,FSAVE,KE2
      REAL K2
      COMMON/SAVE/FSAVE(283),GSAVE(283),NSAVE
      COMMON/PARMTR/KE2,K2,DPTH,HGHT
      DOUBLE PRECISION E,ER,Y1,Y
      DIMENSION T(2),TMAX(2)
      DIMENSION WT0(283),WA0(76),WB0(76),WC0(76),WD0(55),
     *          WT1(283),WA1(76),WB1(76),WC1(76),WD1(55)
      EQUIVALENCE (WT0(1),WA0(1)),(WT0(77),WB0(1)),(WT0(153),WC0(1)),
     *            (WT0(229),WD0(1)),(WT1(1),WA1(1)),(WT1(77),WB1(1)),
     *            (WT1(153),WC1(1)),(WT1(229),WD1(1))
      EQUIVALENCE (C,T(1)),(CMAX,TMAX(1))
C-----------------------------------------------E=DEXP(.2D0,CER=1./E
      DATA E/1.2214027581601698340D/,ER/.81873075307798185910/
      DATA WA0/
     * 2.1969101E-11, 4.1201161E-09,-6.1322980E-09, 7.2479291E-09,
     *-7.9821627E-09, 8.5778983E-09,-9.1157294E-09, 9.6615250E-09,
     *-1.0207546E-08, 1.0796633E-08,-1.1393033E-08, 1.2049873E-08,
     *-1.2708789E-08, 1.3446466E-08,-1.4174300E-08, 1.5005577E-08,
     *-1.5807160E-08, 1.6747136E-08,-1.7625961E-08, 1.8693427E-08,
     *-1.9650840E-08, 2.0869789E-08,-2.1903555E-08, 2.3305308E-08,
     *-2.4407377E-08, 2.6033678E-08,-2.7186773E-08, 2.9094334E-08,
     *-3.0266804E-08, 3.2534013E-08,-3.3672072E-08, 3.6408936E-08,
     *-3.7425022E-08, 4.0787921E-08,-4.1543242E-08, 4.5756842E-08,
     *-4.6035233E-08, 5.1425075E-08,-5.0893896E-08, 5.7934897E-08,
     *-5.6086570E-08, 6.5475248E-08,-6.1539913E-08, 7.4301996E-08,
     *-6.7117043E-08, 8.4767837E-08,-7.2583120E-08, 9.7366568E-08,
     *-7.7553611E-08, 1.1279873E-07,-8.1416723E-08, 1.3206914E-07,
     *-8.3217217E-08, 1.5663185E-07,-8.1482581E-08, 1.8860593E-07,
     *-7.3963141E-08, 2.3109673E-07,-5.7243707E-08, 2.8867452E-07,
     *-2.6163525E-08, 3.6808773E-07, 2.7049871E-08, 4.7932617E-07,
     * 1.1407365E-07, 6.3720626E-07, 2.5241961E-07, 8.6373437E-07,
     * 4.6831433E-07, 1.1916346E-06, 8.0099716E-07, 1.6696015E-06,
     * 1.3091334E-06, 2.3701475E-06, 2.0803829E-06, 3.4012978E-06/
      DATA WB0/
     * 3.2456774E-06, 4.9240402E-06, 5.0005198E-06, 7.1783540E-06,
     * 7.6367633E-06, 1.0522038E-05, 1.1590021E-05, 1.5488635E-05,
     * 1.7510398E-05, 2.2873836E-05, 2.6368006E-05, 3.3864387E-05,
     * 3.9610390E-05, 5.0230379E-05, 5.9397373E-05, 7.4612122E-05,
     * 8.8951409E-05, 1.1094809E-04, 1.3308026E-04, 1.6511335E-04,
     * 1.9895671E-04, 2.4587195E-04, 2.9728181E-04, 3.6629770E-04,
     * 4.4402013E-04, 5.4589361E-04, 6.6298832E-04, 8.1375348E-04,
     * [illegible]-04, 1.2132772E-03, 1.4772052[illegible]-03, 1.8097022E-03,
     * [illegible]-03, 2.698[illegible]E-03, 3.[illegible]E-03, 4.02[illegible]E-03,
```

```
*  [illegible]E-03,  6.0010[illegible]E-03,  [illegible]E-03,  8.[illegible]
*  [illegible]E-02,  1.3340[illegible]E-02,  [illegible]E-02,  1.[illegible]
*  3.4233627E-02,  2.9555499E-02,  3.5[illegible]E-02,  4.3791529E-02,
*  5.3150319E-02,  6.4341372E-02,  7.7506720E-02,  9.2749987E-02,
*  1.0980561E-01,  1.2791555E-01,  1.4525830E-01,  1.5820085E-01,
*  1.6058576E-01,  1.4196085E-01,  8.9781222E-02,-1.0238278E-02,
*-1.5083434E-01,-2.9059573E-01,-2.9105437E-01,-3.7973244E-02,
*  3.8273717E-01,  2.7014118E-01,-4.7342635E-01,  1.9331133E-01,
*  5.3839527E-02,-1.1909845E-01,  9.9317051E-02,-6.6152628E-02,
*  4.0703241E-02,-2.4358316E-02,  1.4476533E-02,-8.6196067E-03/
  DATA WC0/
*  5.2597053E-03,-3.1074602E-03,  1.8822342E-03,-1.1456545E-03,
*  7.0004347E-04,-4.2904226E-04,  2.6354444E-04,-1.6215439E-04,
*  9.9891279E-05,-6.1589037E-05,  3.7996921E-05,-2.3452250E-05,
*  1.4479572E-05,-8.9417427E-06,  5.5227518E-06,-3.4114252E-06,
*  2.1074101E-06,-1.3019229E-06,  8.0433617E-07,-4.9693681E-08,
*  3.0702417E-07,-1.8969219E-07,  1.1720069E-07,-7.2412496E-08,
*  4.4740283E-08,-2.7643004E-08,  1.7079403E-08,-1.0552634E-08,
*  6.5200311E-09,-4.0284597E-09,  2.4890232E-09,-1.5378695E-09,
*  9.5019040E-10,-5.8708696E-10,  3.6273937E-10,-2.2412348E-10,
*  1.3847792E-10,-8.5560821E-11,  5.2865474E-11,-3.2664392E-11,
*  2.0182948E-11,-1.2470979E-11,  7.7057678E-12,-4.7611713E-12,
*  2.9415274E-12,-1.8170081E-12,  1.1221034E-12,-6.9271067E-13,
*  4.2739744E-13,-2.6344388E-13,  1.6297105E-13,-9.9147443E-14,
*  6.0487998E-14,-3.6973097E-14,  2.2817964E-14,-1.4315547E-14,
*  9.1574735E-15,-5.9567236E-15,  3.9209969E-15,-2.5911739E-15,
*  1.6406939E-15,-8.8248590E-16,  3.0195409E-16,  2.2622634E-17,
*-8.0942556E-17,-3.7172363E-17,  1.9299542E-16,-3.3388160E-16,
*  4.6174116E-16,-5.8627358E-16,  7.2227767E-16,-8.7972941E-16,
*  1.0211793E-15,-1.0940039E-15,  1.0789555E-15,-9.7089814E-16/
  DATA WD0/
*  7.4110927E-16,-4.1700094E-16,  8.5977184E-17,  1.3396469E-16,
*-1.7838410E-16,  4.8975421E-17,  1.9398153E-16,-5.0046989E-16,
*  8.3280985E-16,-1.1544640E-15,  1.4401527E-15,-1.6637066E-15,
*  1.7777129E-15,-1.7322187E-15,  1.5247247E-15,-1.1771155E-15,
*  6.9747910E-16,-1.2088956E-16,-4.8382957E-16,  1.0408292E-15,
*-1.5220450E-15,  1.9541597E-15,-2.4107448E-15,  2.9241438E-15,
*-3.5176475E-15,  4.2276125E-15,-5.0977851E-15,  6.1428456E-15,
*-7.3949962E-15,  8.8597601E-15,-1.0515959E-14,  1.2264584E-14,
*-1.3949870E-14,  1.5332490E-14,-1.6146782E-14,  1.6084121E-14,
*-1.4962523E-14,  1.2794804E-14,-9.9286701E-15,  6.6825809E-15,
*-4.0056107E-15,  1.5965079E-15,-7.2732961E-18,-4.0433218E-16,
*-6.5679655E-16,  3.3011866E-15,-7.3545910E-15,  1.2394851E-14,
*-1.7947697E-14,  2.3774303E-14,-3.0279166E-14,  3.9252831E-14,
*-5.5510504E-14,  9.0505371E-14,-1.7064873E-13/
  DATA WA1/
*-4.2129715E-16,  5.3667031E-15,-7.1183962E-15,  8.9478500E-15,
*-1.0767891E-14,  1.2362265E-14,-1.3371129E-14,  1.3284178E-14,
*-1.1714302E-14,  8.4134738E-15,-3.7726725E-15,-1.4263879E-15,
*  6.1279163E-15,-9.1102765E-15,  9.9696405E-15,-9.3649955E-15,
*  8.6009018E-15,-8.9749846E-15,  1.1153987E-14,-1.4914821E-14,
*  1.9314024E-14,-2.3172388E-14,  2.5605477E-14,-2.6217555E-14,
*  2.5057768E-14,-2.2485539E-14,  1.9022752E-14,-1.5198084E-14,
*  1.1422464E-14,-7.9323958E-15,  4.8421406E-15,-2.1875032E-15,
*-3.2177842E-17,  1.8637565E-15,-3.3683643E-15,  4.6132219E-15,
*-5.6209538E-15,  6.4192841E-15,-6.8959928E-15,  6.9895792E-15,
*-6.5355935E-15,  5.6125163E-15,-4.1453931E-15,  2.6358827E-15,
*-9.5104370E-16,  1.4600474E-16,  5.6166519E-16,  8.2899246E-17,
*  5.0032100E-16,  4.3752205E-16,  2.1052293E-15,-9.5451973E-16,
*  6.4004437E-15,-2.1926177E-15,  1.1651003E-14,  5.8415433E-16,
*  1.8044664E-14,  1.0755745E-14,  3.0159022E-14,  3.3506138E-14,
*  5.8709354E-14,  8.1475200E-14,  1.2530006E-13,  1.8519112E-13,
*  2.7441786E-13,  4.1330823E-13,  6.1506209E-13,  9.1921659E-13,
*  1.3698462E-12,  2.0447427E-12,  3.0494477E-12,  4.5501001E-12,
*  6.7870250E-12,  1.0126237E-11,  1.5104976E-11,  2.2536053E-11/
  DATA WB1/
*  3.3617368E-11,  5.0153839E-11,  7.4818173E-11,  1.1161804E-10,
*  1.6651222E-10,  2.4840923E-10,  3.7058109E-10,  5.5284853E-10,
*  8.2474468E-10,  1.2303750E-09,  1.8355034E-09,  2.7382502E-09,
*  4.0849867E-09,  6.0940898E-09,  9.0913020E-09,  1.3562651E-08,
*  2.0233058E-08,  3.0184244E-08,  4.5029477E-08,  6.7176304E-08,
*  [illegible]E-07,  1.4950371E-07,  2.2303208E-07,  3.3272689E-07,
*  [illegible]E-07,  7.4049804E-07,  1.1046805E-[illegible]
```

```
     *  4585014E-06,  3.6677163E-06,  5.4714550E-06,  8.1626422E-06,
     *  2.2176782E-05,  1.8166417E-05,  2.7099223E-05,  4.0428804E-05,
     *  6.0307294E-05,  8.9971508E-05,  1.3420195E-04,  2.0021123E-04,
     *  2.9860417E-04,  4.4545291E-04,  6.6423156E-04,  9.9073275E-04,
     *  1.4767050E-03,  2.2016806E-03,  3.2788147E-03,  4.8837292E-03,
     *  7.2596811E-03,  1.0788355E-02,  1.5973323E-02,  2.3612041E-02,
     *  3.4655327E-02,  5.0608141E-02,  7.2627752E-02,  1.0337889E-01,
     *  1.4207357E-01,  1.8821315E-01,  2.2996815E-01,  2.5088500E-01,
     *  2.0334626E-01,  6.0665451E-02,-2.0275683E-01,-3.5772334E-01,
     * -1.8280529E-01,  4.7014634E-01,  7.2991233E-03,-3.0614594E-01,
     *  3.4781735E-01,-1.1149185E-01,  2.5985386E-02,  1.0850279E-02,
     * -2.2830217E-02,  2.4644647E-02,-2.2895284E-02,  2.0197032E-02/
      DATA WC1/
     * -1.7488968E-02,  1.5057670E-02,-1.2953923E-02,  1.1153254E-02,
     * -9.6138436E-03,  8.2952090E-03,-7.1628361E-03,  6.1882910E-03,
     * -5.3482055E-03,  4.6232056E-03,-3.9970542E-03,  3.4560118E-03,
     * -2.9883670E-03,  2.5840861E-03,-2.2345428E-03,  1.9323046E-03,
     * -1.6709583E-03,  1.4449655E-03,-1.2495408E-03,  1.0805480E-03,
     * -9.3441130E-04,  8.0803899E-04,-6.9875784E-04,  6.0425624E-04,
     * -5.2253532E-04,  4.5186652E-04,-3.9075515E-04,  3.3790861E-04,
     * -2.9220916E-04,  2.5269019E-04,-2.1851585E-04,  1.8896332E-04,
     * -1.6340753E-04,  1.4130796E-04,-1.2219719E-04,  1.0567099E-04,
     * -9.1379828E-05,  7.9021432E-05,-6.8334412E-05,  5.9092726E-05,
     * -5.1100905E-05,  4.4189914E-05,-3.8213580E-05,  3.3045496E-05,
     * -2.8576356E-05,  2.4711631E-05,-2.1369580E-05,  1.8479514E-05,
     * -1.5980307E-05,  1.3819097E-05,-1.1950174E-05,  1.0334008E-05,
     * -8.9364160E-06,  7.7278366E-06,-6.6827083E-06,  5.7789251E-06,
     * -4.9973715E-06,  4.3215167E-06,-3.7370660E-06,  3.2316575E-06,
     * -2.7946015E-06,  2.4166539E-06,-2.0898207E-06,  1.8071890E-06,
     * -1.5627811E-06,  1.3514274E-06,-1.1686576E-06,  1.0106056E-06,
     * -8.7392952E-07,  7.5573750E-07,-6.5353002E-07,  5.6514528E-07,
     * -4.8871388E-07,  4.2261921E-07,-3.6546333E-07,  3.1603732E-07/
      DATA WD1/
     * -2.7329579E-07,  2.3633470E-07,-2.0437231E-07,  1.7673258E-07,
     * -1.5283091E-07,  1.3216174E-07,-1.1428792E-07,  9.8831386E-08,
     * -8.5465227E-08,  7.3906734E-08,-6.3911437E-08,  5.5267923E-08,
     * -4.7793376E-08,  4.1329702E-08,-3.5740189E-08,  3.0906612E-08,
     * -2.6726739E-08,  2.3112160E-08,-1.9986424E-08,  1.7283419E-08,
     * -1.4945974E-08,  1.2924650E-08,-1.1176694E-08,  9.6651347E-09,
     * -8.3580023E-09,  7.2276490E-09,-6.2501673E-09,  5.4048822E-09,
     * -4.6739154E-09,  4.0418061E-09,-3.4951847E-09,  3.0224895E-09,
     * -2.6157226E-09,  2.2602382E-09,-1.9545596E-09,  1.6902214E-09,
     * -1.4616324E-09,  1.2639577E-09,-1.0930164E-09,  9.4519327E-10,
     * -8.1736202E-10,  7.0681930E-10,-6.1122713E-10,  5.2856342E-10,
     * -4.5707937E-10,  3.9526267E-10,-3.4180569E-10,  2.9557785E-10,
     * -2.5560176E-10,  2.2103233E-10,-1.9113891E-10,  1.6528994E-10,
     * -1.4294012E-10,  1.2361991E-10,-8.2740936E-11/
      NONE=0
      IF(NFW.EQ.0) GO TO 100
      NSAVE=0
      Y1=.73588526614797944D0/DBLE(B)
  100 ZHANKS=(0.0,0.0)
      CMAX=(0.0,0.0)
      NF=0
      Y=Y1
      ASSIGN 110 TO M
      I=131
      Y=Y*E
      GO TO 200
  110 TMAX(1)=AMAX1(ABS(T(1)),TMAX(1))
      TMAX(2)=AMAX1(ABS(T(2)),TMAX(2))
      I=I+1
      Y=Y*E
      IF(I.LE.149) GO TO 200
      IF(TMAX(1).EQ.0.0.AND.TMAX(2).EQ.0.0) NONE=1
      CMAX=TOL*CMAX
      ASSIGN 120 TO M
      GO TO 200
  120 IF(ABS(T(1)).LE.TMAX(1).AND.ABS(T(2)).LE.TMAX(2)) GO TO 130
```

```
      IF (...LE.283) GO TO 200
    5 Y=Y1
      ASSIGN 140 TO M
      I=130
      GO TO 200
  140 IF(ABS(T(1)).LE.TMAX(1).AND.ABS(T(2)).LE.TMAX(2).AND.
     *NONE.EQ.0) GO TO 190
      I=I-1
      Y=Y*ER
      IF(I.GT.0) GO TO 200
  190 ISAVE=1
      ZHANKS=ZHANKS/B
      RETURN
  200 G=SNGL(Y)
      IF(NEW) 300,210,300
  210 IF(ISAVE.GT.NSAVF) GO TO 300
      ISAVE0=ISAVE
  220 IF(G.EQ.GSAVE(ISAVE)) GO TO 240
      ISAVE=ISAVE+1
      IF(ISAVE.LE.NSAVF) GO TO 220
      ISAVE=ISAVE0
      GO TO 300
  240 C=FSAVE(ISAVE)
      ISAVE=ISAVE+1
  250 IF(N) 270,260,270
  260 C=C*WTC(I)
      GO TO 280
  270 C=C*WT1(I)
  280 CC1=REAL(C)
      CC2=AIMAG(C)
      IF(ABS(CC1).LT.0.1E-20.AND.ABS(CC2).LT.0.1E-20) C=0.0
      ZHANKS=ZHANKS+C
      GO TO M,(110,120,140)
  300 NSAVE=NSAVE+1
      C=FUN(G)
      NF=NF+1
      FSAVE(NSAVE)=C
      GSAVE(NSAVE)=G
      GO TO 250
  400 RETURN
      END
*END
```

Appendix E

Integration of the total energy flow over a horizontal plane for a vertical magnetic loop.

For a vertical magnetic loop 5-13 is replaced by

$$S = \frac{1}{4}\int (E_r H_\phi^* - E_\phi H_r^*)\, r\,dr\,d\phi . \qquad \text{E-1}$$

If the loop is considered to be in the yz-plane, the Hertz vector for the S_+ term becomes

$$\Pi_x(r,z) = \int J_0(\lambda r)\, e^{-\gamma z}\, \frac{\lambda\, d\lambda}{\gamma} \cdot A \qquad \text{E-2}$$

where

$$A = \left[e^{\mu h} + e^{-\mu h}\, \frac{(n^2\gamma - \gamma_E)}{n^2\gamma + \gamma_E} \right], \qquad \text{E-3}$$

and the Hertz vector for the S_- terms becomes

$$\Pi_x(r,z) = \int J_0(\lambda r)\, e^{-\gamma h}\, \frac{\lambda\, d\lambda}{\gamma} \cdot B \qquad \text{E-4}$$

where

$$B = \left[e^{\gamma z} + e^{-\gamma z}\, \frac{(n^2\gamma - \gamma_E)}{(n^2\gamma + \gamma_E)} \right] . \qquad \text{E-5}$$

Considering the following relations for the electrical and magnetic fields

$$H_r = k^2 \cos\phi\, \Pi_x + \frac{\partial}{\partial r}\, \mathrm{div}\, \vec{\Pi}, \qquad H_\phi = -k^2 \sin\phi\, \Pi_x + \frac{1}{r}\frac{\partial}{\partial \phi}\, \mathrm{div}\, \vec{\Pi}, \qquad \text{E-6}$$

$$E_\phi = i\omega\mu_0 \cos\phi\, \frac{\partial \Pi_x}{\partial z}, \qquad E_r = i\omega\mu_0 \sin\phi\, \frac{\partial \Pi_x}{\partial z},$$

where

$$k^2/i\epsilon\omega = -i\omega\mu_E ,$$

$$\operatorname{div}\vec{\Pi} = \cos\phi \frac{\partial \Pi_x}{\partial r},$$

$$\gamma^2 = \lambda^2 - k^2. \qquad \text{E-7}$$

$\operatorname{div}\vec{\Pi}$ for the S_+ term is:

$$\operatorname{div}\vec{\Pi} = -\cos\phi \int J_1(\lambda r)\, e^{-\gamma z} \frac{\lambda^2 d\lambda}{\gamma} A(h,\lambda), \qquad \text{E-8}$$

$\operatorname{div}\vec{\Pi}$ for the S_- term is:

$$\operatorname{div}\vec{\Pi} = -\cos\phi \int J_1(\lambda r)\, e^{-\gamma h} \frac{\lambda^2 d\lambda}{\gamma} B(z,\lambda), \qquad \text{E-9}$$

consequently

$$S_+ \rightarrow \frac{\partial}{\partial r} \operatorname{div}\Pi = -\cos\phi \int A(\lambda,h)\, e^{-\gamma z} \frac{\lambda^2 d\lambda}{\gamma} \left[\lambda J_0(\lambda r) - \frac{1}{r} J_1(\lambda r)\right]$$

$$S_- \rightarrow \frac{\partial}{\partial r} \operatorname{div}\vec{\Pi} = -\cos\phi \int B(\lambda,z)\, e^{-\gamma h} \frac{\lambda^2 d\lambda}{\gamma} \left[\lambda J_0(\lambda r) - \frac{1}{r} J_1(\lambda r)\right]$$

$$S_+ \rightarrow \frac{1}{r}\frac{\partial}{\partial \phi} \operatorname{div}\Pi = \sin\phi \int A(\lambda,h)\, e^{-\gamma z} \frac{\lambda^2 d\lambda}{\gamma} J_1(\lambda r)/r$$

$$S_- \rightarrow \frac{1}{r}\frac{\partial}{\partial \phi} \operatorname{div}\vec{\Pi} = \sin\phi \int B(z,\lambda)\, e^{-\gamma h} \frac{\lambda^2 d\lambda}{\gamma} J_1(\lambda r)/r$$

$$S_+ \rightarrow i\omega\varepsilon_0 \cos\phi \frac{\partial \Pi_x}{\partial z} = -i\omega\varepsilon_0 \cos\phi \int J_0(\lambda r)\, e^{-\gamma z} \lambda\, d\lambda \cdot A(h,\lambda) \qquad \text{E-10}$$

$$S_- \rightarrow i\omega\varepsilon_0 \cos\phi \frac{\partial \Pi_x}{\partial z} = i\omega\varepsilon_0 \cos\phi \int J_0(\lambda r)\, e^{-\gamma h} \lambda\, d\lambda \left[e^{\gamma z} - e^{-\gamma z} \frac{n^2\gamma - \gamma\varepsilon}{n^2\gamma + \gamma\varepsilon}\right].$$

The four field components for the S_+ term are then deduced as

$$H_r(r,z,\phi) = \cos\phi \int A(h,\lambda) \cdot \frac{\lambda^2}{r\gamma}\, e^{-\gamma z} J_1(\lambda r) \cdot d\lambda$$

$$-\cos\phi \int A(h,\lambda)\, \lambda\gamma\, e^{-\gamma z} J_0(\lambda r)\, d\lambda,$$

$$H_\phi(r,z,\phi) = \sin\phi \int A(h,\lambda) \frac{\lambda^2}{r\gamma}\, e^{-\gamma h} J_1(\lambda r)\, d\lambda$$

$$-\sin\phi \cdot k^2 \int A(h,\lambda) \frac{\lambda}{\gamma}\, e^{-\gamma z} J_0(\lambda r) \cdot d\lambda, \qquad \text{E-12}$$

$$E_r = -i\omega\mu_0 \sin\phi \int J_1(\lambda r)\, e^{-\gamma z}\, \lambda\, d\lambda \cdot A(\lambda, h),$$

$$E_\phi = -i\omega\mu_0 \cos\phi \int J_0(\lambda r)\, e^{-\gamma z}\, \lambda\, d\lambda\; A(h, \lambda),$$

and the same components for the S_- term are

$$H_r(r,\phi,z) = \cos\phi \left[\int B(\lambda, z)\, e^{-\gamma h}\, \frac{\lambda^2}{r\gamma} J_1(\lambda r)\, d\lambda - \int B(\lambda, z)\, e^{-\gamma h}\, \gamma\lambda\, J_0(\lambda r)\, d\lambda \right]$$

$$H_\phi(r,\phi,z) = \sin\phi \left[\int B(\lambda, z)\, \frac{\lambda^2}{r\gamma}\, e^{-\gamma h} J_1(\lambda r)\, d\lambda - k^2 \int B(\lambda, z)\, \frac{\lambda}{\gamma}\, e^{-\gamma h} J_0(\lambda r)\, d\lambda \right] \qquad \text{E-12}$$

$$E_r(r,\phi,z) = i\omega\mu_0 \sin\phi \int \left[e^{\gamma z} - e^{-\gamma z} \frac{n^2\gamma - \gamma\varepsilon}{n^2\gamma + \gamma\varepsilon} \right] e^{-\gamma h} J_0(\lambda r)\, \lambda\, d\lambda$$

$$E_\phi(r,\phi,z) = i\omega\mu_0 \cos\phi \int \left[e^{\gamma z} - e^{-\gamma z} \left(\frac{n^2\gamma - \gamma\varepsilon}{n^2\gamma + \gamma\varepsilon} \right) \right] e^{-\gamma h} J_1(\lambda r)\, \lambda\, d\lambda .$$

Thus the S_+ term is:

$$\frac{1}{2} \mathrm{Re} \int_r \int_\phi E_r H_\phi^*\, r\, dr\, d\phi = \frac{1}{2}\pi\mu_0\omega\, \mathrm{Re}(i) \cdot \left\{ k^2 \int_\lambda e^{-z(\gamma+\gamma^*)} A(h,\lambda) \cdot A^*(h,\lambda) \frac{\lambda}{\gamma^*}\, d\lambda \right.$$
$$- \int_\lambda \int_{\ell=\lambda}^{\infty} e^{z(\gamma(\lambda)+\gamma^*(\ell))} A(\lambda, h)\, A^*(\ell, h)\, \frac{\ell}{\gamma^*(\ell)}\, d\ell$$
$$\left. - \tfrac{1}{2} \int A(h,\lambda)\, e^{-z\gamma}\, d\lambda \cdot \int A^* e^{-z\gamma^*} \frac{\lambda^2 d\lambda}{\gamma} \right\}$$

$$-\frac{1}{2} \mathrm{Re} \int_r \int_\phi E_\phi H_r^*\, r\, dr\, d\phi = \frac{1}{2}\pi\mu_0\omega\, \mathrm{Re}(i) \cdot \left\{ - \int_\lambda e^{-z(\gamma+\gamma^*)} A(h,\lambda) A^*(h,\lambda)\, \lambda\, \gamma^*\, d\lambda \right.$$
$$+ \int_\lambda \int_{\ell=\lambda}^{\infty} e^{-z[\gamma(\lambda)+\gamma^*(\ell)]} A(h,\lambda)\, A^*(\ell,h)\, \frac{\ell}{\gamma^*(\ell)}\, d\ell \qquad \text{E-13}$$
$$\left. + \tfrac{1}{2} \int A(h,\lambda)\, e^{-z\gamma}\, d\lambda \cdot \int A^* e^{-z\gamma^*} \frac{\lambda^2 d\lambda}{\gamma^*} \right\}$$

$$S_+ = \frac{1}{2}\pi\mu_0\omega\, \mathrm{Re} \left\{ i \int_\lambda (e^{-z\gamma} A(h,\lambda))(e^{-z\gamma^*} A^*(h,\lambda))\, \lambda \left(\frac{2k^2 - \lambda^2}{\gamma^*} \right) d\lambda \right.$$

Introducing a further simplification, for the situation where the z-plane approaches the h-plane:

$$z = h \pm \epsilon \quad \text{thus} \quad |z-h| = \epsilon \ll h \quad z+h = 2h \qquad \text{E-14}$$

and E-13 yields to:

$$S_+ = \frac{\pi\omega\gamma_0}{2} \operatorname{Re}\left\{ i \left[-\int_\lambda e^{-\epsilon(\gamma+\gamma^*)} \frac{\lambda}{\gamma^*}(-2k^2+\lambda)\, d\lambda \right.\right.$$
$$- \int_\lambda e^{2h\gamma^*} \frac{n^{*2}\gamma^* - \gamma_\varepsilon^*}{n^{*2}\gamma^* + \gamma_\varepsilon^*} \frac{\lambda}{\gamma^*}(\lambda^2 - 2k^2)\, d\lambda - \int_\lambda e^{-2h\gamma} \frac{n^2\gamma - \gamma_\varepsilon}{n^2\gamma + \gamma_\varepsilon} \frac{\lambda}{\gamma^*}(\lambda - 2k^2) d\lambda$$
$$\left.\left. - \int_\lambda e^{-2h(\gamma+\gamma^*)} \frac{\lambda}{\gamma^*} \frac{(n^{*2}\gamma^* - \gamma_\varepsilon^*)(n^2\gamma - \gamma_\varepsilon)}{(n^{*2}\gamma^* + \gamma_\varepsilon^*)(n^2\gamma + \gamma_\varepsilon)} (\lambda - 2k^2) d\lambda \right] \right\}$$

The S_- term proceeding as above results as follows:

$$S_- = \frac{1}{2} \int_r \int_\phi E_r H_\phi^* \, r\, dr\, d\phi =$$

$$\frac{1}{2} \pi\omega\gamma \operatorname{Re}\left\{ i \left[\int_\lambda C(\lambda, z)\, B^*(\lambda, z)\, e^{-h(\gamma+\gamma^*)} \frac{\lambda}{\gamma^*}(-2k^2 - \lambda)\, d\lambda \right] \right\} \qquad \text{E-15}$$

where

$$C = e^{\gamma z} - e^{-\gamma z} \frac{(n^2\gamma - \gamma_\varepsilon)}{(n^2\gamma + \gamma_\varepsilon)} .$$

Introducing E-14 in E-15,

$$S_- = \frac{1}{2} \pi\gamma\omega_0 \operatorname{Re}\left\{ i \left[\int_\lambda e^{-\epsilon(\gamma+\gamma^*)} \frac{\lambda}{\gamma^*}(\lambda^2 - 2k^2)\, d\lambda + \int_\lambda \frac{\lambda}{\gamma^*} e^{-2\gamma^* h} \frac{n^{*2}\gamma^* - \gamma_\varepsilon^*}{n^{*2}\gamma^* + \gamma_\varepsilon^*} \frac{\lambda}{\gamma^*}(\lambda^2 - 2k^2) d\lambda \right.\right.$$
$$\left.\left. - \int e^{-2\gamma h} \frac{n^2\gamma - \gamma_\varepsilon}{n^2\gamma + \gamma_\varepsilon} \frac{\lambda}{\gamma}(\lambda^2 - 2k^2)\, d\lambda - \int e^{-2(\gamma+\gamma^*)h} \frac{n^2\gamma - \gamma_\varepsilon}{n^2\gamma + \gamma_\varepsilon} \frac{n^{*2}\gamma^* - \gamma_\varepsilon^*}{n^{*2}\gamma^* + \gamma_\varepsilon^*} d\lambda \right] \right\}$$

Applying the same simplification to the A, B, and C terms:

$$e^{-2\gamma} A(\lambda,h) \cong e^{-\epsilon\gamma} + e^{-2h\gamma} \frac{n^2\gamma - \gamma_E}{n^2\gamma + \gamma_E}$$

$$e^{-2\gamma^*} A^*(\lambda,\gamma) \cong e^{-\epsilon\gamma^*} + e^{-2h\gamma^*} \frac{n^{*2}\gamma^* - \gamma_E^*}{n^{*2}\gamma^* + \gamma_E^*}$$

E-16

$$e^{-h\gamma} B(\lambda,z) \cong e^{\epsilon\gamma^*} + e^{-2h\gamma^*} \frac{n^{*2}\gamma^* - \gamma_E^*}{n^{*2}\gamma + \gamma_E^*}$$

$$e^{-h\gamma} C(\lambda,z) \cong e^{-\epsilon\gamma} - e^{-2h\gamma} \frac{n^2\gamma - \gamma_E}{n^2\gamma + \gamma_E}$$

and finally W is obtained as:

$$W = S_+ - S_- = \frac{2\pi k^2}{\omega\epsilon_0} \mathrm{Re}(i) \left[\frac{1}{2} \int_\lambda e^{-\epsilon(\gamma_1^* + \gamma)} \frac{\lambda}{\gamma^*} (\lambda^2 - 2k^2)\, d\lambda + \frac{1}{2} \int_\lambda e^{-2\gamma_1^* h} \frac{n_1^{*2}\gamma^* - \gamma_{1\varepsilon}^*}{n_1^{*2}\gamma_1^* + \gamma_{1\varepsilon}^*} \cdot \frac{\lambda}{\gamma_1^*} (\lambda^2 - 2k^2)\, d\lambda \right]$$

$$\mathrm{Re}(-i/2) \int_\lambda e^{-\epsilon(\gamma_1^* + \gamma)} \frac{\lambda}{\gamma_1^*} (\lambda^2 - 2k^2)\, d\lambda = \frac{2}{3} k^3$$

$$\mathrm{Re}(-i/2) \int_\lambda e^{-2\gamma_1^* h} \frac{\lambda}{\gamma_1^*} (\lambda^2 - 2k^2)\, d\lambda = k^3 \left[\frac{\sin J}{J} - \frac{\sin J - J\cos J}{J^3} \right]$$

where $J = 2kh$

$$V = \mathrm{Re}(i) \int e^{-2\gamma_1^* h} \frac{\gamma_{1\varepsilon}^*}{n_1^{*2}\gamma^* + \gamma_{1\varepsilon}^*} \frac{\lambda}{\gamma_1^*} (\lambda^2 - 2k^2)\, d\lambda$$

$$W = \frac{2\pi k^5}{\omega\epsilon_0} \left[\frac{2}{3} + \frac{\sin J}{J} - \frac{\sin J - J\cos J}{J^3} + V \right]$$